

AD-A055 635

AIR FORCE INST OF TECH WRIGHT-PATTERSON AFB OHIO SCH--ETC F/6 17/7
PSEUDO-RANGE MEASUREMENTS USED TO INCREASE THE SAMPLING RATE OF--ETC(U)

DEC 77 J M PETEK

AFTT/GA/FE/77-4

UNCLASSIFIED

1 OF 2
AD
A055 635

NL



DISCLAIMER NOTICE

**THIS DOCUMENT IS BEST QUALITY
PRACTICABLE. THE COPY FURNISHED
TO DDC CONTAINED A SIGNIFICANT
NUMBER OF PAGES WHICH DO NOT
REPRODUCE LEGIBLY.**

AFIT/GA/EE/77-4

AD No. / DDC FILE COPY

AD A 055635

1

9 Master's thesis,

6
PSEUDO-RANGE MEASUREMENTS
USED TO INCREASE THE SAMPLING
RATE OF THE AIDED TRACK ALGORITHM.

THESIS

14

AFIT/GA/EE/77-4

10

James M. Petek
Captain USAF

DDC

JUN 22 1978

REF ID: A64214
E

11 Dec 77

12 155p.

Approved for public release; distribution unlimited

78 06 13 176

012225

6

AFIT/GA/EE/77-4

PSEUDO-RANGE MEASUREMENTS
USED TO INCREASE THE SAMPLING
RATE OF THE AIDED TRACK ALGORITHM

THESIS

Presented to the Faculty of the School of Engineering
of the Air Force Institute of Technology
Air University
in Partial Fulfillment of the
Requirements for the Degree of
Master of Science

ACKNOWLEDGMENT FOR	
NTS	White Section <input checked="" type="checkbox"/>
DDG	Buff Section <input type="checkbox"/>
UNARMONIZED <input type="checkbox"/>	
JUSTIFICATION.....	
.....	
BY	
DISTRIBUTION/AVAILABILITY CODES	
DIS.	AVAIL. AND/OR SPECIAL
A	2345

by

James M. Petek, B.S.

Captain USAF

Graduate Astronautical Engineering

December 1977

Approved for public release; distribution unlimited.

Preface

From the start, my objective was to develop a low-cost method of increasing the sampling rate of a rate aided pointing and tracking system by using information already available within the system. After determining the best of alternative pseudo-measurement schemes, the system proved to be very effective against highly maneuverable targets. Although only a two dimensional analysis with simplified dynamics was used, it is expected that the general results will carry over in a satisfactory manner to three dimensional systems with more complicated dynamics.

My sincere appreciation goes to Prof. James E. Negro for his advice and patient guidance in this effort. Most of all, I must express my gratitude to my wife, Berni, for her encouragement and endurance of many lonely hours during the preparation of this work.

Contents

	<u>Page</u>
Preface	ii
List of Figures	v
List of Tables	xi
List of Symbols	x
Abstract	xii
I. Introduction	1
Background	1
Purpose of Study	2
Outline of Report	3
II. Aided Track	4
III. Simulation Model	8
Reference Frames	8
Truth Model	10
Transformation T_1	12
Kalman Filter Equations	13
Transformation T_2	18
Transformation T_3	19
W_{aid}	19
IV. Design Improvements	22
Filter Changes	22
Modification One	24
Modification Two	25
Modification Three	25
Modification Four	25
Modification Five	26
Modification Six	26
Scenarios	27
V. Results Analysis	37
Q33 Analysis	37
Generating W_{aid}	39
Modification Selection	41
Performance Comparison	42
VI. Conclusion and Recommendations	49

	<u>Page</u>
Bibliography	51
Appendix A: Program Listing: A Rate Aided Pointing and Tracking Algorithm for a Two- Dimensional System	52
Appendix B: Truth Model Formulation	68
Appendix C: Steady-State Perturbation Analysis . .	70
Appendix D: Program Listings for Each Modifica- tion Method Tested	74
Appendix E: Supportive Material: Plots of Tracking Error Versus Time for Various Modifications and Scenarios	81
Vita	138

List of Figures

<u>Figure</u>		<u>Page</u>
1	Pointing and Tracking System Model	1
2	Azimuth Channel of Pointing and Tracking System	4
3	Aided Track Model	9
4	Target Geometry	10
5	Aided @ 0.01 Second Rate by Modification Two, H Matrix Unchanged - Sinusoidal Corruption, Scenario One	23
6	Scenario One, Straight Flyby	29
7	Scenario Two, Flyby to 100 G turn	29
8	Scenario Three, Slower Flyby to 10 G turn.	31
9	Scenario Four, Flyby to Deceleration	34
10	Scenario Five, Flyby to Pursuit to Deceleration	34
11	Q_{33} Analysis	38
12	Aided at 0.01 second rate by Modification Two with computational delay, Scenario One	82
13	Aided at 0.01 second rate by Modification Two with instantaneous update, Scenario One	83
14	Aided at 0.01 second rate by Modification Two with predicted update, Scenario One	84
15	Aided at 0.01 second rate by Modification Two with computational delay, Scenario Two	85
16	Aided at 0.01 second rate by Modification Two with instantaneous update, Scenario Two	86
17	Aided at 0.01 second rate by Modification Two with predicted update, Scenario Two	87
18	Aided at 0.10 second rate by Modification Two with computational delay, Scenario Five	88

<u>Figure</u>		<u>Page</u>
19	Aided at 0.01 second rate by Modification Two with instantaneous update, Scenario Five . . .	89
20	Aided at 0.01 second rate by Modification Two with predicted update, Scenario Five	90
21	Aided at 0.01 second rate by Modification Six with computational delay, Scenario One	91
22	Aided at 0.01 second rate by Modification Six with instantaneous update, Scenario One	92
23	Aided at 0.01 second rate by Modification Six with predicted update, Scenario One	93
24	Aided at 0.01 second rate by Modification Six with computational delay, Scenario Two	94
25	Aided at 0.01 second rate by Modification Six with instantaneous update, Scenario Two	95
26	Aided at 0.01 second rate by Modification Six with predicted update, Scenario Two	96
27	Aided at 0.01 second rate by Modification One, Scenario Two	97
28	Aided at 0.01 second rate by Modification One with measurement noise, Scenario Two	98
29	Aided at 0.01 second rate by Modification Two, Scenario Two	99
30	Aided at 0.01 second rate by Modification Two with measurement noise, Scenario Two	100
31	Aided at 0.01 second rate by Modification Three, Scenario Two	101
32	Aided at 0.01 second rate by Modification Three with measurement noise, Scenario Two . . .	102
33	Aided at 0.01 second rate by Modification Five, Scenario Two	103
34	Aided at 0.01 second rate by Modification Five with measurement noise, Scenario Two . . .	104
35	Aided at 0.01 second rate by Modification Six, Scenario Two	105

<u>Figure</u>	<u>Page</u>
36 Aided at 0.01 second rate by Modification Six with measurement noise, Scenario Two	106
37 Unaided Tracking of Scenario One	107
38 Aided at 0.1 second rate, $Q_{33} = 1.0$, Scenario One	108
39 Aided at 0.01 second rate with laser range-finder, Optimal modification, Scenario One	109
40 Aided at 0.1 second rate, $Q_{33} = P_{33} = 0.0$, Scenario One	110
41 Aided at 0.01 second rate by Modification Four, $Q_{33} = P_{33} = 0.0$, Scenario One	111
42 Aided at 0.01 second rate by Modification Six, Scenario One	112
43 Unaided tracking of Scenario Two	113
44 Aided at 0.1 second rate, $Q_{33} = 1.0$, Scenario Two	114
45 Aided at 0.01 second rate with laser range-finder, Optimal modification, Scenario Two	115
46 Aided at 0.01 second rate by Modification Six, Scenario Two	116
47 Aided at 0.1 second rate, with noise, Scenario Two	117
48 Aided at 0.01 second rate by Modification Six, with measurement noise, Scenario Two	118
49 Unaided tracking of Scenario Five	119
50 Aided at 0.1 second rate, Scenario Five	120
51 Aided at 0.01 second rate by Modification Six, Scenario Five	121
52 Aided at 0.01 second rate by Modification Two, Scenario One	122
53 Aided at 0.1 second rate, with noise, Scenario One	123

<u>Figure</u>		<u>Page</u>
54	Aided at 0.01 second rate by Modification Two, with noise, Scenario One	124
55	Unaided tracking of Scenario Three	125
56	Aided at 0.1 second rate, Scenario Three . . .	126
57	Aided at 0.01 second rate by Modification Two, Scenario Three	127
58	Aided at 0.1 second rate, with noise, Scenario Three	128
59	Aided at 0.01 second rate by Modification Two, with noise, Scenario Three	129
60	Unaided Tracking of Scenario Four	130
61	Aided at 0.1 second rate, Scenario Four . . .	131
62	Aided at 0.01 second rate by Modification Two, Scenario Four	132
63	Aided at 0.1 second rate, with noise, Scenario Four	133
64	Aided at 0.01 second rate by Modification Two, with noise, Scenario Four	134
65	Aided at 0.01 second rate by Modification Two, Scenario Five	135
66	Aided at 0.1 second rate, with noise, Scenario Five	136
67	Aided at 0.01 second rate by Modification Two, with noise, Scenario Five	137

List of Tables

<u>Table</u>		<u>Page</u>
I	Listing of Modifications	27
II	Scenario One	28
III	Scenario Two and Scenario Three	32
IV	Scenario Four	35
V	Scenario Five	36
VI	Performance of Techniques Used to Generate W _{aid}	40
VII	Performance of Modifications Against Scenario Two	43
VIII	Peak and RMS Tracking Errors	47

List of Symbols

<u>Symbol</u>	<u>Computer Code</u>	<u>Definition</u>
$\dot{\eta}_T, \ddot{\eta}_T, \ddot{\ddot{\eta}}_T$	ETAT, ETATD, ETATDD	True target angle, angular rate, and angular acceleration
$\eta_p, \dot{\eta}_p, \ddot{\eta}_p$	ETAP, ETAPD, ETAPDD	Tracker pointing angle, angular rate, and angular acceleration
ϵ	ETAERR	Error signal, ETAT-ETAP
W_{aid}	WAID	Angular rate aiding signal
W_{cmd}	WCMD	Commanded angular rate
W_A	WA	Angular rate output from the compensator
$\eta_m, \dot{\eta}_m$	ETAM, WCMD	Measured angle and angular rate
R_m, \dot{R}_m	RM, RMD	Measured range and range rate
R'_m	--	Pseudo-range measurement
X_{1m}, X_{2m}	X1M, X1MD, X2M, X2MD	Planar coordinate pseudo-measurements
\underline{A}	\underline{A}	State transition matrix
\underline{P}	\underline{P}	Covariance matrix
\underline{H}	\underline{H}	Measurement matrix
\underline{G}	\underline{G}	Kalman gain matrix
\underline{Q}	\underline{Q}	Uncertainty matrix
\underline{R}	\underline{R}	Measurement covariance matrix
$E\{ \}$	--	Expectation
$\hat{R}, \dot{\hat{R}}$	ER, RMD	Estimates of range and range rate

<u>Symbol</u>	<u>Computer Code</u>	<u>Definition</u>
$\hat{R}, \dot{\hat{R}}$	ER, RMD	Estimates of range and range rate
$\hat{n}, \dot{\hat{n}}, \ddot{\hat{n}}$	EETA, EETAD, EETADD	Estimates of $n_T, \dot{n}_T, \ddot{n}_T$
$\delta R, \delta \dot{R}$	- -	Error in range and range rate
ΔT	DT	Measurement sampling interval
ΔT_T	DDT	Filter interval
ΔT_c	- -	Computational interval of Differential equation solving routine.

Abstract

This thesis investigates the use of internally generated pseudo-range measurements to increase the sampling speed of a rate aided pointing and tracking system known as Aided Track. Six separate methods for generating pseudo-range measurements were developed for a two dimensional analysis of the problem. Five target scenarios of various complexity were used to test the systems. The results obtained indicate that the use of a pseudo-range measurement generated by using the internal estimate of range provided the best performance of all methods tested. This method demonstrated a definite improvement over the slower system when tracking highly maneuverable targets.

PSEUDO-RANGE MEASUREMENTS
USED TO INCREASE THE SAMPLING
RATE OF THE AIDED TRACK ALGORITHM

I. Introduction

Background

The problem of accurately pointing a gimbaled sensor at a target and then precisely tracking that target has always been important. Conventional methods of pointing and tracking have an inherent pointing error caused by dynamic lag. This error is unacceptable for many applications.

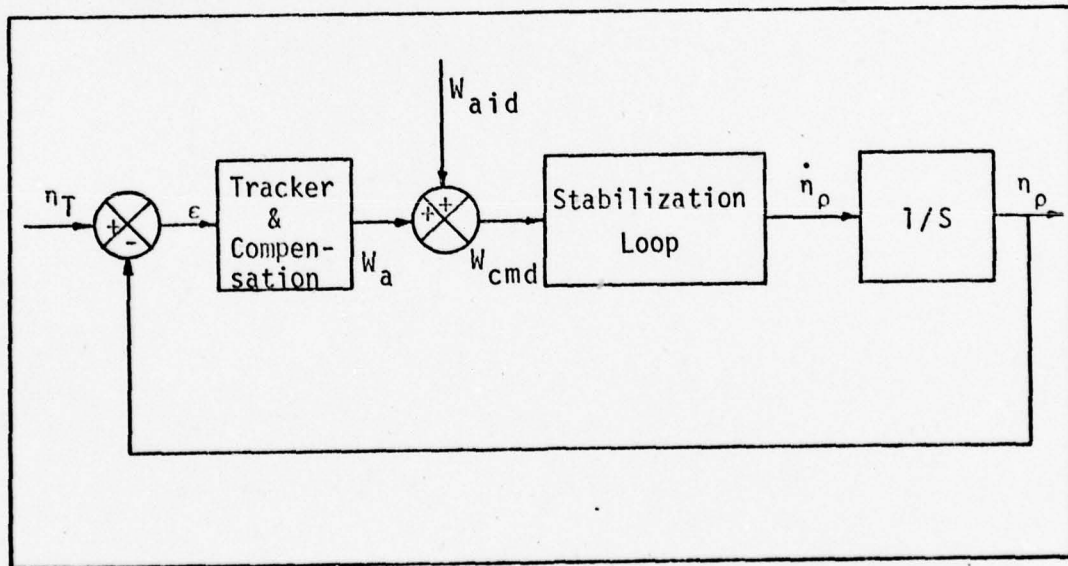


Fig. 1. Pointing and Tracking System Model

A new approach to the pointing and tracking problem was developed by Fitts (Ref 1,2,3). In this approach,

known as Aided Track, an auxiliary signal W_{aid} is input to the rate command signal as shown in Figure 1. Ideally, if W_{aid} is chosen properly, the tracking error ϵ would be forced to zero. The Aided Track concept is covered in greater depth in Chapter II.

In order to generate W_{aid} , Aided Track uses recursive Kalman filtering techniques to weight and incorporate the measurements of range and gimbal rotation rates. Nominally, the gimbal rate information can be provided at 0.01 second intervals by gyros attached directly to the gimbaled sensor. Whereas, accurate range information is only available every 0.1 seconds from a laser rangefinder. Aided Track, as developed by Fitts, operates at the slower 10 samples/second data rate due to the laser rangefinder limitation (Ref 1:37).

Purpose of the Study

At the current sample rate, nine out of ten measurements of gimbal rate are being ignored. Logically, it would seem that if these nine measurements could be incorporated in some way, that an improvement in the system could be realized. The simplest way to do this would be to increase the sample rate of the laser rangefinder, however, this is not possible due to heat dissipation limitations. Therefore, some other means of obtaining range measurements to couple with the nine gimbal rate measurements must be used. The purpose of this study is to determine the

best method of internally generating pseudo-range measurements to combine with the extra gimbal rate measurements and to determine if and how much of an improvement in tracking performance can be gained.

Outline of the Report

In this study, a two dimensional analysis of the problem is presented. This approach allows for a more simplified computer simulation with the results being easily related to the more complicated three dimensional case. The actual computer simulation developed is listed in Appendix A.

Chapter II presents a discussion of Aided Track and some of the rationale behind it. The actual transformations and associated equations are presented in Chapter III.

Chapter IV then describes each modification of the program that was used to generate the pseudo-range measurements. The rationale for each modification is also presented along with the problems encountered and how they were remedied.

Next, Chapter V presents an analysis of the results which shows an agreement, in part, with those obtained by Fitts (Ref 1,2,3). Any attainable improvement in tracking performance is shown to be dependent on target motion.

Finally, Chapter VI presents the conclusions and recommendations regarding the overall analysis.

II. Aided Track

The analysis of Aided Track presented here is for a simplified two dimensional model. Figure 2 depicts a model of the azimuth channel of a pointing and tracking system wherein the stabilization loop is modeled by the transfer function

$$G_S(s) = \frac{w_n^2}{s^2 + 2\zeta w_n s + w_n^2} \quad (1)$$

which is a second order approximation of the actual stabilization loop.

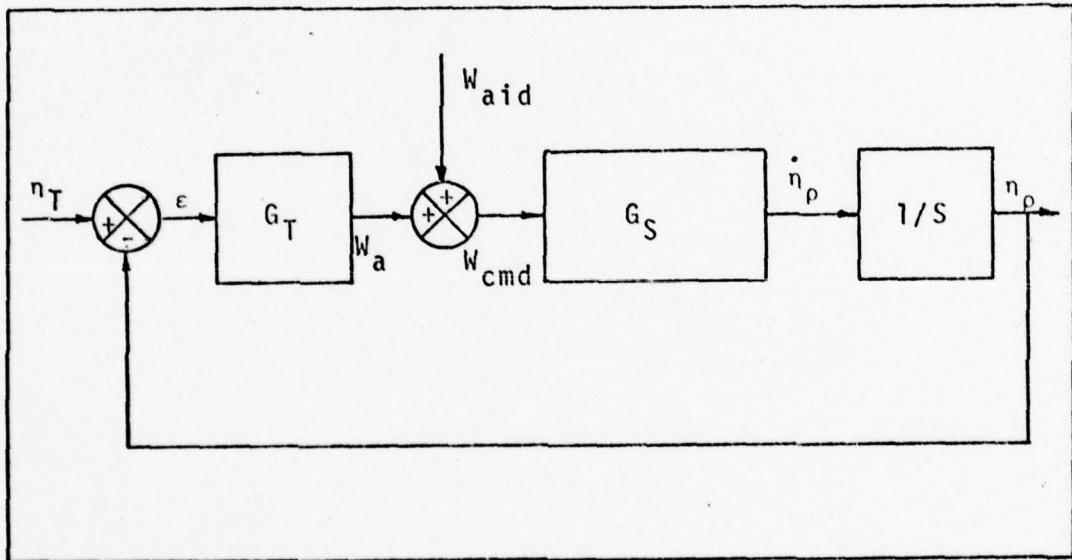


Fig. 2. Azimuth channel of Pointing and Tracking System (Ref 4:41)

The natural frequency w_n and the damping ratio ζ of the stabilization loop are 220 radians/second and 0.7 respectively (Ref 2:40).

The tracker and proportional plus integral compensation is accurately modeled by the transfer function

$$G_T(s) = \frac{K_T(s/W_T + 1)}{s} \quad (2)$$

For this analysis, the tracker sensor sampling period (T) is 0.01 seconds. Therefore, a gain K_T of 700 seconds $^{-2}$ and a frequency W_T of 18 radians/second give suitable closed loop characteristics (Ref 3:41-44).

Ideally, one would like W_{aid} to be chosen so that the tracking error ϵ is forced to zero. From inspection of Figure 2, one sees that zero error implies

$$W_{aid}(s) = S n_T(s)/G_S(s) \quad (3)$$

Substituting for $G_S(s)$ yields

$$W_{aid}(s) = [s + (2\zeta/W_n)s^2 + s^3/W_n^2]n_T(s) \quad (4)$$

Now, taking the inverse transform of both sides of Eq (4) yields

$$W_{aid}(t) = \ddot{n}_T + 2\zeta \ddot{n}_T/W_n + \text{higher order terms} \quad (5)$$

The problem of generating W_{aid} is that the derivatives of the target angle specified in Eq (5) are not available from direct measurements. However, Fitts determined that sufficiently accurate estimates of these derivatives could be generated by using a Kalman filter external to the servo loop (Ref 1). Eq (5) then becomes

$$W_{aid}(t) = \dot{\hat{n}}_T + G_A \ddot{\hat{n}}_T \quad (6)$$

where

$$G_A = 2\xi/W_n + 3.5 \Delta TT/2\pi \quad (7)$$

is the quadratic stabilization loop correction term. The first term of the gain G_A follows from Eq (5). The second term, however, was selected by Fitts to compensate for the lag due to the discretization of the actual aided track signal (Ref 1:16).

In order to generate the estimates of gimbal rate and acceleration, Fitts elected to use a linear Kalman filter. This approach requires several transformations. First, the measurements R_m , n_m , \dot{n}_m along with the estimate of range rate from the filter must be transformed into an inertial coordinate frame. The measurement sample interval for the Fitts model is $\Delta T = 0.1$ seconds. This interval will be decreased in this study to $\Delta T = 0.01$ seconds to incorporate pseudo-range measurements. The filter, however, operates at $\Delta TT = 0.01$ seconds already, in order to provide a smooth W_{aid} command signal compatible with the servo loop 8.0 Hz frequency. Estimates of the target position, velocity, and acceleration in an inertial frame are output from the filter. These estimates must then be transformed back into polar coordinates to provide the estimate of range rate for the filter and estimates of gimbal rate and acceleration for generation of W_{aid} .

This chapter has presented a very basic description of the Aided Track concept as developed by Fitts. It again should be emphasized that the design rationale is the desire to use a linear Kalman filter with precomputed gains rather than on-line gain calculations required in an Extended Kalman filter approach for non-linear systems. Details of the Aided Track approach are included in Chapter III.

III. Simulation Model

The Aided Track model, as discussed in Chapter II, is depicted in Figure 3. In this chapter, the reference frames in which the target motion is modeled, are defined. Also, the equations representing the truth model and Kalman filter are presented along with their associated transformations.

Reference Frames

Fitts defines several reference frames in order to accommodate tracker motion in his three dimensional analysis (Ref 1,2,3). For purposes of this study, the tracker will be assumed non-translating with respect to inertial space, thereby requiring only two coordinate frames to be defined. The orientation of these reference frames is arbitrary, but usually chosen for convenience.

An inertial coordinate system Y_1, Y_2 is defined to be fixed on the surface of the earth with the tracker located at the origin. For convenience, the Y_1 axis is defined to be pointing directly at the target at $t = 0$.

A similar inertially non-rotating coordinate system X_1, X_2 is defined for the Kalman filter. However, it is initialized when the filter is turned on so that the X_1 axis is pointing directly at the estimated position of the target. The target geometry can now be described as illustrated in Figure 4. The angle θ_0 is fixed at the instant the filter is activated and is used to make transformations from the filter frame back to the truth model

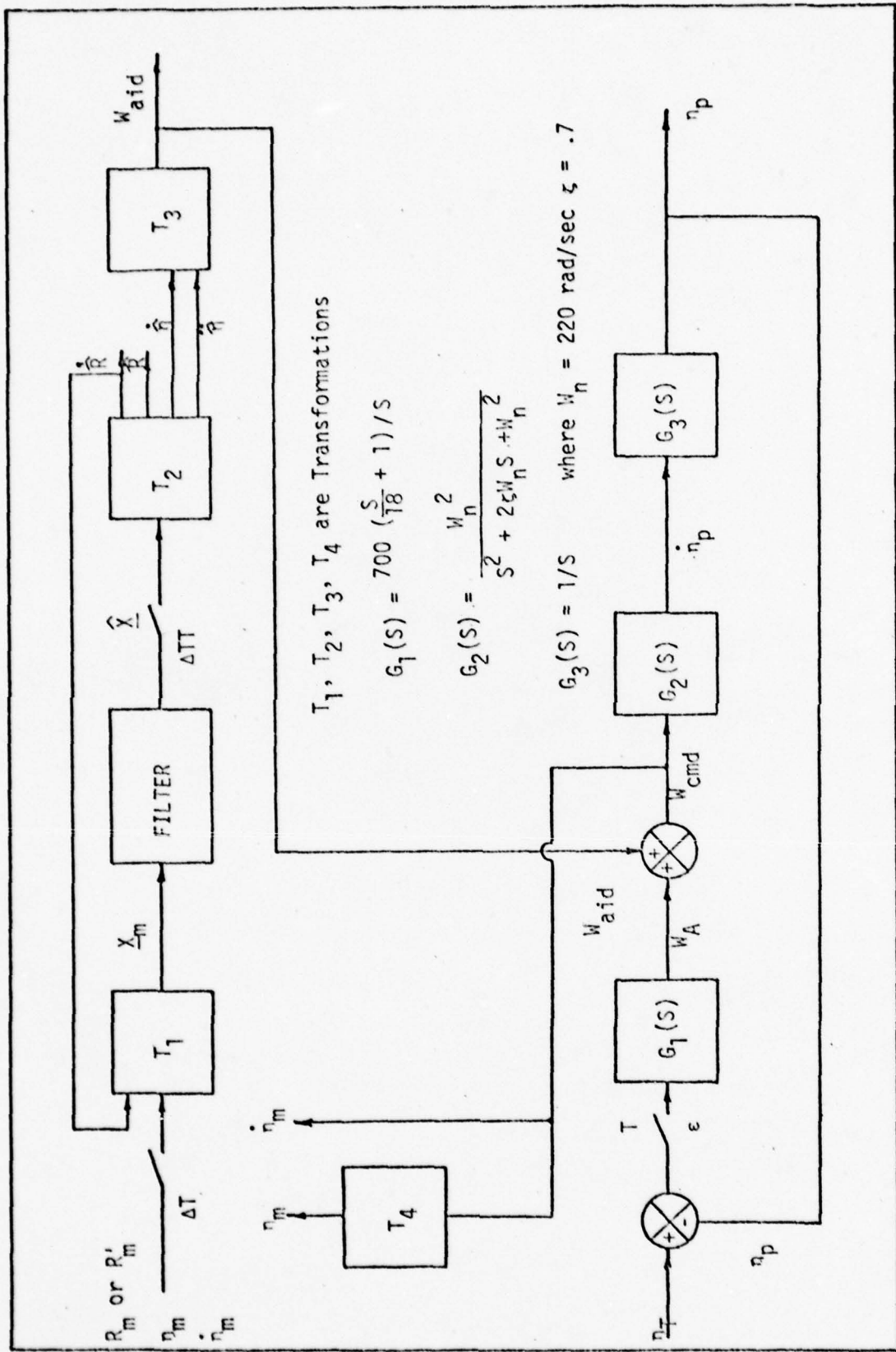


Figure 3: Aided Track Model

inertial frame. This angle is used only as a simulation artifice to relate the filter frame to the simulation frame.

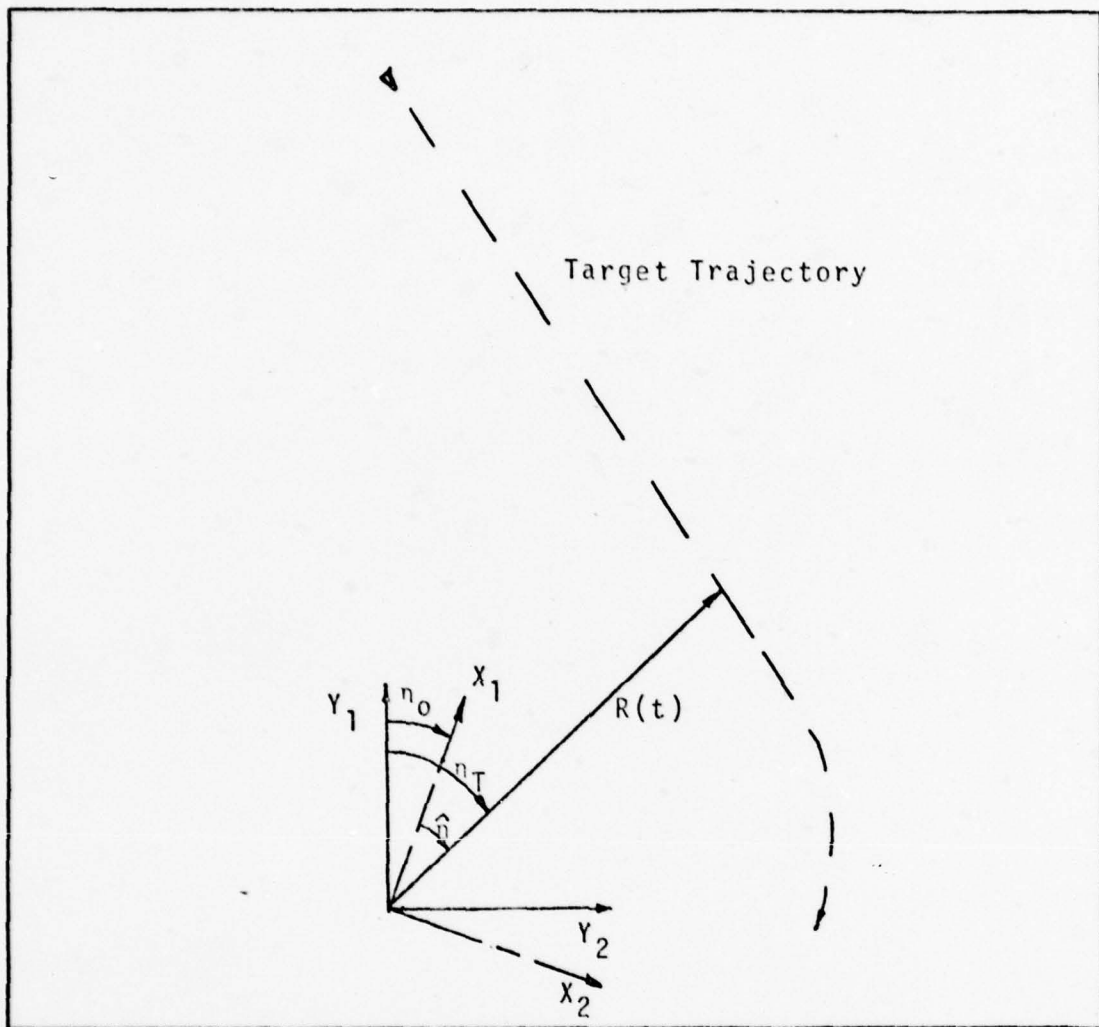


Fig. 4. Target Geometry

Truth Model

The truth model consists of the differential equations that model both the target motion and the gimbal dynamics. The matrix expression for the truth model is shown in Eq (8). The formulation of this expression is

$$\begin{bmatrix} \dot{C} \\ \dot{\eta}_p \\ \ddot{\eta}_p \\ \ddot{\eta}_p \\ \dot{\chi}_1 \\ \ddot{\chi}_1 \\ \dot{\chi}_2 \\ \ddot{\chi}_2 \end{bmatrix} =
 \begin{bmatrix} 0 & -700 & 0 & 0 & [700 \operatorname{ARCTAN}(\chi_2/\chi_1)] \\ 0 & 0 & 1 & 0 & 0 \\ 0 & 0 & 0 & 1 & 0 \\ \omega_n^2 & -\frac{700}{18}\omega_n^2 & -\omega_n^2 & -2G_{th} \left[\frac{700}{18}\omega_n^2 \operatorname{ARCTAN}(\chi_2/\chi_1) \right] & 0 \\ 0 & 0 & 0 & 0 & 0 \\ 0 & 0 & 0 & 0 & 0 \\ 0 & 0 & 0 & 0 & 0 \\ 0 & 0 & 0 & 0 & 0 \end{bmatrix} +
 \begin{bmatrix} 0 & 0 \\ 0 & 0 \\ 0 & 0 \\ 0 & 0 \\ 0 & 0 \\ 0 & 0 \\ 0 & 0 \\ 0 & 0 \end{bmatrix} +
 \begin{bmatrix} 0 & 0 \\ 0 & 0 \\ 0 & 0 \\ 0 & 0 \\ 0 & 0 \\ 0 & 0 \\ 0 & 0 \\ 0 & 0 \end{bmatrix} +
 \begin{bmatrix} A_1 \\ A_2 \end{bmatrix}$$

Equation 8

developed in Appendix B. This matrix expression of the truth model is solved by a differential equation solving routine using a variable step size down to 1.0 E-6 seconds. Output is actually provided every hundredth of a second in order to simulate the 100 Hz sample rate of the servo loop. The laser rangefinder is then simulated by sampling the true target position every 0.1 seconds. Similarly, the gimbal rate measurement is simulated by sampling W_{cmd} every 0.01 seconds. Transformation T_4 in Figure 3 also uses W_{cmd} in the equation

$$\text{where } n_m(K+1) = n_m(K) + \Delta TT \cdot W_{cmd} \quad (9)$$
$$K+1 = \Delta TT + t_k$$

to generate n_m . At filter turn on time t_0 , the angle n_m is initialized to zero.

Transformation T_1

In order to utilize a linear Kalman filter as mentioned in Chapter II, the polar coordinate measurements (R_m , \dot{R}_m , n_m , \dot{n}_m) must be transformed into a planar coordinate pseudo-measurements (x_{1m} , \dot{x}_{1m} , x_{2m} , \dot{x}_{2m}). The measurement of range rate \dot{R}_m , and target angle n_m , are not readily available. However, the target angle n_m is provided as was shown in Eq (9), and range rate \dot{R}_m initially can be obtained from a weighted combination of the last three laser range measurements by the equation

$$\dot{R}_m(t_0) = [3R_m(t_0) - 4R_m(t_0 - \Delta T) + R_m(t_0 - 2\Delta T)]/2\Delta T_L \quad (10)$$

where t_0 is the filter turn on time and $\Delta T_L = 0.1$ seconds (Ref 1:39). Subsequently, an estimate of range rate \dot{R}_m is available from the filter. The pseudo-measurement generation can now be expressed as follows:

$$\begin{aligned} x_{1m} &= R_m \cos n_m \\ x_{2m} &= R_m \sin n_m \\ \dot{x}_{1m} &= \dot{R}_m \cos n_m - R_m w_{CMD} \sin n_m \\ \dot{x}_{2m} &= \dot{R}_m \sin n_m + R_m w_{CMD} \cos n_m \end{aligned} \quad (11)$$

The pseudo-measurements are now ready to be processed by the filter.

Kalman Filter Equations

The Kalman filter propagates target position, velocity, and acceleration estimates forward in time up to the next measurement update time. At that point, the estimates are optimally combined with the measurements to provide the new best estimate of target position, velocity, and acceleration. The propagation and update equations are separate processes and are presented accordingly.

Propagation Equations. The propagation process utilizes the state transition matrix (Ref 4:356)

$$A = \begin{bmatrix} 1 & \Delta T & \Delta T^2/2 \\ 0 & 1 & \Delta T \\ 0 & 0 & 1 \end{bmatrix} \quad (12)$$

The estimates are propagated by the matrix equation

$$\hat{x}(t_k + \Delta T) = \begin{bmatrix} \hat{x}_i(t_k + \Delta T) \\ \dot{\hat{x}}_i(t_k + \Delta T) \\ \ddot{\hat{x}}_i(t_k + \Delta T) \end{bmatrix} = A \begin{bmatrix} \hat{x}_i(t_k) \\ \dot{\hat{x}}_i(t_k) \\ \ddot{\hat{x}}_i(t_k) \end{bmatrix}^+ \quad (12)$$

$i=1,2$

where the minus sign designates the estimates just prior to incorporation of the next measurement and the plus sign designates the estimates just after the last update.

Update Equations. Before the estimates can be updated, the appropriate Kalman gains must be computed by the following equations (Ref 2:35):

$$\underline{P}(K+1)^- = A \underline{P}(K)^+ A^T + Q \quad (3 \times 3 \text{ matrix}) \quad (14A)$$

$$\underline{G}(K+1) = \underline{P}(K+1)^- H^T [H \underline{P}(K+1)^- H^T + R]^{-1} \quad (3 \times 2 \text{ matrix}) \quad (14B)$$

$$\underline{P}(K+1)^+ = [I - \underline{G}(K+1) H] \underline{P}(K+1)^- \quad (3 \times 3 \text{ matrix}) \quad (14C)$$

$$K+1 = t_k + \Delta T, \quad K = 0, 1, 2, \dots$$

H can be referred to as the measurement matrix. Since position and velocity are the only pseudo-measurements, H becomes the 2×3 matrix

$$\underline{H} = \begin{bmatrix} 1 & 0 & 0 \\ 0 & 1 & 0 \end{bmatrix} \quad (15)$$

The Kalman gain matrix G is a 3×2 matrix expressed as

$$\underline{G} = \begin{bmatrix} G_{11} & G_{12} \\ G_{21} & G_{22} \\ G_{31} & G_{32} \end{bmatrix} \quad (16)$$

\underline{Q} is a 3x3 matrix describing the covariance of assumed unknown target motion or assumed modeling error. For this case where target acceleration is assumed constant over the sampling interval, target motion can be modeled as follows:

$$\dot{\underline{x}}(t) = \underline{F} \underline{x}(t) + \underline{b} w(t)$$

$$\begin{bmatrix} \dot{x}(t) \\ \dot{v}(t) \\ \dot{a}(t) \end{bmatrix} = \begin{bmatrix} 0 & 1 & 0 \\ 0 & 0 & 1 \\ 0 & 0 & 0 \end{bmatrix} \begin{bmatrix} x(t) \\ v(t) \\ a(t) \end{bmatrix} + \begin{bmatrix} 0 \\ 0 \\ 1 \end{bmatrix} w(t) \quad (17)$$

where $w(t)$ is a zero mean, Gaussian, random white noise sequence modeling the unknown change in acceleration. For a discrete time simulation

$$E[w(t)w(s)] = q\delta(t-s) \quad (18)$$

where q is considered the strength of the white noise sequence or a measure of the uncertainty in the target model. If the target acceleration is constant then $q = 0$, otherwise q would increase appropriately. The covariance equation for the target model would be

$$\underline{P}(t_k + \Delta T) = \underline{A} \underline{P}(t_k) \underline{A}^T + \int_0^{\Delta T} \underline{A} \underline{b} q(\tau) \underline{b}^T \underline{A}^T d\tau \quad (19)$$

Approximating the integration process with an Euler integration for a discrete time system yields Eq (14A) where

$$\underline{Q} = \underline{A} \underline{b} \underline{q} \underline{b}^T \underline{A}^T \Delta T$$

$$= \begin{bmatrix} \Delta T / 4 & \Delta T^3 / 2 & \Delta T^2 / 2 \\ \Delta T^3 / 2 & \Delta T^2 & \Delta T \\ \Delta T^2 / 2 & \Delta T & 1 \end{bmatrix} q \Delta T \quad (20)$$

\underline{Q} then is a function of the sampling interval ΔT and q the uncertainty of the target acceleration profile. Fitts (Ref 4:356-357) elected to normalize the \underline{Q} , \underline{R} , and \underline{P} matrices and ignore products of ΔT since $\Delta T \ll 1$. Therefore \underline{Q} reduces to

$$\underline{Q} = \begin{bmatrix} 0 & 0 & 0 \\ 0 & 0 & 0 \\ 0 & 0 & Q_{33} \end{bmatrix} \quad (21)$$

This approximation is logical since target acceleration is the only state that was assumed constant over the interval. Through experimentation, Fitts determined $Q_{33} = 1.0$ to be optimal against maneuvering targets when $\Delta T = 0.1$ seconds (Ref 2:71).

\underline{R} is the measurement covariance matrix. The values expressed in it are approximated by processing the covariance of the laser rangefinder and the gimbal rate sensor through Eq (11), to get

$$\underline{R} = \begin{bmatrix} 1 & 0 \\ 0 & R_{22} \end{bmatrix} \quad (22)$$

Since the velocity measurements are dependent on estimated range rate, the R_{22} term cannot be explicitly calculated. Through experimentation, $R_{22} = 16$ was found to be optimal (Ref 5:B35).

\underline{P} is the covariance matrix of the estimate errors. Taking into account that $R_m(t_0)$ and $\dot{R}_m(t_0)$ are correlated by Eq (10), and that the pseudo-measurements are correlated indirectly by Eq (11), Fitts calculated

$$\underline{P}(t_0) = \begin{bmatrix} 1 & 1.5/\Delta T_L & 0 \\ 1.5/\Delta T_L & 6.5/\Delta T_L^2 & 0 \\ 0 & 0 & 1 \end{bmatrix} \quad (23)$$

where ΔT_L is the sampling period of the laser rangefinder (Ref 4:361).

Eq (23) is derived using the orientation of the X_1 axis at filter turn on and the definition of the covariance of a zero mean process.

Define $\underline{z} = \begin{bmatrix} \bar{R}_m - E(R_m) \\ \dot{\bar{R}}_m - E(\dot{R}_m) \end{bmatrix} = \begin{bmatrix} z_1 \\ z_2 \end{bmatrix} \quad (24)$

then

$$P_0 = \begin{bmatrix} \underline{z} \underline{z}^T & 0 \\ 0 & 1 \end{bmatrix} \quad (25)$$

Now, from Eq (10), assuming $R_m(t_0)$, $R_m(t_0 - \Delta T)$, and $R_m(t_0 - 2\Delta T)$ are independent and $E\{z_1^2\} = E[(R_m - E\{R_m\})^2] = 1$ (because of the normalization with the R matrix, $R_{11} = 1$).

$$E\{z_1 z_2\} = E\{z_1^2\} 1.5/\Delta T_L = 1.5/\Delta T_L \quad (26)$$

$$E\{z_2^2\} = E\{(1.5/\Delta T_L)^2 z_1^2 + (2/\Delta T_L)^2 z_1^2 + \quad (27)$$

$$(1/2\Delta T_L)^2 z_1^2\} = (6.5/\Delta T_L^2) E\{z_1^2\} = 6.5/\Delta T_L^2$$

Once the Kalman gain matrix G is calculated, the estimates and measurements are combined by the formula (Ref 1:33-34)

$$\hat{x}_i(K)^+ = \hat{x}_i(K)^- + \underline{G}(K)[\underline{x}_{im}(K) - \underline{H}\hat{x}_i(K)^-], \quad i=1,2 \quad (28)$$

Transformation T₂

Once the estimates \hat{x}_i are generated by the filter, whether they are updated or propagated estimates, they must be transformed back into polar coordinates to generate the W_{aid} for the gimbals and \dot{R} for the filter. The following equations are used in T_2 to perform this transformation.

$$\begin{aligned}
 \hat{R} &= (\hat{x}_1^2 + \hat{x}_2^2)^{1/2} \\
 \hat{n} &= \text{ARCTAN} (\hat{x}_2 / \hat{x}_1) \\
 \dot{\hat{R}} &= (\hat{x}_1 \dot{\hat{x}}_1 + \hat{x}_2 \dot{\hat{x}}_2) / \hat{R} \\
 \dot{\hat{n}} &= (\hat{x}_1 \dot{\hat{x}}_2 - \hat{x}_2 \dot{\hat{x}}_1) / \hat{R}^2 \\
 \ddot{\hat{n}} &= (\hat{x}_1 \ddot{\hat{x}}_2 - \hat{x}_2 \ddot{\hat{x}}_1) / \hat{R}^2 - 2 \dot{\hat{n}} \dot{\hat{R}} / \hat{R}
 \end{aligned} \tag{29}$$

Transformation T_3

Filter estimates of gimbal rate and acceleration are used in T_3 to generate W_{aid} as discussed in Chapter II. Eqs (6) and (7) are restated here:

$$W_{\text{aid}}(K) = \hat{n}(K) + G_A \ddot{\hat{n}}(K) \tag{30}$$

where $G_A = 2\zeta/W_n + (3.5/2\pi)\Delta TT$ (31)

W_{aid}

From a close look at Figure 3, it can be seen that W_{aid} is dependent on W_{cmd} , which itself is generated by the sum of W_{aid} and W_A . It is important to note that there are three possible methods of handling this loop in the system.

Delayed. A conventional method of handling it is to generate a new W_{cmd} with the W_{aid} that was calculated using the last W_{cmd} . This implies an inherent computational delay in the system and is the method normally implemented in hardware. In equation form

$$W_{cmd}(K+1) = W_A(K+1) + W_{aid}(K)^+ \quad (32)$$

The sequence of events for this case would be as follows:

1. Filter updates at K and generates $W_{aid}(K)^+$
2. Truth Model integrates from K to K+1 using $W_{aid}(K)^+$
3. Filter propagates from K to K+1
4. Filter updates at K+1 and generates $W_{aid}(K+1)^+$

Instantaneous. The second method of handling this system loop is to assume a zero computational delay. This implies that the filter equations could generate the W_{aid} instantaneously. This is an ideal situation although not practically implementable. In equation form

$$W_{cmd}(K) = W_A(K) + W_{aid}(K)^+ \quad (33)$$

The sequence of events for this case is as follows:

1. Filter updates at K and generates $W_{aid}(K)^+$
2. Truth Model integrates from K to K+1 using $W_{aid}(K)^+$
3. Filter propagates from K to K+1
4. Filter updates at K+1 and generates $W_{aid}(K+1)^+$

Predicted. The third method of handling the system loop is to use the filter to propagate the estimates forward which would generate a prediction for W_{aid} . This method is an attempt to solve the computational delay and approach the performance of the "ideal" instantaneous method. In equation form

$$W_{cmd}(K) = W_A(K) + W_{aid}(K)^- \quad (34)$$

The sequence of events would be as follows:

1. Filter updates at K and generates $W_{aid}(K)^+$
2. Filter propagates from K to $K+1$ and generates $W_{aid}(K+1)^-$
3. Truth Model integrates from K to $K+1$ using $W_{aid}(K)^-$
4. Filter updates at $K+1$ and generates $W_{aid}(K+1)^+$

In this analysis, all three methods are considered.

The results are presented in Chapter V.

IV. Design Improvements

The simulation discussed in Chapter III must now be modified to produce the pseudo-range measurements so as to increase the sampling rate. Five basic modifications are used along with a modification simulating actual range measurements being available every 0.01 seconds. This latter modification is performed so as to determine the optimum improvement possible. This chapter will first discuss what changes are made in the basic equations in order to accept the pseudo-range measurements. Then, the modifications are presented with supporting rationale. Finally, the scenarios used to test the changes are discussed.

Filter Changes

Several of the modifications to be mentioned were incorporated into the simulation with no change to the filter equations. Upon inspection of the output, a sinusoidal response was found to be corrupting the system response as seen in Figure 5 (a plot of tracking error versus time). A steady-state perturbation analysis (Appendix C) revealed that the inherent errors in the pseudo-range measurements were being amplified through the propagation process until a new accurate laser range measurement could be incorporated. Therefore, the filter had to be altered to make it rely more heavily on the angle and angular rate measurements and much less on the pseudo-range

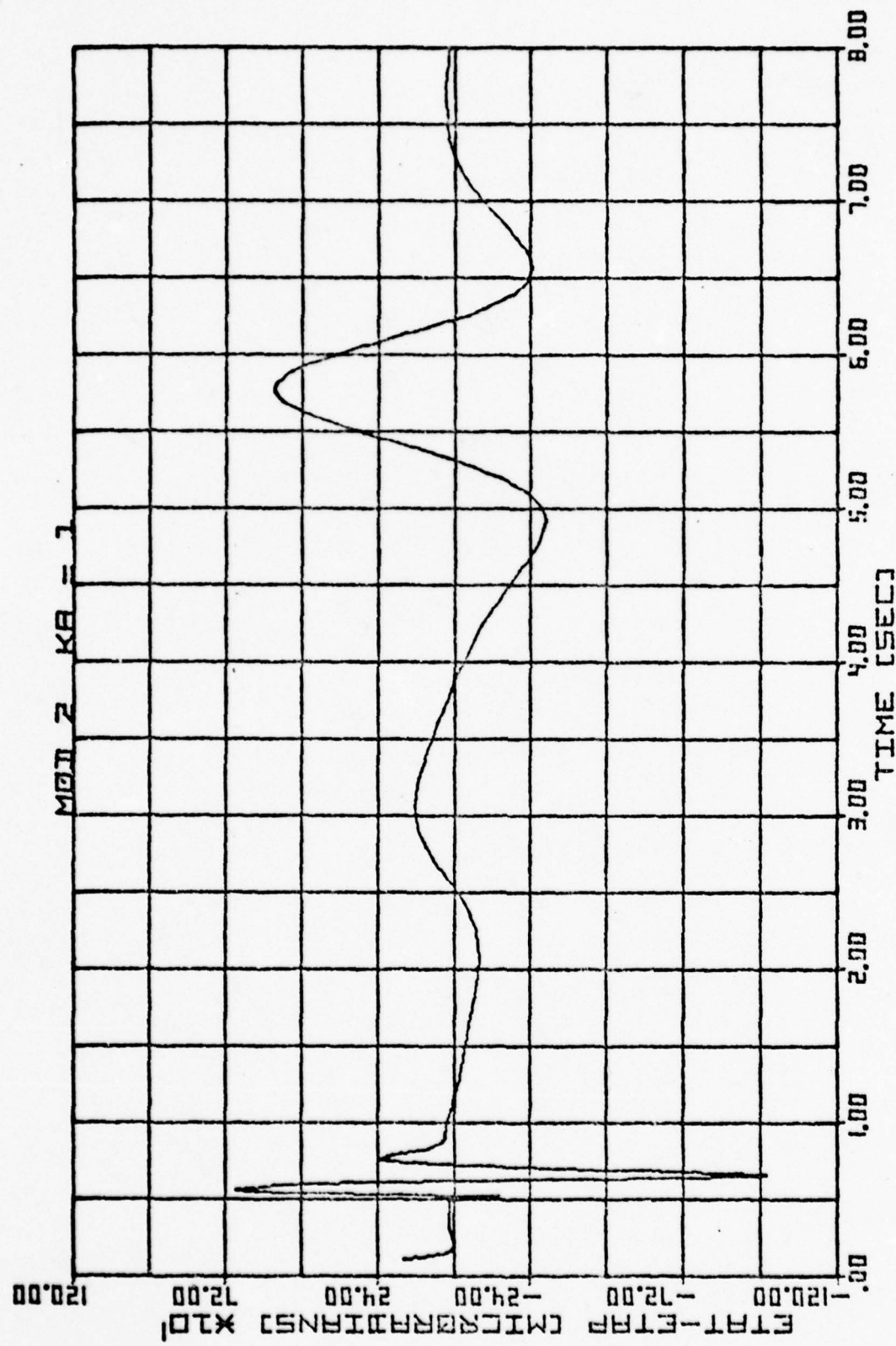


Fig. 5. Aided at 0.01 second rate by Modification Two, H matrix unchanged - Sinusoidal corruption, Scenario One.

measurements. The method chosen to do this was to alter the H matrix during the incorporation of the pseudo-range measurements from

$$\underline{H} = \begin{bmatrix} 1 & 0 & 0 \\ 0 & 1 & 0 \end{bmatrix} \quad (35)$$

to

$$\underline{H} = \begin{bmatrix} 0 & 0 & 0 \\ 0 & 1 & 0 \end{bmatrix} \quad (36)$$

The H_{11} term was set to zero, thereby ignoring the pseudo-measurements of target position x_{1m} , x_{2m} until the next laser range measurement could be taken. This had to be done for all modifications where pseudo-range information was used. The sinusoidal corruption was eliminated when this change was made to the algorithm.

Another change to the filter equations is the rescaling of the Q matrix. When the sampling rate is increased the Q matrix must be scaled accordingly, as shown by Eq (20). For this study Q_{33} is changed from 1.0 to 0.1. A study of Q_{33} versus RMS pointing error performance was accomplished. The results of this analysis are presented in the next chapter.

Modification One

In modification one, range is assumed to be constant over the sample interval. This modification is the simplest

to implement, and demonstrates the feasibility of the overall study.

Modification Two

Modification two propagates the last laser range measurement forward by use of the internally generated estimate of range rate. Recall that this estimate of range rate is recomputed every 0.01 seconds by the filter. This method was scrutinized for possible stability problems due to the likelihood that errors in the estimate of range rate could propagate larger errors. This method did result in a rather large sinusodial type response until the change to the H matrix was made. This change eliminated the problem.

Modification Three

The possible instability of the last method was the motivation for modification three. In this method, range is propagated by the estimated range rate obtained at the last laser range measurement time. By holding this estimate constant over the 0.1 second interval, the propagation of errors was minimized. However the sinusoidal response was still present until the change was again made to the H matrix.

Modification Four

This modification simulates actual laser range measurements every 0.01 seconds. The motivation for this method was to determine the best possible performance available

from increasing the sample rate and to use this method as a comparison for the others. Also, the results from this modification demonstrate that the sinusoidal response obtained by using the other methods was due to the propagation of errors and not due to increasing the computation rate of the filter equations since this modification showed no sinusoidal corruption with the H matrix unchanged.

Modification Five

The motivation for this method again comes from the instability problem of modification two. In this method, range is propagated by a constant range rate obtained by a linear combination of the last three laser range measurements. This modification has a unique problem when noise is introduced into the system. When this is done, the differenced range rate becomes more noisy than the estimated range rate. Again, the sinusoidal corruption disappeared when the H matrix was changed.

Modification Six

This method of generating pseudo-range measurements is simply to use the estimated range available from the filter. Initially, this method was ignored because it was the method tried by Fitts (Ref 1:77) which reportedly demonstrated poor performance. However, Fitts considered only flyby type scenarios. Once the results of Modification Two demonstrated the capabilities of this concept

against maneuvering targets, the use of the estimated range was again considered. This method also required the H matrix to be changed.

All of the modifications mentioned, as well as the altering of the H matrix, are handled by the update equations of the filter. Appendix D contains a listing of these changes as they are implemented in the computer program. Table I is a listing of the modifications.

Table I
Listing of Modifications

Modification	Method used to Generate
One	Range held constant from last measurement.
Two	Range propagated by estimated range rate.
Three	Range propagated by constant range rate obtained from last estimate.
Four	Laser range measurements every 0.01 seconds.
Five	Range propagated by constant range rate obtained from differenced range measurements.
Six	Estimated Range.

Scenarios

Initially, a straight flyby scenario was used as shown in Figure 6. This scenario is very similar to that used by Fitts (Ref 1,2,3) and was chosen so that a comparison could be made to insure that the results agree. Table II

presents a listing of range, range rate, and angular rate versus time for scenario one.

TABLE II
SCENARIO ONE

Time (sec)	Range (meters)	Range Rate (meters/sec)	Angular Rate (radians/sec)	Acceleration (G-s)
0.5	5590	-984	.0320	0
1.0	5099	-981	.0385	0
1.5	4610	-976	.0471	0
2.0	4123	-970	.0588	0
2.5	3640	-961	.0755	0
3.0	3162	-949	.1000	0
3.5	2693	-928	.1379	0
4.0	2236	-894	.2000	0
4.5	1803	-832	.3077	0
5.0	1414	-707	.5000	0
5.5	1118	-447	.8000	0
6.0	1000	-20	1.000	0
6.5	1118	447	.8000	0
7.0	1414	707	.5000	0
7.5	1803	832	.3077	0
8.0	2236	894	.2000	0

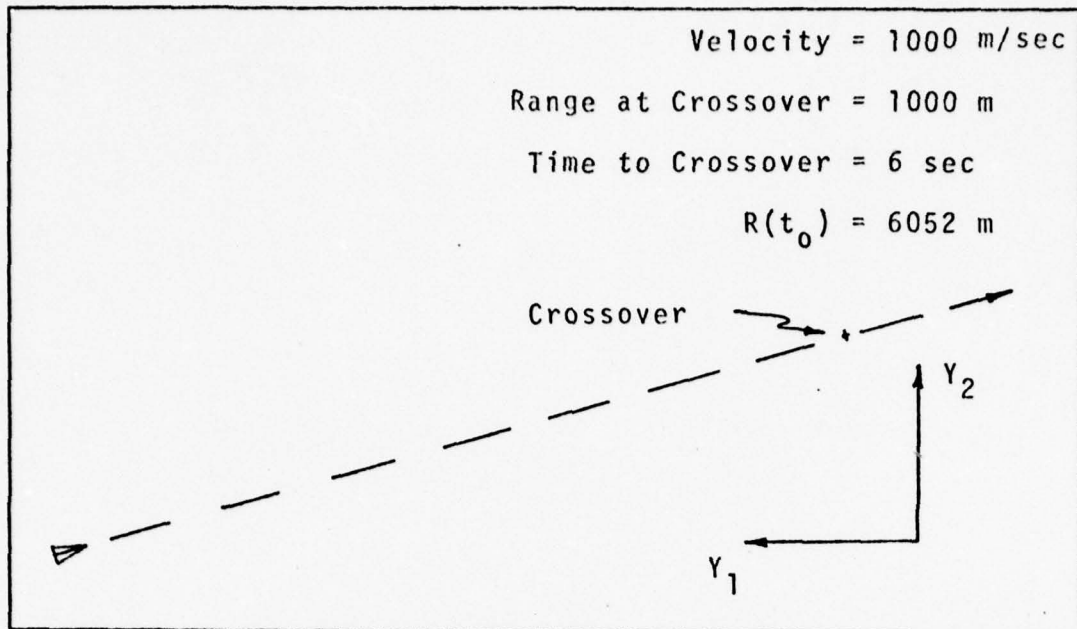


Fig. 6. Scenario One, Straight Flyby

The second scenario used is almost identical to the first except that at crossover the target enters a constant radius, constant velocity turn around the tracker as shown in Figure 7. This scenario was chosen in order to determine

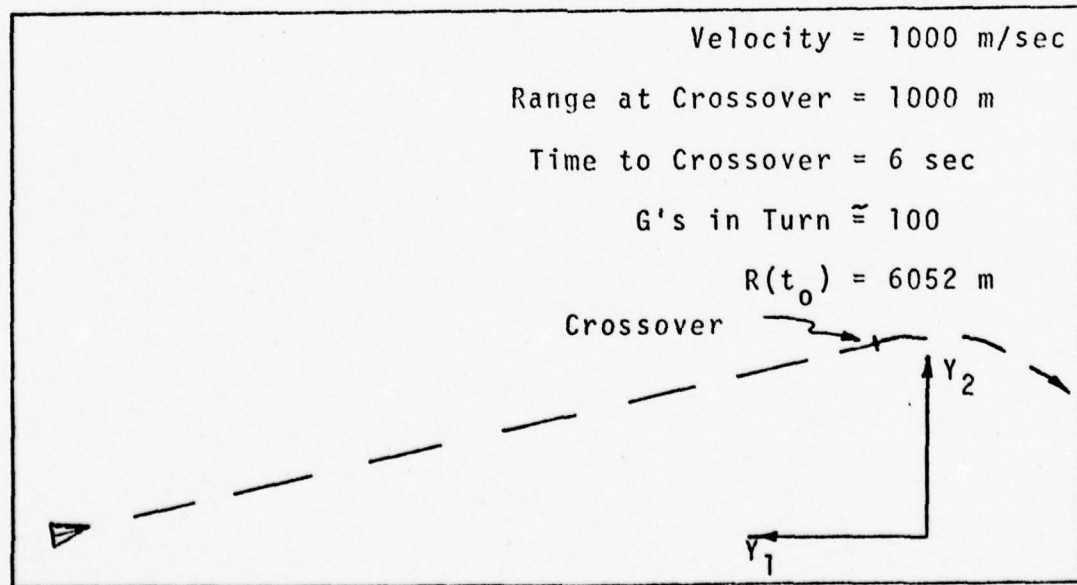


Fig. 7. Scenario Two, Flyby to 100 G Turn

how well this system performs against an unmodeled acceleration. The acceleration in the turn is approximately 100 G's and definitely accentuates any difficulties in handling unmodeled accelerations.

These first two scenarios were used to select which modification performed the best. Once this was determined, the best modification was tested against the following, more realistic, scenarios.

Scenario three is a reduced version of scenario two, with respect to velocity and G forces, as shown in Figure 8. Velocity is held constant at 300 meters/second and at crossover the target enters approximately a 9.2 G turn. Table III is a tabulation of range, range rate, angular rate, and acceleration versus time for scenario two and three.

Figure 9 illustrates scenario four which is an adaptation of scenario one. Velocity is held constant at 1000 meters/second until $t = 4.5$ seconds. At that time, the target undergoes a deceleration modeled by the drag on a 90 kilogram missile with a radius of 15 centimeters and a coefficient of drag $C_D = .25$. The time history of scenario four is presented in Table IV.

Scenario five begins as in scenario one until $t = 2$ seconds. At that time, the target enters approximately a 16 G turn toward the tracker until it is pointed approximately at the tracker. The target then rolls out and

Velocity = 300 m/sec

Range at Crossover = 1000 m

Time at Crossover = 3 sec

G's in turn = 9.2

$R(t_0) = 1345$ m

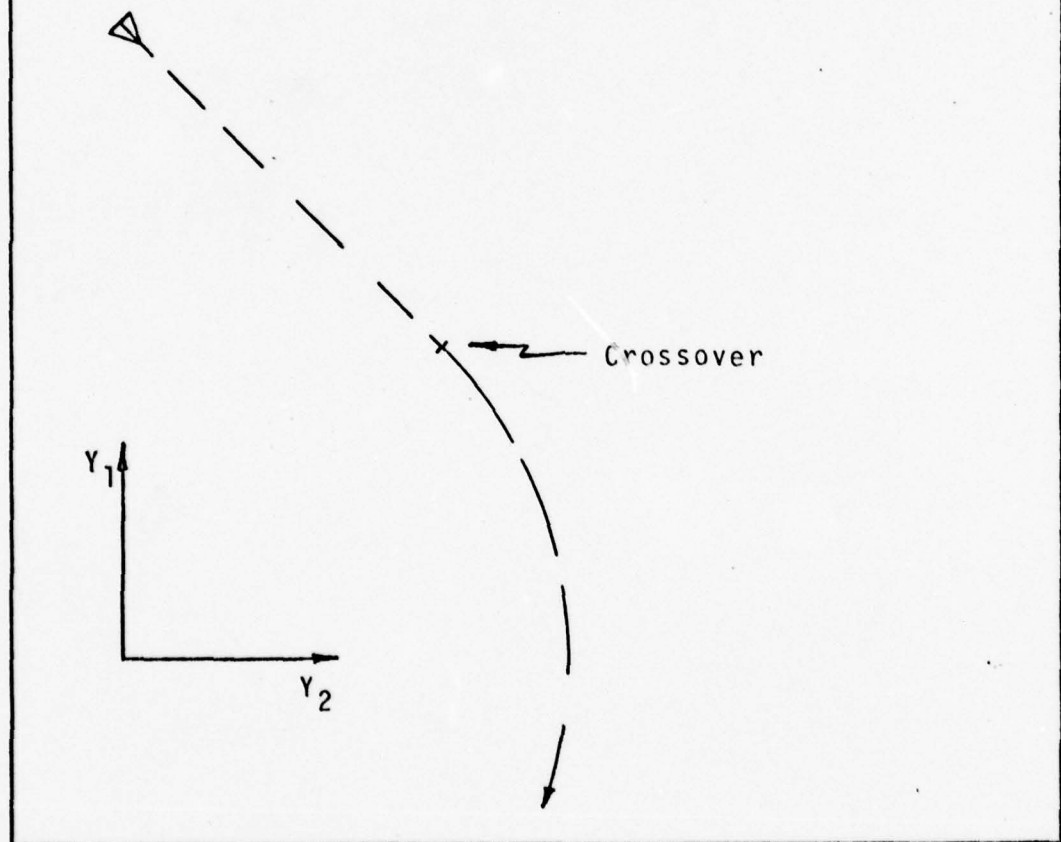


Fig. 8. Scenario Three, Slower Flyby to 10 G Turn

TABLE III

SCENARIO TWO

Time (seconds)	Range (meters)	Range Rate (meters/sec)	Angular Rate (radians/sec)	Acceleration (G's)
0.5	5590	-984	.0320	0

SAME DATA AS SCENARIO ONE

***** constant G turn (approximately)

6.0	1000	-20	1.0000	102
6.5	990	-20	1.005	102
7.0	980	-19	1.005	102
7.5	970	-19	1.005	102

SCENARIO THREE

Time (seconds)	Range (meters)	Range Rate (meters/Sec)	Angular Rate (radians/Sec)	Acceleration (G's)
0.5	1250	-180	.1920	0
1.0	1165	-154	.2206	0
1.5	1097	-123	.2495	0
2.0	1044	-86	.2752	0
2.5	1011	-44	.2934	0
3.0	1000	-1.8	.3000	9.2
3.5	999	-1.8	.3004	9.2
4.0	998	-1.8	.3007	9.2
4.5	997	-1.8	.3009	9.2

experiences the same deceleration mentioned in scenario four. This scenario is illustrated in Figure 10. The time history for this scenario is presented in Table V.

It is important to note that for scenarios two, three, four and five the conversion from one acceleration profile to another was modeled as an instantaneous change. Although this instantaneous change in profiles is not realistic, it again accentuates the response characteristics of the system.

Velocity = 1000 m/sec
 Range at Crossover = 1000 m
 @ $t = 4.5$ $D = -\frac{1}{2} \rho C_D A V^2$
 $C_D = .25$ $W = 90 \text{ kg}$
 radius = 15 cm deceleration = 7 G's

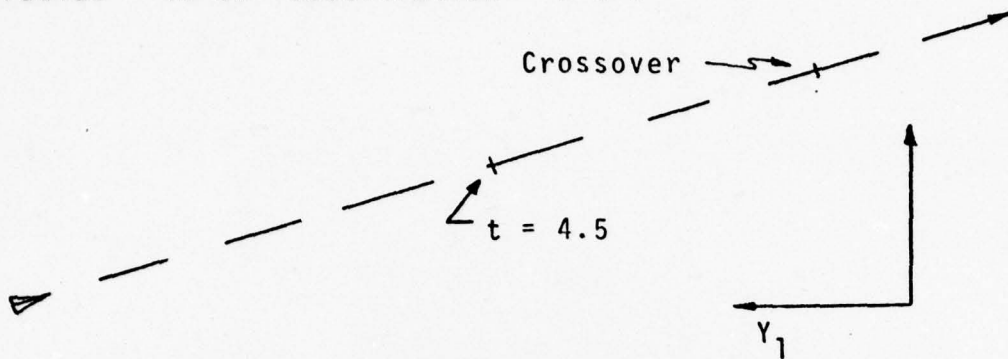


Fig. 9. Scenario Four, Flyby to Deceleration

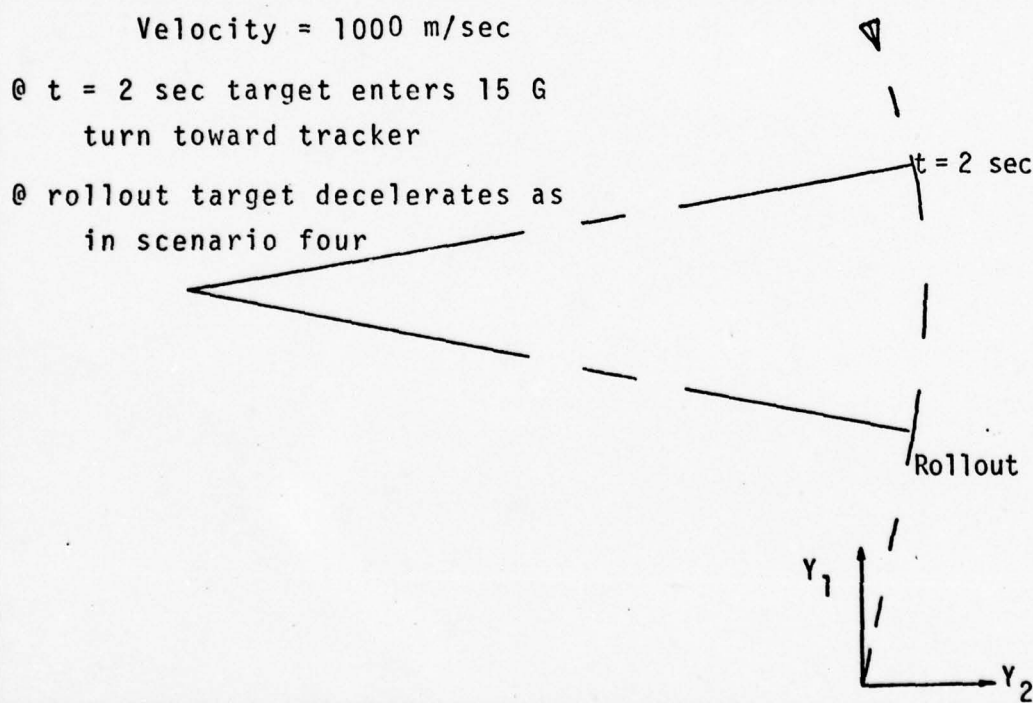


Fig. 10. Scenario Five, Flyby to Pursuit to Deceleration

TABLE IV

SCENARIO FOUR

Time (sec)	Velocity (m/sec)	Range (meters)	Range Rate (m/sec)	Angular Rate (rad/sec)	Acceleration (G's)
0.5	1000	5590	-984	.0320	0

SAME DATA AS SCENARIO ONE

***** decelerate *****

4.5	1000	1803	-832	.3072	-7.8
5.0	962	1421	-683	.4760	-7.2
5.5	927	1135	-439	.7193	-6.7
6.0	896	1003	-73.4	.8896	-6.3
6.5	866	1062	292	.7675	-5.9
7.0	838	1271	517	.5190	-5.5
7.5	812	1559	623	.3339	-5.2
8.0	787	1884	667	.2219	-4.9

TABLE V

SCENARIO FIVE

Time (sec)	Range (meters)	Range Rate (m/sec)	Angular Rate (rad/sec)	Velocity (m/sec)	Acceleration (G's)
0.5	5590	-984	.0320	1000	0
1.0	5099	-980	.0385	1000	0
1.5	4610	-976	.0471	1000	0
***** 15.6 G turn toward tracker *****					
2.0	4123	-970	.0585	1000	15.6
2.5	3635	-981	.0533	1000	15.6
3.0	3142	-988	.0454	1000	15.6
3.5	2646	-996	.0327	1000	15.6
4.0	2147	-999	.099	1000	15.6
***** rollout and decelerate *****					
4.5	1652	-973	.0004	973	-7.4
5.0	1174	-938	.0009	938	-6.9
5.5	713	-906	.0008	906	-6.4

V. Results Analysis

This chapter presents the basic results of the study with an analysis of what the results signify. Initially, an analysis of the parameter Q_{33} versus RMS tracking error is presented in order to determine the optimum value of Q_{33} . Next, the results of using a computational delay, instantaneous update, and prediction update in generating W_{aid} are presented. Subsequently, with Q_{33} set at the optimum value and the best method of generating W_{aid} used, the results indicating that Modification Six demonstrated the best performance are presented. Finally, a comparison of the results from the faster 0.01 second sample rate pseudo-range system versus the slower 0.1 second sample rate system is presented.

The measurement noise in this simulation was modeled as a white, Gaussian, zero mean sequence. The standard deviation in range is 5 meters and in pointing angle, 10 micro-radians. The same sequence was used for each simulation.

Q_{33} Analysis

Figure 11 is a graph of Q_{33} versus RMS tracking error. Curves 1 and 2 represent the time averaged RMS tracking performance during 1.5 seconds of the 100 G turn in scenario two, with and without noise respectively. From these curves a value of $Q_{33} = 1.0$ appears to be optimal. However, curves 3 and 4 represent the RMS tracking performance during the non-accelerating portion of scenario two, with and without noise

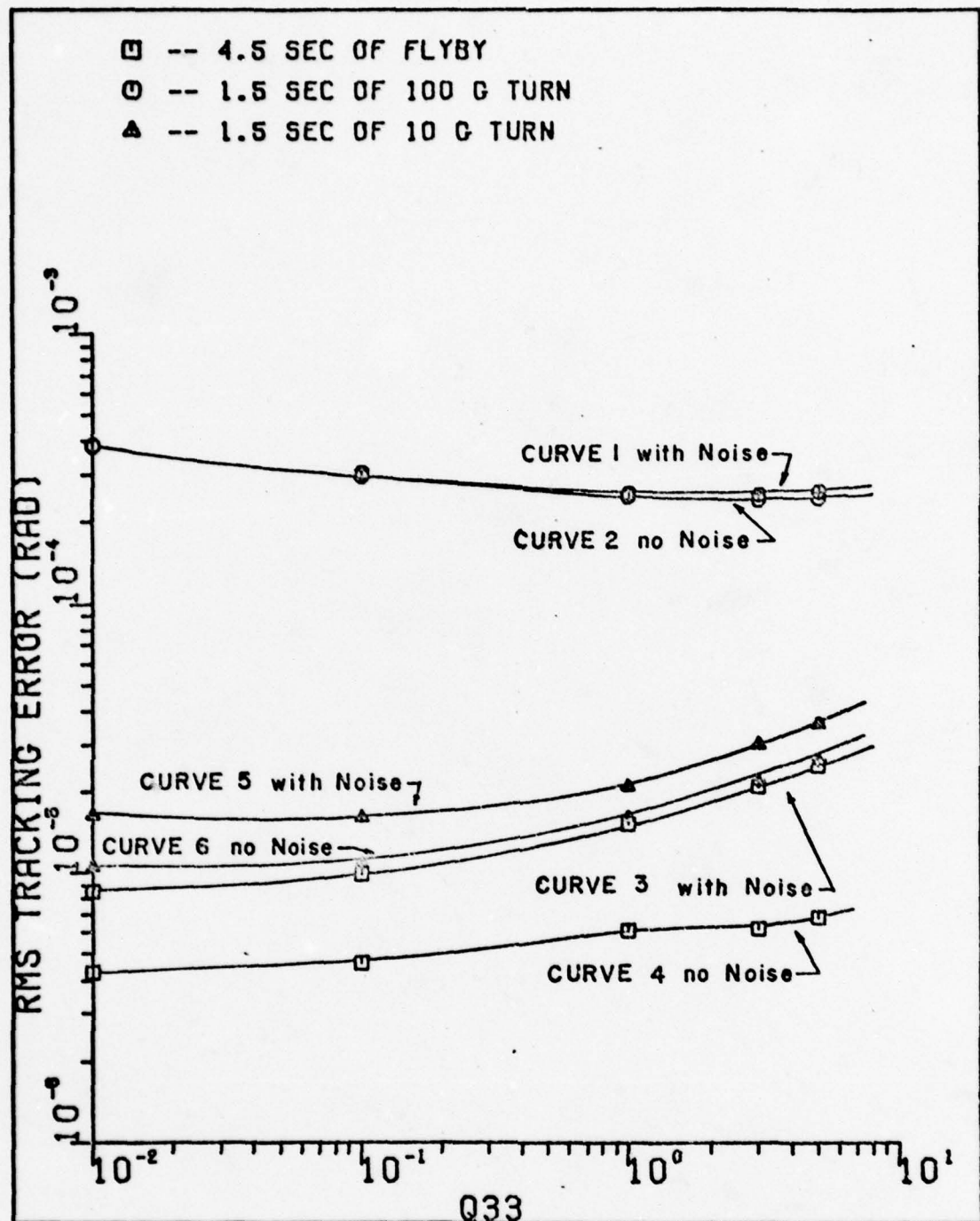


Fig. 11. Q_{33} Analysis

respectively. These curves indicate that Q_{33} should be set as low as possible when tracking a non-accelerating target. On the other hand, curves 5 and 6, which represent the performance during 1.5 seconds of the 10 G turn in scenario three, indicate a Q_{33} of approximately 0.01 to be optimal. Since actual target motion is unknown, a tradeoff must be made between $Q_{33} = 0.0$ and 1.0, because to choose either one exactly would cause substantial errors if the target motion was just the opposite. From analysis of Figure 11, $Q_{33} = 0.1$ was chosen as the optimum tradeoff value to handle both highly accelerating and non-accelerating targets. Ideally, the value of Q_{33} should be set according to the bandwidth of the random or unknown target motion as indicated by Fitts (Ref 3:73).

Generating W_{aid}

The results of the discussion in Chapter III about the various techniques of generating W_{aid} are shown in Figures 12 through 26. (Note: Figures 12 through 67 are contained in Appendix E and are plots of tracking error versus time.) Table VI gives a listing of the RMS and peak tracking errors for each technique. Originally, Modification Two was used for this analysis. Later, Modification Six was compared to deduce what conclusions could be drawn for it. A close observation of Figures 12 through 26 and of Table VI yields the following:

TABLE VI
Performance of Techniques
Used to Generate Waid

Modification Two	Peak Error (microradians)	RMS Error (microradians)		
		1.5 - 6 sec	6-8 sec	1.5 - 8 sec
**** Scenario One ****				
Delayed	-35.5	9.6	13.4	10.7
Instantaneous	20	4.6	9.1	6.3
Prediction	15.7	4.4	7.0	5.3
**** Scenario Two ****				
Delayed	531.9	9.5	296	149.4
Instantaneous	533.9	4.6	297	149.6
Prediction	527.0	4.4	294	147.8
**** Scenario Five ****				
Delayed	96.2			26.9
Instantaneous	82.0			28.0
Prediction	95.4			26.8
Modification Six				
**** Scenario One ****				
Delayed	-32.8	8.2	12.8	9.7
Instantaneous	15.1	2.7	6.5	4.2
Prediction	15.3	3.8	6.6	4.8
**** Scenario Two ****				
Delayed	388.9	8.1	207	104.3
Instantaneous	390.4	2.7	208	104.7
Prediction	406	3.9	215	108.3

1. When Modification Two was used against scenario one, the predicted update technique showed better overall performance in terms of peak and RMS errors than the computational delay or instantaneous update technique. However, when Modification Six was used, the instantaneous technique demonstrated the best performance.
2. When Modification Two was used against scenario two, the predicted update technique was again superior. On the other hand, Modification Six showed mixed results. The computational delay technique provided slightly lower peak and RMS errors during the 10 G turn. Whereas, the instantaneous technique was substantially better in the unaccelerated portion of the trajectory than the other two techniques.
3. Against scenario five, the results are inconclusive. Figures 18 through 20 show no appreciable difference. For this reason, Modification Six was not compared against scenario five.

From the above results, it appears that the predicted update technique improves the tracking performance of Modification Two over that obtained using the "ideal" instantaneous update technique. However, when Modification Six was compared, the instantaneous update technique provided the best overall performance. Throughout the remainder of this study the instantaneous update technique was used.

Modification Selection

The five different methods of generating the pseudo-range measurement were used to track the target modeled by scenario two. Figures 27 through 36 illustrate the tracking performance attained by each method with and without noisy measurements.

A comparison of Figures 28, 30, 32, 34, and 36 show that noise has relatively the same effect on each modification with the exception of Modification Five as predicted in Chapter IV. Noise in the measurements is propagated more by the differenced range rate expression than by any of the other methods.

A comparison of Figures 27 through 36 and of the tabulated data in Table VII, clearly shows Modification Six (using the estimated range) provides the best overall tracking performance.

Performance Comparison

This section presents a compilation of the most significant results of this study. The results from scenarios one, two, and five are analyzed here. Table VIII provides a tabulation of peak and RMS tracking errors used in making the comparisons.

Scenario One. Figure 37 illustrates the tracking error obtained when a conventional pointing and tracking system is used to track target motion modeled by scenario one. Peak tracking error is 927 microradians with the RMS tracking error being 492 microradians. Figure 38 illustrates the performance obtained when the 0.1 second Aided Track system is used. Peak error is reduced to a maximum value of 8.25 microradians. RMS tracking error is also reduced to 2.75 microradians.

TABLE VII

Performance of Modifications Against Scenario Two

Modification	Peak Error (microradians)	RMS Error (microradians)	Flyby	100 G Turn	Overall
One	533.0	26.1	286.6		145.7
One with Noise	552.3	36.9	295.5		151.6
Two	533.9	4.6	297.7		149.6
Two with Noise	566.6	11.3	305.6		153.8
Three	528.8	4.3	294.9		148.3
Three with Noise	561.6	11.1	302.8		152.4
Five	571.2	4.4	313.0		157.5
Five with Noise	599.8	17.8	322.8		162.8
Six	390.4	2.67	208.4		104.7
Six with Noise	385.5	6.77	207.8		104.6

Flyby - 1.5 to 6 seconds

100 G turn - 6 to 8 seconds

Overall - 1.5 to 8 seconds

Time average RMS calculations were begun 1.0 seconds after filter was activated to allow for transients to die out.

Results shown in Figure 39 demonstrate the best possible performance attainable by the system. These were obtained using Modification Four. The peak error is increased slightly from that shown in Figure 38 to a value of 9.61 microradians. The RMS tracking error is also increased to 3.3 microradians. This demonstrates the degradation in performance mentioned by Fitts when the sample rate is increased (Ref 1:91,97). However, the flyby scenario is a constant velocity, zero acceleration model. The filter propagates a constant acceleration over the sampling interval. Therefore, if Q_{33} and P_{33} are set to zero, then the filter model matches the target model. Figures 40 and 41 show that when this is done, the degradation is no longer present. On the other hand, the faster system shows no improvement over the slower system other than eliminating the estimation oscillations.

Figure 42 illustrates the performance obtained when Modification Six is used. Peak tracking error is increased even more to 15.2 microradians and the RMS tracking error to 4.23 microradians. This increased degradation is due to the use of the pseudo-range measurements.

Scenario Two. Figures 43 through 48 illustrate the results obtained when target motion was modeled by scenario two. A close look at Figure 43 clearly shows that a conventional unaided pointing and tracking system produces essentially zero tracking error during the 100 G, constant radius, constant velocity turn. On the other hand, Figures

44 through 46 demonstrate the fact that any aiding process results in relatively large errors during this same 100 G turn. This is due to the basic filter model assuming constant acceleration over the sample interval, which is not true in this case. However, aiding practically eliminates the large tracking error prior to the 100 G turn as seen in Figure 43.

A comparison of Figure 44 and 45 shows that a definite improvement in the tracking performance of the 0.1 second system during the 100 G turn is possible by increasing the sampling rate of the system. Figure 45 however, is a graph of the tracking performance of the optimal modification using actual laser rangefinder measurements every 0.01 seconds. A comparison of Figure 44 and 46 illustrates that the use of pseudo-range measurements to increase the sampling rate still results in an improvement. The peak tracking error during the 100 G turn is reduced from 699 microradians in Figure 44 to 390 microradians in Figure 46. Similarly, the RMS tracking error during the 100 G turn is reduced from 369 microradians for the unmodified case to 208 microradians for the system using Modification Six.

Figures 47 and 48 show the effect noisy measurements have on the 0.1 second system and the Modification Six system respectively. Both appear to be affected to about the same degree.

Another interesting result can be seen by comparing the RMS tracking errors for the non-accelerating portion

(that portion prior to crossover) of scenario two shown in Table VIII. The 0.1 second Aided Track system has an RMS error of 2.04 microradians for this portion of the trajectory; whereas, the 0.01 second Modification Four system has only a 1.88 microradian RMS error. This is in contradiction to the degradation prediction found when the entire trajectory of scenario one was considered. However, Modification Four uses actual laser rangefinder measurements. When the pseudo-range measurements in Modification Six are used, the RMS tracking error increases up to 2.67 microradians. The primary differences between Modification Four, Modification Six, and the unmodified systems can be seen by comparing Figures 38, 39, and 41 from scenario one and Figures 44, 45, and 46 from scenario two. Modification Four totally eliminates the range correction oscillations in the tracking error curves seen in the unmodified system and the Modification Six system.

Scenario Five. The results obtained when target motion was modeled by the more realistic scenario five are depicted in Figures 49 through 51. The tracking performance of a conventional unaided system is shown in Figure 49. The jumps in the curve at 2.0 seconds and 4.4 seconds are from the 16 G turn toward the tracker and the deceleration model respectively. The small jump at 5.0 seconds is due to the target reentering the 16 G turn profile momentarily because of a simulation modeling error. The peak tracking

TABLE VIII

Peak and RMS Tracking Errors

Scenario One	Peak error (microradians)	RMS error (microradians)
No aiding	927	492
0.1 second rate	8.25	2.75
Modification Four	9.61	3.3
Modification Two	20	6.34
Modification Six	15.2	4.23

Scenario Two	Peak error	RMS error
		in flyby in turn
No aiding	927 (in flyby)	365 20.9
0.1 second rate	699 (in turn)	2.04 369
with noise	770 (in turn)	8.08 366
Modification Four	356 (in turn)	1.88 277
Modification Two	533.9 (in turn)	4.63 297
Modification Six	390.4	2.67 208.4
with noise	385.5	6.77 207.8

Scenario Five	Peak error	RMS error
No aiding	-100	37
0.1 second rate	240	67
Modification Two	82	28
Modification Six	95	27

error in this case is approximately -100 microradians, which occurs just as the target is rolling out aimed at the tracker. Once the target rolls out and begins to decelerate, the conventional system appears to track very accurately. The overall RMS tracking error is 37 microradians.

The 0.1 second Aided Track system results are shown in Figure 50. This system appears to have great difficulty at close ranges and head-on attacks. The peak tracking error occurs during the head-on attack portion of the trajectory, the value being approximately 240 microradians. The overall RMS tracking error is 67 microradians, which is worse than the conventional system.

The performance obtained by using Modification Six is shown in Figure 51. A substantial improvement over the conventional system and the 0.1 second Aided Track system can be seen. The peak tracking error is only 95 microradians and the RMS error is only 27 microradians. This system tracks the head-on attack much better than the 0.1 second aided system and also handles the 16 G turn better than either the conventional system or the 0.1 second Aided Track system.

The remaining Figures 52 through 67 are provided as supportive material.

VI. Conclusions and Recommendations

Conclusions

1. A value of $Q_{33} = 0.1$ provided the optimum trade-off at the 0.01 second sample rate. This conclusion is consistent with that made by Fitts.
2. Generating W_{aid} by the instantaneous update technique is the "ideal" situation and provided the best performance of the three computational techniques when Modification Six was used. However, the predicted update technique performed almost as well. The instantaneous technique is not realistic in terms of hardware whereas the prediction technique is.
3. Modification Six, which uses the estimate of range from the filter as a pseudo-range measurement, demonstrated the best performance of all the modifications tested.
4. The faster sample rate results in a degradation in performance when tracking simple target motion, such as the flyby scenario, with $Q_{33} = 0.1$ and $P_{33} = 1.0$. However, when $Q_{33} = P_{33} = 0.0$, there is no degradation but there is no improvement either.
5. The faster sample rate does result in an improvement in tracking performance when tracking highly maneuverable targets, especially when the target is attacking the tracker.

Recommendations

1. From the Q_{33} analysis, a tuneable Q_{33} is desirable, dependent upon the maneuverability of the target being tracked.

2. The predicted update technique for generating W_{aid} should be incorporated in the system.

3. When tracking flyby or non-accelerating type targets, the faster sample rate system should not be used.

4. When tracking highly maneuverable targets, Modification Six should be incorporated to improve the performance.

5. In order to implement this algorithm, the following steps should be taken.

a.) Set $\Delta T = 0.01$

b.) Set

$$\underline{H} = \begin{bmatrix} 0 & 0 & 0 \\ 0 & 1 & 0 \end{bmatrix}$$

between laser rangefinder measurements and

$$\underline{H} = \begin{bmatrix} 1 & 0 & 0 \\ 0 & 1 & 0 \end{bmatrix}$$

at laser range measurement time.

Remark: The Kalman gains can still be precomputed and stored, since the \underline{H} matrix is changed in a periodic manner.

c.) Use the estimate of range from the filter as the pseudo-range measurement between the laser range updates.

d.) Use the predicted update technique for generating W_{aid} in order to improve the performance of the system.

Bibliography

1. Fitts, J. M. HAT Aided Tracking Analysis. Report No. P71-2154. Culver City, California: Hughes Aircraft Company, June 1971.
2. Fitts, J. M. A Strapdown Approach to HAT Aided Tracking. Report No. P71-351. Culver City, California: Hughes Aircraft Company, September 1971.
3. Fitts, J. M. HAT Position and Rate Aided Tracking Analysis. Report No. P71-471. Culver City, California: Hughes Aircraft Company, December 1971.
4. Fitts, J. M. "Aided Tracking as Applied to High Accuracy Pointing Systems." IEEE Transactions on Aerospace and Electronic Systems. 9:350-368 (May 1973).
5. User Manual for OSUAPT-3.0 and FROAPT, Report ER-73-R-22-003. Stillwater, Oklahoma: Oklahoma State University, January 1974.

Supplemental Bibliography

Airborne Pointing and Tracking System (U), AFWL-TR-72-124, Kirtland Air Force Base, New Mexico: Air Force Weapons Laboratory: 1972.

Negro, J. E. and Robert R. Wilde, "An Aid for Improving The Precision Pointing of the FTT." Laser Digest, AFWL-TR-72-243, Kirtland Air Force Base, New Mexico: Air Force Weapons Laboratory, December 1972.

Sebesta, H. R. and L. R. Ebbesen. Studies of Advanced Simulation Concepts. Stillwater, Oklahoma: Oklahoma State University, October 1974.

Appendix A

Program Listing: A Rate Aided Pointing and Tracking
Algorithm for a Two-Dimensional System.

THE FOLLOWING IS AN ALPHABETICAL LISTING OF THE VARIABLES USED

STATE TRANSITION MATRIX	
D	DUMMY VARIABLE
DT	• 01 SEC. ITERATION
SETA	• 1 SEC. ITERATION
FETA0	ESTIMATE OF TARGET ANGLE FROM FILTER X1 AXIS
SETA0D	ESTIMATE OF TARGET ANGULAR RATE
SETAERP	ESTIMATE OF TARGET'S ANGLE FROM PSEUDO-INERTIAL FRAME
STAT	MEASURED ANGLE FROM FILTER X1 AXIS
FTAY	ANGLE OF FILTER FRAME FROM PSEUDO-INERTIAL FRAME
STAO	POINTED ANGLE FROM PSEUDO-INERTIAL X1 AXIS
ETAP	POINTER ANGULAR RATE
FTAPD0	POINTER ANGULAR POSITION FROM PSEUDO-INERTIAL X1 AXIS
FTAPD0D	TRUE ANGULAR POSITION FROM PSEUDO-INERTIAL X1 AXIS
ETAT	TRUE ANGULAR RATE
FTATD0	TRUE ANGULAR ACCELERATION
ER	ESTIMATE OF TARGET RANGE
EX1	ESTIMATE OF TARGET POSITION IN FILTER X1 DIRECTION
EX2	ESTIMATE OF TARGET POSITION IN FILTER X2 DIRECTION
FX1D0	ESTIMATE OF TARGET VELOCITY IN FILTER X1 DIRECTION
FX2D0	ESTIMATE OF TARGET VELOCITY IN FILTER X2 DIRECTION
FX1D0D	ESTIMATE OF TARGET ACCELERATION IN FILTER X1 DIRECTION
FX2D0D	ESTIMATE OF TARGET ACCELERATION IN FILTER X2 DIRECTION
FX1T	ESTIMATE OF TARGET POSITION IN PSEUDO-INERTIAL X1 AXIS
FX2T	ESTIMATE OF TARGET POSITION IN PSEUDO-INERTIAL X2 AXIS
FX1D1	ESTIMATE OF TARGET RATE ALONG PSEUDO-INERTIAL X1 AXIS
FX2D1	ESTIMATE OF TARGET RATE ALONG PSEUDO-INERTIAL X2 AXIS
FX1D01	ESTIMATE OF TARGET ACCEL. ALONG PSEUDO-INERTIAL X1 AXIS
FX2D01	ESTIMATE OF TARGET ACCEL. ALONG PSEUDO-INERTIAL X2 AXIS
GA	KALMAN GAIN MATRIX
GA	AIDED TRACK SIGNAL GAIN
H	MEASUREMENT MATRIX
KACCEL	KEYING VARIABLE FOR SELECTING TARGET PROFILE

L	L SWITCH	COUNTING VARIABLE
P	P SWITCH	SWITCHING VARIABLE FOR FILTER
PI	PI	COVARIANCE MATRIX
Q	Q	COMPUTED VALUE FOR PI
R	R	NOISE MATRIX
RMD	RMD	MEASUREMENT NOISE MATRIX
PT	PT	MEASURED RANGE RATE
RTO	RTO	TRUE RANGE RATE
TT	TT	TOTAL TIME
WA	WA	ANGULAR ROTATION RATE GENERATED BY EPROP SIGNAL
WCMD	WCMD	ANGULAR ROTATION RATE PROVIDED BY FILTER
WN	WN	COMMANDED ANGULAR ROTATION RATE
ZETA	ZETA	GIMBAL DYNAMICS PARAMETER (NATURAL FREQUENCY)
0	0	GIMBAL DYNAMICS DAMPING PARAMETER

```

PROGRAM POINT(INPUT,OUTPUT,TAPES,TAPES=OUTPUT,JT)
C JUL, ONLY TAPES AND KALMAN GAINS ON-LINE
C THIS PROGRAM IS A TWO DIMENSIONAL SIMULATION OF THE AIDED TRACK
C ALGORITHM. MEASUREMENTS ARE TAKEN EVERY .1 SECONDS WHILE EVERYTHING
C ELSE IS RUN AT A .01 SECOND ITERATION TIME.
COMMON /PT/ TT,L,DT,DDT,LSWITCH,Y(8),YP(8),WCMD,WAIN,WA,WN,TETA,RT
+ ,PTD,ETAT,ETADD,ETATDD,ETAPDD,PTD,EX1,EX2,EX10,EX20,EX100,EX200,
+ ,ER,EEETA,EEETAD,EEETADD,PI,ETAO,ETAI,KACCEL,EX11,EX21,EX1D1,
+ EX2D1,EX1DD1,EX2DD1,ETAM
+ COMMON /ACCE/ KA,U
EQUIVALENCE (Y(1),C),(Y(2),ETAP),(Y(3),ETAPD),(Y(4),ETAPDD),
+ (Y(5),X1),(Y(6),X1D),(Y(7),X2),(Y(8),X2D)
DIMENSION A(3,3),H(2,3),P(3,3),Q(3,3),R(2,2),G(3,2)
READ*,LSWITCH,TIME,KACCEL,YP(6),YP(9),P(3,3),Q(3,3)
THETA=ATAN(1.0/6.0)
X1=1.0/6.*SIN(THETA)
X2=0.
X1D=-1.0/6.*COS(THETA)
X2D=1.0/6.*SIN(THETA)
DT=.1 $ DDT=.01 $ WN=220 $ PI=ACOS(-1.0)
U=5.0-PI/2.0+THETA
KA=KACCEL
PRINT*, "LSWITCH = ",LSWITCH," TIME = ",TIME," KA = ",KA," X1 = ",X1," X2 = ",X2," X2D = ",X2D," A1 = ",YP(6),
+ " A2 = ",YP(8)," P33 = ",P(3,3)," J33 = ",J33
PRINT* $ PRINT*
PRINT*, "FOR TARGET PROFILE ",KACCEL," THE FOLLOWING RESULTS WERE 0000360
+ RETAINED."
PRINT* $ PRINT*
CALL INITIAL
WRITE(6,5)
FORMAT(/,1X,4HTIME,8X,6HETAERR,13X,9HETAI-ETAT,9X,10HETAD-ETAD,8X000410
+ ,12HETADD-ETADD,6X,9HHAID-WCMD,/)
TT=TT+.01
L=L+1
CALL SCOLVE

```

```

CALL XFORMAT(GT,200) GO TO 50
50 IF(LSWITCH.GT.200) GO TO 50
    GO TO 51
    IF(MOD(L,10).NE.0) GO TO 51
    WRITE(6,52) RT,RTD,ETAT,ETATO,ETATO
    WRITE(6,53) FTAP,ETAPD,ETAPDD,WA
    52 FORMAT(1X,4HRT =,G12.4,6H RTD =,G12.4,7H ETAT =,G12.4,
        +8H ETATO =,G12.4,9HETATO =,G12.4)
    53 FORMAT(1X,6HETAP =,G12.4,8H ETAPD =,G12.4,9H ETAPDD =,
        +G12.4,5H WA =,G12.4)
    54 CONTINUE
    IF(L.LT.LSWITCH) WRITE(6,6) TT,ETAERR
    IF(L.LT.LSWITCH) WRITE(8,*)
    55 FORMAT(1X,F5.3,G18.8)
    C INITIALIZE RANGE RATE
    IF(L.EQ.LSWITCH-1) RM2=RT
    IF(L.EQ.LSWITCH-2) RM3=RT
    C INITIALIZE AND TURN ON FILTER
    IF(L.EQ.LSWITCH) GO TO 10
    GO TO 100
    56 M1=FT
    RMN=(3*RM1-4*RM2+RM3)/(2*DT)
    PRINT*, "*****FILTER TURNED ON*****"
    CALL FJLINT(A,H,P,C,R)
    CALL XFOPMF
    CALL XFOPMI
    EFP2=ETAI-ETAT
    EDERR=ETAD-ETATO
    EDDERR=ETATO-ETATO
    WEPR=WA10-WCMD
    WRITE(6,7) TT,ETAERR,EEP2,EDERR,EDJERR,WERR
    WRITE(8,*)
    57 FORMAT(1X,F5.3,5G18.8)
    IF(MOD(L,10).NE.0) GO TO 100
    PRINT*, "RT = ",RT," RTD = ",RTD," ETAT = ",ETAT," ETATO = ",
        +",ETATO = ",ETATO
    GO TO 50
    000460
    000470
    000480
    000490
    000500
    000510
    000520
    000530
    000540
    000550
    000560
    000570
    000580
    000590
    000600
    000610
    000620
    000630
    000640
    000650
    000660
    000670
    000680
    000690
    000700
    000710
    000720
    000730
    000740
    000750
    000760
    000770
    000780
    000790
    000800
    000810

```

```

103  CONTINUE
      IF(L.GT.LSWITCH) GO TO 11
      GO TO 102
11   CALL FILTER
      CALL XFORMI
      CALL XFORMF
      FEPF=ETAI-ETAT
      FEDF=ETAD-ETATO
      WEPF=WAID-WCMD
      ENDERR=EETADD-ETATO
      WRITE(6,7) TT,ETAEPF,EEPR,EDERR,EDJERR,WERF
      WRITE(8,*) TT,ETAEPF
      IF(MOD(L,10).NE.0) GO TO 103
      PRINT*, " RT = ", RT, " RTD = ", RTD, " ESTAT = ", ETATO = "", ETATD = "", ETATD0=0350
      *, " ETATO = ", ETATD0
      WRTTE(6,20) ETAP,ETAI,ETAPD,EETAD,WAID
      FORMAT(1X,6HETAP =,G12.4,7H ETAI =,G12.4,8H ETAPD =,G12.4,
      +9H EETAD =,G12.4,5H WA =,G12.4,7H WAID =,G12.4)
      CONTINUE
      LDIF=L-LSWITCH
      IF(MOD(LDIF,10).EQ.0) GO TO 12
      GO TO 102
12   CALL UDATE(A,H,P,N,R,G)
      CALL XFORMI
      CALL XFORMF
      FEPF=ETAI-ETAT
      FEDF=ETAD-ETATO
      ENDERR=EETADD-ETATO
      WERF=WAID-WCMD
      WRITE(6,5)
      WRITE(6,7) TT,ETAERR,ERR,EDERR,EDJERR,WERF
      WRITE(8,*) TT,ETAERR
      IF(TT.LE.TIME) GO TO 1
      STOP
      END

```

```

C
C      SUBROUTINE INITIAL
C
C      *****
C      COMMON /PT/ TT,L,DT,DT,LSWITCH,Y(8),YP(3),WCMD,WAID,WA,WN,ZETA,RT
C      + ,RTD,ETAT,ETATD,ETATDD,ETAFRR,RM,FX1,EX2,EX10,EX20,EX100,EX200,001230
C      + ,ER,FETA,ETAD,ETAD0,ETAI,ETAD,ETAI,KACCEL,EX1I,EX2I,EX10I,
C      + EX2DI,EX10DI,EX2DDI,ETAM
C      + EQUIVALENCE (Y(1),C),(Y(2),ETAP),(Y(3),ETAPD),(Y(4),ETAPDD),
C      + (Y(5),X1),(Y(6),X10),(Y(7),X2),(Y(8),X20)
C      + T=0 $ L=0 $ WAID=0 $ C=0
C      ETAP=0 $ ETAPD=X2D/X1 $ ETAPDD=0
C      CALL XFORMT
C      RETURN
C      END
C
C      *****
C      SUBROUTINE SOLVE
C
C      *****
C      COMMON /PT/ TT,L,DT,DT,LSWITCH,Y(8),YP(3),WCMD,WAID,WA,WN,ZETA,RT
C      + ,RTD,ETAT,ETATD,ETATDD,ETAFRR,RM,FX1,EX2,EX10,EX20,EX100,EX200,001230
C      + ,ER,EETA,ETAD,ETAD0,ETAI,ETAD,ETAI,KACCEL,EX1I,EX2I,EX10I,
C      + EX2DI,EX10DI,EX2DDI,ETAM
C      + EXTERNAL F
C      DIMENSION IWORK(5),WORK(270),Z(8),TP(8)
C      IFLAG=1 $ NEQN=8
C      TOUT=.C1
C      TIN=0
C      DO 10 I=1,8
C      10 Y(I)=Y(I)
C      RELEERR=ABSEERR=1.0E-8
C      CALL ONE(F,NEQN,Z,TIN,TOUT,RELEERR,ABSEERR,IFLAG,WORK,IWORK)
C      DO 11 I=1,8
C      11 Y(I)=7(I)

```



```

+ ER,EEETA,EEETADD,PI,ETAC,ETAI,KACCEL,EX1I,EX2I,EX10I, 001890
+ EX20I,EX100I,EX200I,ETAM 001900
+ EQUIVALENCE (Y(1),C),(Y(2),ETAP),(Y(3),ETAPD),(Y(4),ETAPDD), 001910
+ (Y(5),X1),(Y(6),X1D),(Y(7),X2),(Y(8),X2D) 001920
+ RT=SQRT(Y(5)**2+Y(7)**2) 001930
+ ETAT=ATAN2(Y(7),Y(F)) 001940
+ PTp=(Y(5)*Y(6)+Y(7)*Y(8))/RT 001950
+ ETATD=(Y(5)*Y(8)-Y(7)*Y(6))/PT**2 001960
+ FTATDD=(PT**2*(Y(5)*YP(8)-Y(7)*YP(5))-2*(Y(5)*Y(8)-Y(7)*Y(6))* 001970
$ (Y(5)*Y(6)+Y(7)*Y(8)))/RT**4 001980
+ ETAEPR=ETAT-ETAP 001990
+ IF(L.EQ.1LSWITCH+1) C=1 002000
+ WA=700*ETAEPR/18+C 002010
+ WCMD=WF+WA17 002020
+ RETURN 002030
+ FND 002040
+ **** 002050
+ **** 002060
+ **** 002070
+ **** 002080
+ **** 002090
+ COMMON /PT/ TT,L,DT,DJT,LSWITCH,Y(3),YP(8),WCMD,WA,WN,ZETA,RT 002100
+ ,RTD,ETAT,ETAD,FTATDC,ETAFRR,RM2,EX1,EX2,EX10,EX20,EX100,EX2DD, 002110
+ ER,EEETA,EEETADD,EEETAD,PI,ETAC,ETAI,KACCEL,EX1I,EX2I,EX10I, 002120
+ EX20I,EX100I,EX200I,ETAM 002130
+ EQUIVALENCE (Y(1),C),(Y(2),ETAP),(Y(3),ETAPD),(Y(4),ETAPDD), 002140
+ (Y(5),X1),(Y(6),X1D),(Y(7),X2),(Y(8),X2D) 002150
+ DIMENSION A(3,3),H(2,3),P(3,3),Q(3,3),R(2,2) 002160
+ EX1=RT 002170
+ EX2=6 002180
+ ETAM=0 002190
+ ETAD=ETAP 002200
+ FX1D=PM'D 002210
+ FX1DD=RT*WCMD 002220
+ FX10D=FX200=0 002230
+ A(1,1)=A(2,2)=A(3,3)=1.0 002240

```

```

A(1,2)=A(2,3)=0 002250
A(1,3)=.5*DT*2 002260
A(2,1)=A(3,1)=A(3,2)=0 002270
H(1,1)=H(2,2)=1.0 002290
H(1,2)=H(1,3)=H(2,1)=H(2,3)=0 002290
R(1,1)=1 002300
P(2,2)=16 002310
P(1,2)=P(2,1)=0 002320
P(1,1)=1 002330
P(1,2)=P(2,1)=1.5/DT 002340
P(2,2)=6.5/DT*2 002350
C P33 AND 033 READ-IN, ALL OTHER 0 ELEMENTS ZERO BY SYSTEM DEFAULT 002360
RETURN 002370
END 002380
***** 002390
002400
SUBROUTINE FILTER 002410
002420
COMMON /PT/, TT,L,DT,DNT,LSWITCH,Y(8),YP(8),WCND,WAID,WN,ZETA,RT,02440
+ ,RTD,ETAT,ETAD,FTATDD,ETATERR,RMJ,EX1,EX2,EX2D,EX10D,EX20D,002450
+ ,ER,EETA,EETAD,EETADD,PI,ETAD,ETAI,KACCEL,EX1I,EX2I,EX1D, 002450
+ ,EX2D,EX10D,EX20D,ETAM 002470
+ ETAM=ETAM+DNT*WCMD 002480
EX1=EX1+DNT*EX1D+DNT**2*EX10D/2 002490
EX2=EX2+DNT*EX2D+DNT**2*EX20D/2 002500
EX1D=EX1D+DNT*EX10D 002510
EX2D=EX2D+DNT*EX20D 002520
EX10D=EX10D 002530
EX20D=EX20D 002540
RETURN 002550
END 002560

```



```

RETURN
FND
*****+
C   SUBROUTINE ACCEL(A1,A2,TD)
C
C   ****+
C   COMMON /PT/ TT,L,DT,DTT,LSWITCH,Y(8),YP(8),WCMD,WAID,HA,WN,ZETA,RT
C   +,RTD,ETAT,ETAD,ETATDD,ETADDD,ETAERR,RY),EX1,EX2,EX1D,EX2D,EX1DD,EX2DD
C   COMMON /ACC/ KA,U
C   IF(KA.FQ.2 .AND. TD.GT.5.99) GO TO 1
C   A1=0
C   A2=0
C   GO TO 2
C   1   A1=-RT*ETATD**2*COS(ETATD*TD-U)
C   2   A2=-RT*ETATD**2*SIN(ETATD*TD-U)
C   RETURN
FND
004330
004340
004350
004360
004370
004380
004390
004390
004400
004410
004420
004430
004440
004450
004460
004470
004480
004490
004500

```

Appendix B

Truth Model Formulation

In order to model the target motion in two dimensions, all that is needed is the target acceleration in the Y_1 , Y_2 coordinate system defined in Chapter II, and a set of initial conditions. The differential equations can then be written in matrix form as

$$\begin{bmatrix} \dot{Y}_1 \\ \ddot{Y}_1 \end{bmatrix} = \begin{bmatrix} 0 & 1 \\ 0 & 0 \end{bmatrix} \begin{bmatrix} Y_1 \\ \dot{Y}_1 \end{bmatrix} + \begin{bmatrix} 0 \\ 1 \end{bmatrix} A_1 \quad (B1)$$

$$\begin{bmatrix} \dot{Y}_2 \\ \ddot{Y}_2 \end{bmatrix} = \begin{bmatrix} 0 & 1 \\ 0 & 0 \end{bmatrix} \begin{bmatrix} Y_2 \\ \dot{Y}_2 \end{bmatrix} + \begin{bmatrix} 0 \\ 1 \end{bmatrix} A_2 \quad (B2)$$

where A_1 and A_2 are the modeled target acceleration expressions in the Y_1 , Y_2 directions respectively.

The differential equations describing the gimbal dynamics can be written by inspection of the closed loop servo portion of Figure 3. By looking at the $G_2(s)$ and $G_3(s)$ transfer functions the following matrix equation is obtained:

$$\begin{bmatrix} \dot{\eta}_p \\ \ddot{\eta}_p \\ \dddot{\eta}_p \\ \ddot{\eta}_p \end{bmatrix} = \begin{bmatrix} 0 & 1 & 0 \\ 0 & 0 & 1 \\ 0 & -w_n^2 & -2\zeta w_n \end{bmatrix} \begin{bmatrix} \eta_p \\ \dot{\eta}_p \\ \ddot{\eta}_p \\ \ddot{\eta}_p \end{bmatrix} + \begin{bmatrix} 0 \\ 0 \\ w_n^2 \end{bmatrix} w_{cmd} \quad (B3)$$

And from the $G_1(S)$ transfer function the following proportional plus integral compensation relationship is obtained:

$$W_A = (700/18 + 700/S)\epsilon \quad (B4)$$

Now let

$$C = (700/S)\epsilon \quad (B5)$$

then

$$\dot{C} = 700\epsilon = 700 (n_T - n_p) \quad (B6)$$

but

$$n_T = \text{Arctan } (Y_2/Y_1) \quad (B7)$$

Therefore,

$$W_A = 700 (\text{Arctan } (Y_2/Y_1) - n_p)/18 + C \quad (B8)$$

By combining Eq (B1), (B2), (B6), and (B8) with the relationship

$$W_{cmd} = W_A + W_{aid} \quad (B9)$$

the overall truth model matrix can be written as seen in Eq (8).

Appendix C

Steady-State Perturbation Analysis

The use of pseudo-range measurements to increase the sample rate of the Aided Track algorithm is susceptible to the problem of error propagation. Modification Two is the worst case since estimates of range rate are used every 0.01 seconds to propagate the last range measurement. This case is analyzed here.

Range is propagated by the equation

$$R'(K+1) = R'(K) + \hat{R}(K)\Delta T \quad (C1)$$

where the prime denotes pseudo-range and $R'(0)$ is the last laser range measurement. Assuming that the laser range measurement is perfect, the estimate of range rate \hat{R} and the pseudo-range terms can be expressed as the sum of their true values plus some error.

$$\hat{R}(K) = R(K) = \delta \hat{R}(K), \quad K=0,1,\dots,9 \quad (C2)$$

$$R'(K) = R(K) + \delta R'(K), \quad K=1,2,\dots,9 \quad (C3)$$

where $\delta R(0) = 0$. Eq (C1) can be rewritten as

$$R'(K+1) = R(K) + \delta R(K) + R(K)\Delta T + \delta R(K)\Delta T, \quad K=1,\dots,9 \quad (C4)$$

But the first and third terms represent the true range. Therefore, the error in the pseudo-range propagation can be written as

$$\delta R'(K+1) = \delta R'(K) + \dot{\delta R}(K)\Delta T, \quad K=1, \dots, 9 \quad (C5)$$

were $\delta R'(0) = 0$.

The pseudo-range measurements are used in Eq (6) through (9) which are restated here.

$$x_{1m} = R' \cos \eta_m$$

$$x_{2m} = R' \sin \eta_m$$

(C6)

$$\dot{x}_{1m} = \dot{R} \cos \eta_m - R' W \sin \eta_m$$

$$\dot{x}_{2m} = \dot{R} \sin \eta_m + R' W \cos \eta_m$$

Assuming that η_m and W are known perfectly, the perturbations caused in Eq (C6) by the use of pseudo-range measurements are expressed as

$$\delta x_{1m} = [\delta R' + \dot{\delta R}\Delta T] \cos \eta_m$$

$$\delta x_{2m} = [\delta R' + \dot{\delta R}\Delta T] \sin \eta_m$$

(C7)

$$\delta \dot{x}_{1m} = \dot{R} \cos \eta_m - [\delta R' + \dot{\delta R}\Delta T] W \sin \eta_m$$

$$\delta \dot{x}_{2m} = \dot{R} \sin \eta_m + [\delta R' + \dot{\delta R}\Delta T] W \cos \eta_m$$

Assume the nominal, steady-state conditions to be

$$\eta_m = 90^\circ$$

$$W = 1 \text{ radian/second}$$

$$\Delta T = 0.01 \text{ seconds}$$

$$\dot{\delta R}(0) = 0.01 \text{ meters/second}$$

Then Eq (C7) becomes

$$\delta \dot{x}_1 = 0$$

$$\delta \dot{x}_2 = \delta R' + \delta \dot{R} \Delta T$$

(C8)

$$\delta \dot{x}_1 = -[\delta R' + \delta \dot{R} \Delta T]$$

$$\delta \dot{x}_2 = \delta \dot{R}$$

Eq (C8) is further simplified if only the errors after the first iteration are considered (i.e. $\delta R'(0) = 0$).

$$\delta \dot{x}_1 = 0$$

$$\delta \dot{x}_2 = 0.001$$

(C9)

$$\delta \dot{x}_1 = -0.0001$$

$$\delta \dot{x}_2 = 0.01$$

These perturbations are processed through the filter by the following set of equations:

$$\begin{aligned} \delta \hat{x}_1^+ &= \delta \hat{x}_1^- + G_{11}(\delta x_1 - \delta \hat{x}_1^-) + G_{12}(\delta \dot{x}_1 - \delta \dot{\hat{x}}_1^-) \\ \delta \hat{x}_2^+ &= \delta \hat{x}_2^- + G_{21}(\delta x_2 - \delta \hat{x}_2^-) + G_{22}(\delta \dot{x}_2 - \delta \dot{\hat{x}}_2^-) \\ \delta \dot{\hat{x}}_1^+ &= \delta \dot{\hat{x}}_1^- + G_{11}(\delta x_1 - \delta \hat{x}_1^-) + G_{12}(\delta \dot{x}_1 - \delta \dot{\hat{x}}_1^-) \\ \delta \dot{\hat{x}}_2^+ &= \delta \dot{\hat{x}}_2^- + G_{21}(\delta x_2 - \delta \hat{x}_2^-) + G_{22}(\delta \dot{x}_2 - \delta \dot{\hat{x}}_2^-) \end{aligned} \quad (C10)$$

Substituting in the steady-state Kalman gains, the values expressed in Eq (C9), and assuming $\delta\hat{x}_1(0) = \delta\hat{x}_2(0) = \dot{\delta\hat{x}}_1(0) = \dot{\delta\hat{x}}_2(0) = 0$ Eq (C10) becomes

$$\begin{aligned}\delta\hat{x}_1 &= (.26)(0) + (.03)(-.0001) = 3.0E-6 \\ \delta\hat{x}_2 &= (.26)(.0001) + (.03)(.01) = 3.26E-4 \\ \dot{\delta\hat{x}}_1 &= (.48)(0) + (.11)(-.0001) = 1.1E-5 \\ \dot{\delta\hat{x}}_2 &= (.48)(.0001) + (.11)(.01) = 1.148E-3\end{aligned}\tag{C11}$$

The perturbations expressed in Eq (C11) are transformed into the change of the error in the estimate of range rate by

$$\begin{aligned}\Delta\dot{\delta R} &= \frac{\delta\hat{x}_1\dot{\delta\hat{x}}_1 + \delta\hat{x}_2\dot{\delta\hat{x}}_2}{(\delta\hat{x}_1^2 + \delta\hat{x}_2^2)^{1/2}} \\ &= 1.148E-3\end{aligned}\tag{C12}$$

Therefore, the new error in the estimate of range rate becomes

$$\begin{aligned}\dot{\delta R}(1) &= \dot{\delta R}(0) + \Delta\dot{\delta R}(0) \\ &= .01 + .001148 \\ &= .01148\end{aligned}\tag{C13}$$

Thus it has been shown that the use of pseudo-range measurements creates a stability problem of errors in the estimates of range rate generating larger errors in the next estimate of range rate.

APPENDIX D

Program Listings for Each Modification Method Tested.

```

***** MODIFICATION ONE ****
C
C   SUBROUTINE UPDATE(A,H,P,Q,R,G)
C
C   ****
C   COMMON /PT/ TT,L,DT,DDT,LSWITCH,Y(3),YP(8),WCMD,WAID,WA,WN,ZETA,RT
C   ,R7D,ETAT,ETATO,ETATD,ETAFRR,R4),EX1,FX2,EX1D,EX2D,EX100,EX200,
C   +,ER,FEETA,EEETAD,EEETAD,PI,ETAD,ETAI,KACCEL,EX1I,EX2I,EX10I,
C   +,EX20I,EX100I,EX200I,ETAM,RM1,RM2,RM3
C   + DIMENSION A(3,3),H(2,3),P(3,3),Q(3,3),R(2,2),G(3,2)
C   N=3  S  M=2
C   LDTF=L-LSWITCH
C   IF (MCD(LDTF,10).EQ.0) GO TO 1
C   GO TO 2
C   P=R*T
C   1   H(1,1)=1.0
C   GO TO 2
C   2   P=P*P
C   H(1,1)=0.0
C   CONTINUE
C   CALL P*PCOV(P,A,Q,H)
C   CALL KALG(P,H,R,N,M,G)
C   CALL CCVUP(P,G,H,N,M)
C   CE=COS(ETAM)  S SE=SIN(ETAM)
C   X1M=RP*CE
C   X2M=RP*SE
C   X1M0=RN*D*CE-RQ*WCMD*SE
C   X2M0=PD*SE+RR*WCMD*CE
C   FX1=EX1+G(1,1)*(X1M-EX1)+G(1,2)*(X1M)-EX1D)
C   EX2=EX2+G(1,1)*(X2M-EX2)+G(1,2)*(X2M)-EX2D)
C   EX1D=EX1D+G(2,1)*(X1M-EX1)+G(2,2)*(X1M)-EX1D)
C   EX2D=EX2D+G(2,1)*(X2M-EX2)+G(2,2)*(X2M)-EX2D)
C   EX10D=EX10D+G(3,1)*(X1M-EX1)+G(3,2)*(X1M)-EX10)
C   EX20D=EX20D+G(3,1)*(X2M-EX2)+G(3,2)*(X2M)-EX20)
C   RETURN
C   END

```



```

***** SUBROUTINE UPDATE(A, H, P, Q, R, F) ***** MODIFICATION THREE *****

      COMMON /PT/ TT,L,DT,DTT,LSWITCH,Y(8),YP(8),WCMD,WAID,WA,WN,ZETA,RT
      +,RTD,ETAT,ETATO,ETATDD,ETAERR,RTD,EX1,EX2,EX1D,EX2D,EX10D,EX20D,
      +,EP,EETA,EETAD,EETAND,PI,ETAJ,ETAI,KACCEL,EX1I,EX2I,EX10I,
      +,EX20I,EX10NI,EX20DI,ETAM,RT1,RT2,RT3
      + DIMENSION A(3,3),H(2,3),P(3,3),Q(3,3),R(2,2),G(3,2)

      N=3 $ M=2
      LDTF=L-LSWITCH
      IF(MOD(LDTF,10).EQ.0) GO TO 1
      GO TO 2

      1      RR=RT
      CRM0=PRD 3 H(1,1)=1.0
      GO TO 3
      PR=RP+RT*CRM0

      2      H(1,1)=0.0
      CONTINUE
      CALL PPPCOV(P,A,Q,N)
      CALL KALG(P,H,R,N,M,G)
      CALL CCVUP(P,G,H,N,M)
      CE=COS(ETAM) $ SE=SIN(ETAM)
      X1M=PR*CE
      X2M=PR*SE
      X1M=RYD*CE-PR*WCMD*SE
      X2M=RYD*SE+PR*WCMD*CE
      FX1=EX1+G(1,1)*(X1M-EX1)+G(1,2)*(X1MD-EX1D)
      FX2=EX2+G(1,1)*(X2M-EX2)+G(1,2)*(X2MD-EX2D)
      FX1D=EX1D+G(2,1)*(X1M-FX1)+G(2,2)*(X1MD-EX1D)
      FX2D=EX2D+G(2,1)*(X2M-FX2)+G(2,2)*(X2MD-EX2D)
      FX1DD=EX1DD+G(3,1)*(X1M-EX1)+G(3,2)*(X1MD-EX1D)
      FX2DD=EX2DD+G(3,1)*(X2M-EX2)+G(3,2)*(X2MD-EX2D)
      RETURN
      END

```

***** MODIFICATION FOUR *****

S 6 SUBROUTINE UPDATE(A, H, P, N, R, G)

```
*****  
COMMON /PT/ TT,L,DT,DOT,LSWITCH,Y(6),YP(8),WCMD,WAID,WA,WN,ZETA,RT  
+ ,R7D,ETAT,ETATD,ETATD,ETAERR,R7D,EX1,EX2,EX10,EX20,EX10D,EX20D,  
+ ,ER,EETA,EETAD,ETAD,ETAD,PI,ETAJ,ETAI,KACCEL,EXII,EX2I,EX10I  
+ ,EX20I,EX10DI,EX20DI,ETAM,RM1,RM2,RM3  
+ DIMENSION A(3,3),H(2,3),P(3,3),Q(3,3),R(2,2),G(3,2)  
N=3 S M=2  
P=R*T  
CALL PEGCOV(P,A,Q,N)  
CALL KALG(P,H,R,N,M,G)  
CALL CRYUP(P,G,H,N,M)  
CE=COS(ETAM) S SE=SIN(ETAM)  
X1M=FR*CE  
X2M=FP*SE  
X1MD=PI*N*CE-RP*WCMD*SE  
X2M7=R*D*SE+R*WCMD*CE  
FX1=EX1+G(1,1)*(X1M-EX1)+G(1,2)*(X1M)-EX10)  
FX2=FX2+G(1,1)*(X2M-EX2)+G(1,2)*(X2M)-EX20)  
EX10=EX10+G(2,1)*(X1M-EX1)+G(2,2)*(X1M)-EX10)  
EX20=EX20+G(2,1)*(X2M-EX2)+G(2,2)*(X2M)-EX20)  
EX10D=FX10D+G(3,1)*(X1M-EX1)+G(3,2)*(X1M)-EX10)  
EX20D=FX20D+G(3,1)*(X2M-EX2)+G(3,2)*(X2M)-EX20)  
RETURN  
END
```

```

***** **** MODIFICATION FIVE ****
C
C   SUBROUTINE UPDATE(A,H,P,Q,R,G)
C
* **** **** ****
COMMON /PT/ TT,L,DT,DTT,LSWITCH,Y(3),YP(3),WCMD,WAID,WA,WN,ZETA,RT
* ,RTD,ETAT,ETATD,ETATD,ETAEP,RTD,EX1,FX2,EX1D,EX2D,EX1DD,EX2DD,
* ,ER,ETA,ETAD,ETAD,ETAJ,ETAI,KACCEL,EX1I,EX2I,EX1D,
* EX2II,EX10DI,EX20DI,ETAM,RY1,RM2,RM3
* DIMENSION A(3,3),H(2,3),P(3,3),Q(3,3),R(2,2),G(3,2)
N=2 $ M=2
LDIF=L-LSWITCH
IF(IND(LDIF,10).EQ.0) GO TO 1
GO TO 2
1  RR=RT $ RM3=RM2 $ RM2=RM1 $ RM1=RT
SRD=(3*RM1-4*RM2+RM3)/(.2)
H(1,1)=1.0
GO TO 2
RR=RR+SRD*DT $ H(1,1)=0.0
2  CONTINUE
CALL PFCOV(P,A,Q,N)
CALL KALG(P,H,R,N,M,G)
CALL CCOVUP(P,G,H,N,M)
CE=COS(ETAM) $ SE=SIN(ETAM)
X1M=RR*CE
X2M=RR*SE
X1MD=RRD*CE-RR*WCMD*SE
X2MD=RRD*SE+RR*WCMD*CE
EX1=EX1+G(1,1)*(X1M-EX1)+G(1,2)*(X1MD-EX1D)
EX2=EX2+G(1,1)*(X2M-FX2)+G(1,2)*(X2MD-EX2D)
EX10=EX10+G(2,1)*(X1M-EX1)+G(2,2)*(X1MD-EX1D)
EX2D=EX2D+G(2,1)*(X2M-FX2)+G(2,2)*(X2MD-EX2D)
EX1DD=FX10D+G(3,1)*(X1M-FX1)+G(3,2)*(X1MD-EX1D)
EX2DD=FX2DD+G(3,1)*(X2M-FX2)+G(3,2)*(X2MD-EX2D)
RETURN
END

```

```

***** MODIFICATION SIX ****
C
C   SUBROUTINE UPDATE(A, H, P, Q, R, S)
C
C   **** COMMON /PT/ TT,L,DT,DJT,L SWITCH, Y(8), YP(8), WCMD, WAI0, WA, WN, ZETA, RT
C   +, RT0, ETAT, ETATD, ETAT0, ETAEER, R'MD, EX1, EX2, EX1D, EX2D, EX10D, EX20D,
C   +, ER, EETA, EETAD, EETADD, PI, ETAD, ETAI, KACCEL, EX1I, EX2I, EX10I,
C   +, EX20I, EX100I, EX200I, ETAM, RM1, RM2, RM3
C
C   DIMENSION A(3,3), H(2,3), P(3,3), Q(3,3), R(2,2), S(3,2)
C
C   H=3   $   M=2
C   LDIF=L-L SWITCH
C   IF(MOD(LDIF,10).EQ.0) GO TO 1
C   GO TO 2
C
C   RR=RT
C   H(1,1)=1.0
C   GO TO 2
C   RR=EP
C   H(1,1)=0.0
C
C   CONTINUE
C   CALL PFPcov(P,A,Q,N)
C   CALL KALG(P,H,R,N,M,G)
C   CALL CCVUP(P,G,H,N,M)
C   CE=COS(ETAM) $ SE=SIN(ETAM)
C   X1M=RR*CE
C   X2M=RR*SE
C   X1N=RR*CE-RR*WCMN*SE
C   X2M=RR*SE+RR*WCMN*CE
C   FX1=EX1+G(1,1)*(X1M-EX1)+G(1,2)*(X1M-EX1D)
C   FX2=EX2+G(1,1)*(X2M-EX2)+G(1,2)*(X2M-EX2D)
C   FX1D=EX1D+G(2,1)*(X1M-EX1)+G(2,2)*(X1M-EX1D)
C   FX2D=EX2D+G(2,1)*(X2M-EX2)+G(2,2)*(X2M-EX2D)
C   EX10D=EX10D+G(3,1)*(X1M-EX1)+G(3,2)*(X1M-EX1D)
C   EX20D=EX20D+G(3,1)*(X2M-EX2)+G(3,2)*(X2M-EX2D)
C
C   RETURN
CEND

```

APPENDIX E

Supportive Material: Plots of Tracking Error Versus Time
for Various Modifications and Scenarios.

AD-A055 635

AIR FORCE INST OF TECH WRIGHT-PATTERSON AFB OHIO SCH--ETC F/G 17/7
PSEUDO-RANGE MEASUREMENTS USED TO INCREASE THE SAMPLING RATE OF--ETC(U)

DEC 77 J M PETEK

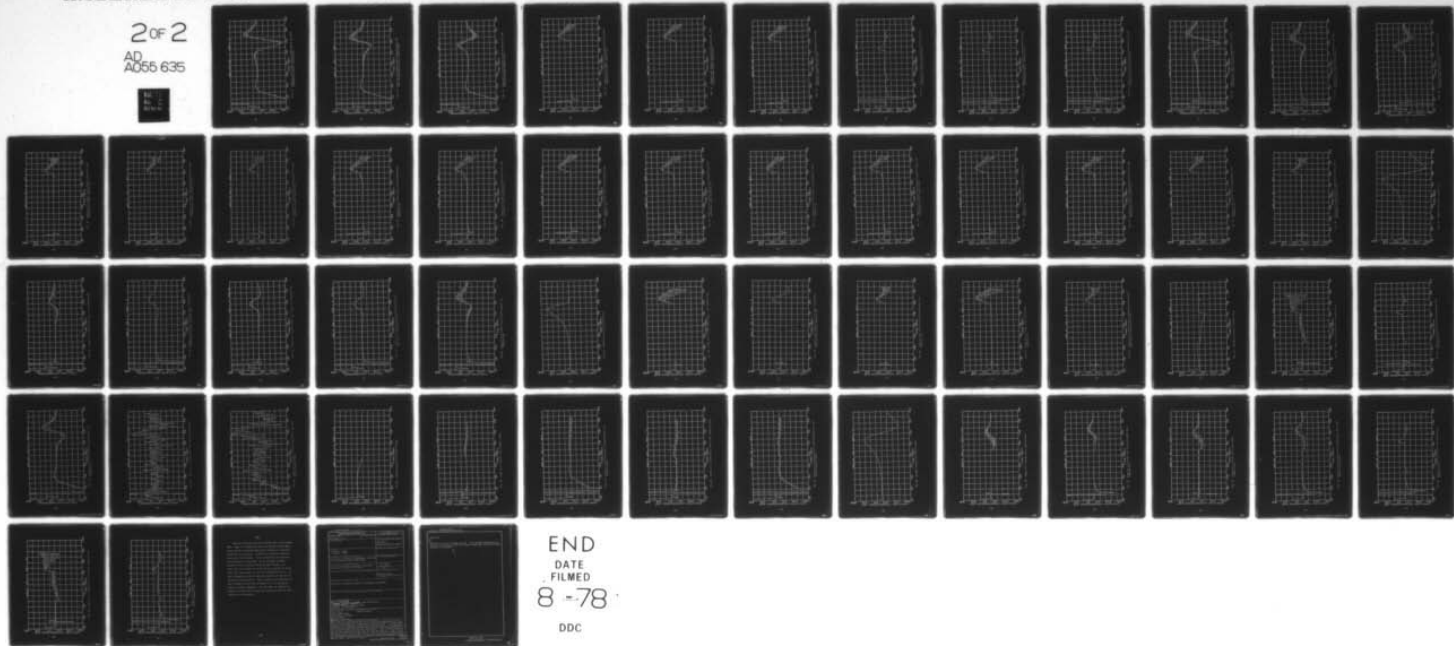
UNCLASSIFIED

AFTT/GA/FE/77-4

NL

2 OF 2
AD
A055 635

FF



END
DATE
FILED
8-78
DDC

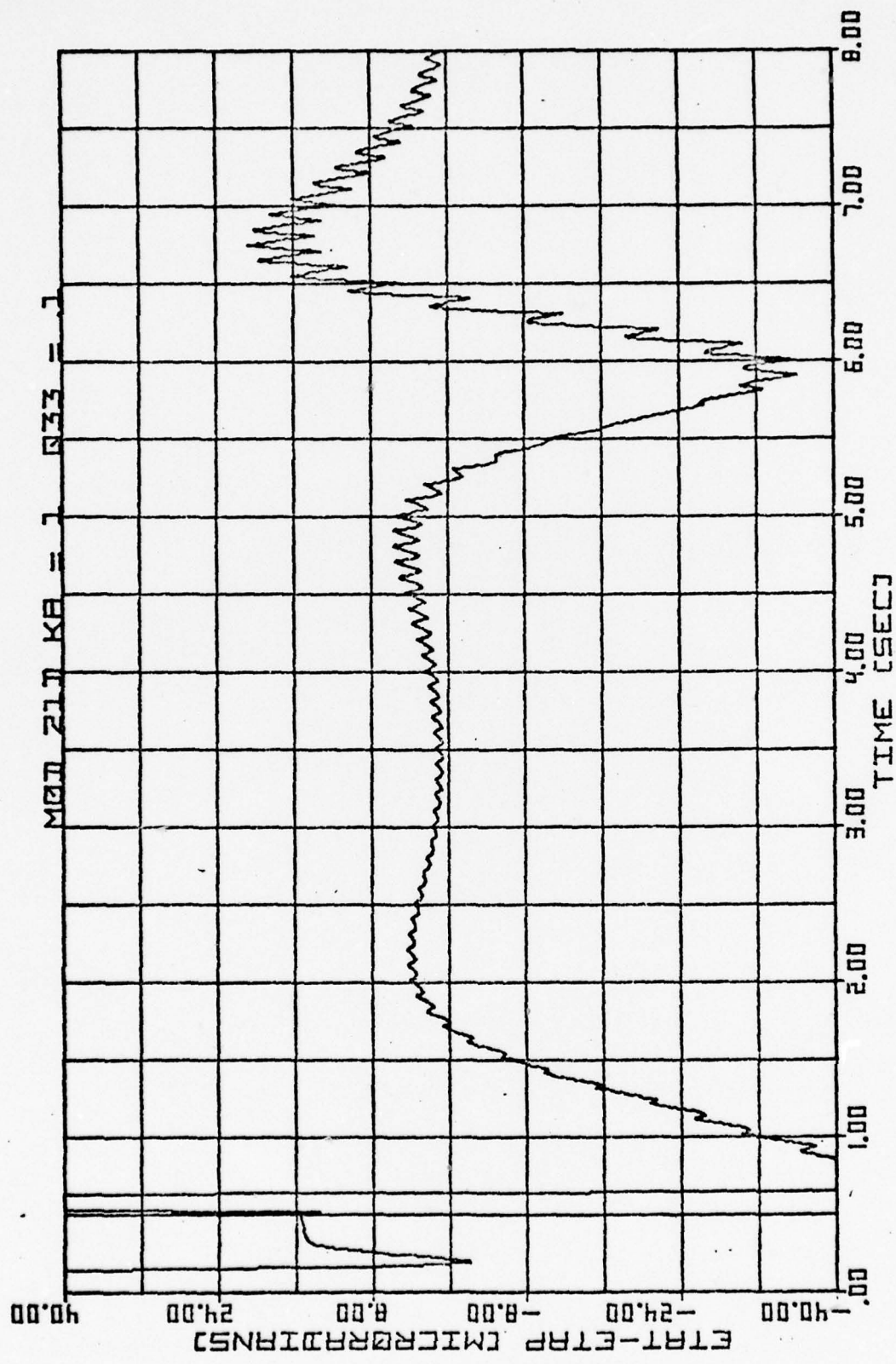
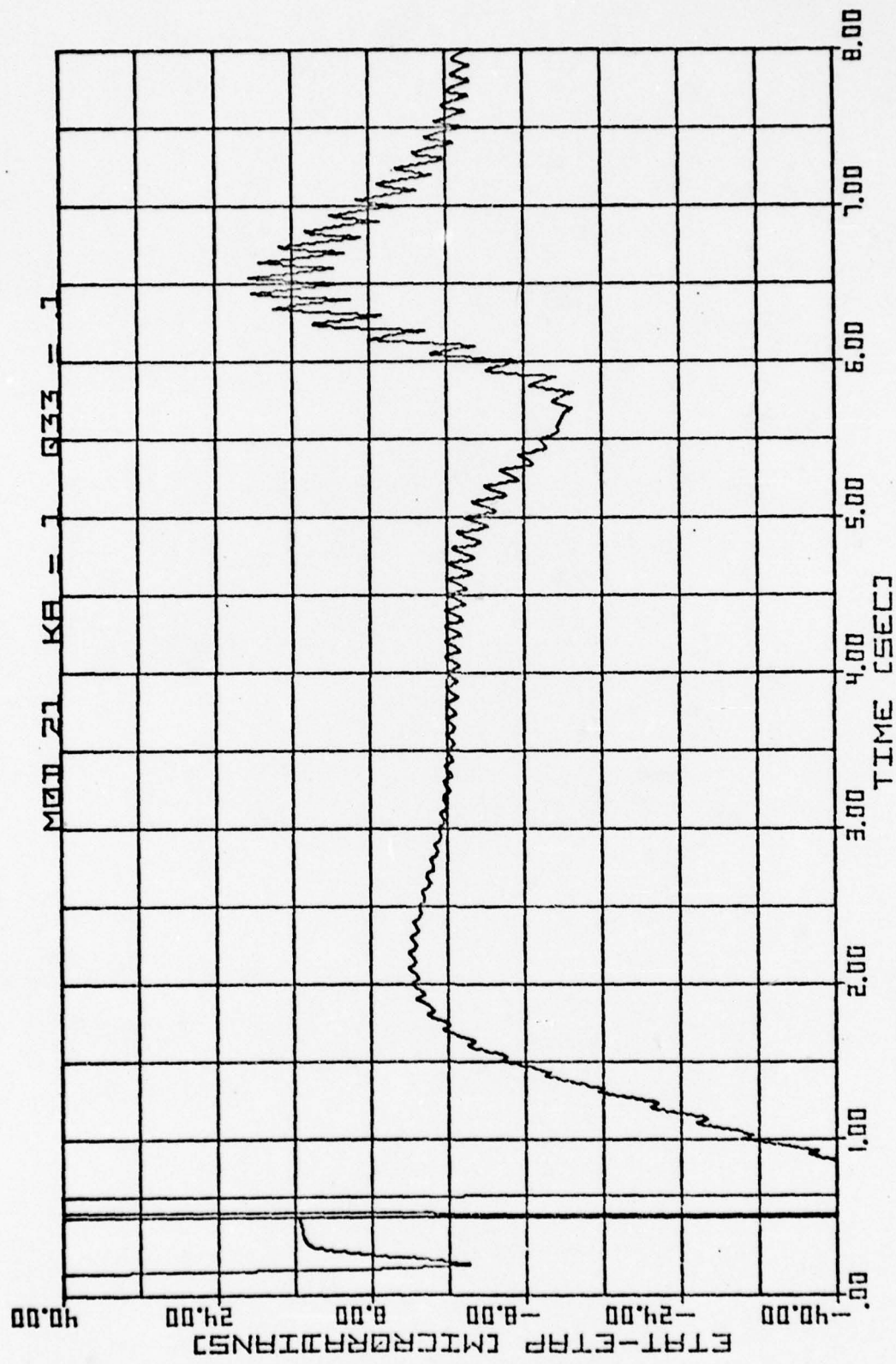
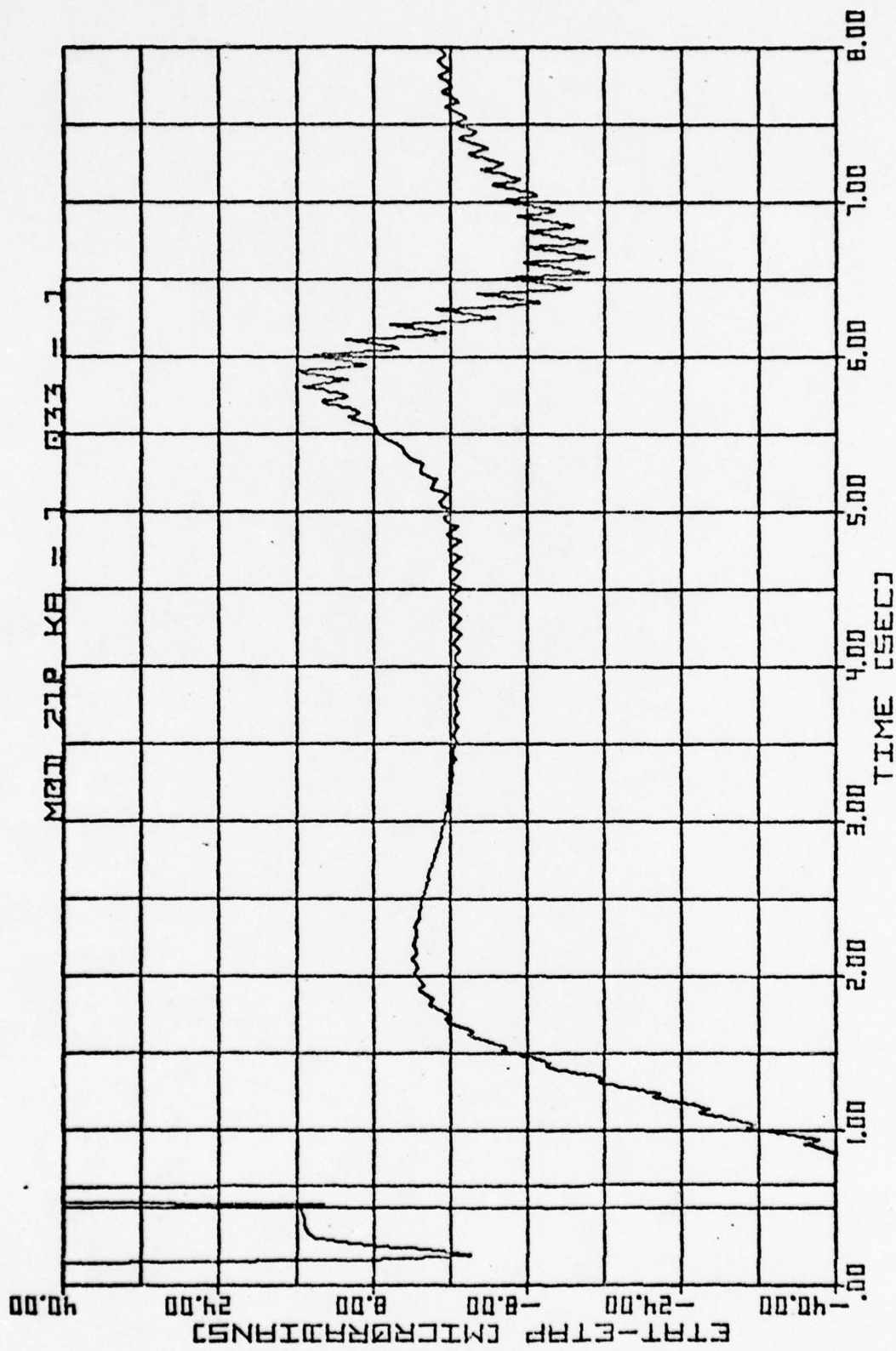


Fig. 12. Aided at 0.01 second rate by Modification Two with computational delay, Scenario One.





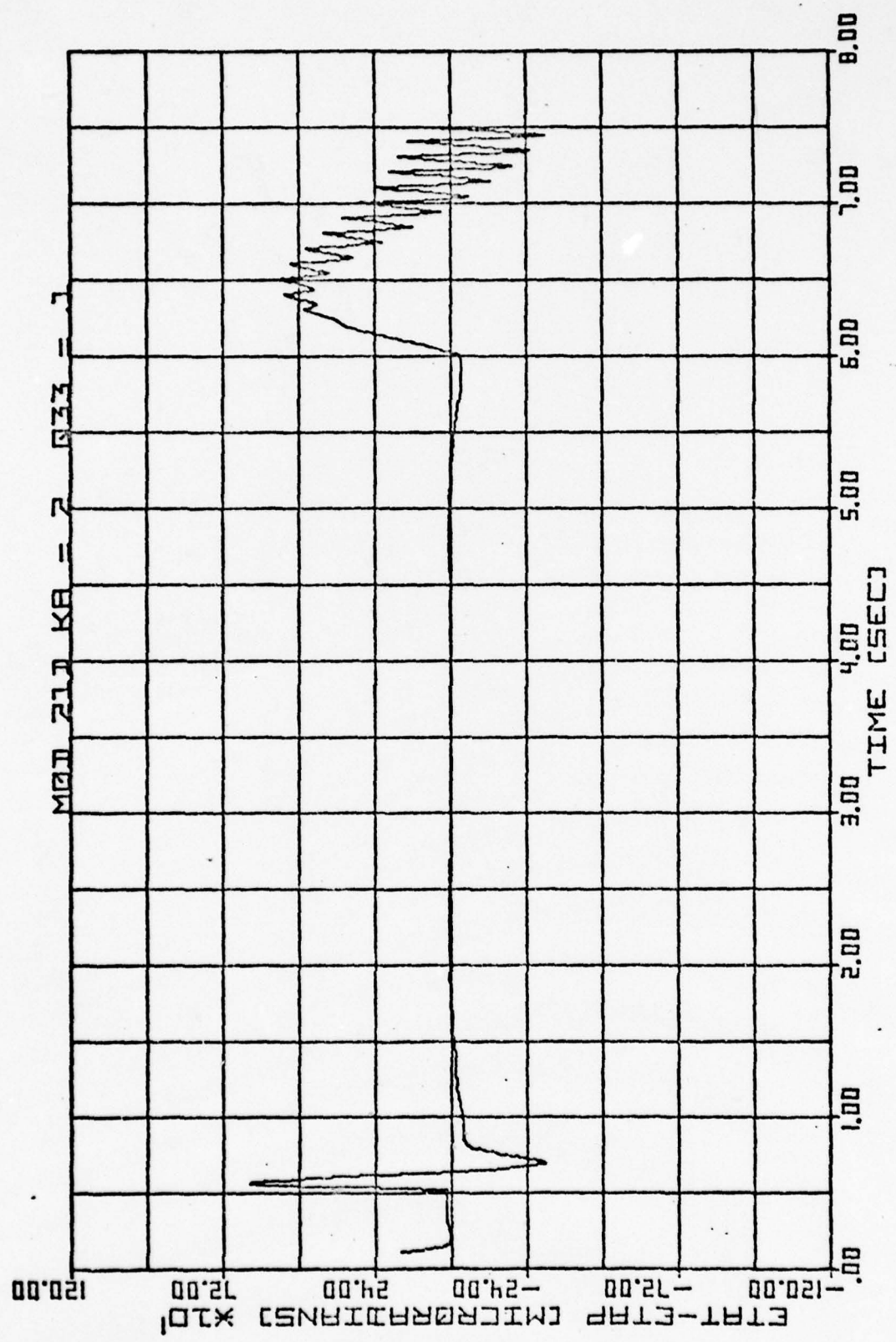


Fig. 15. Aided at 0.01 second rate by Modification Two with computational delay, Scenario Two.

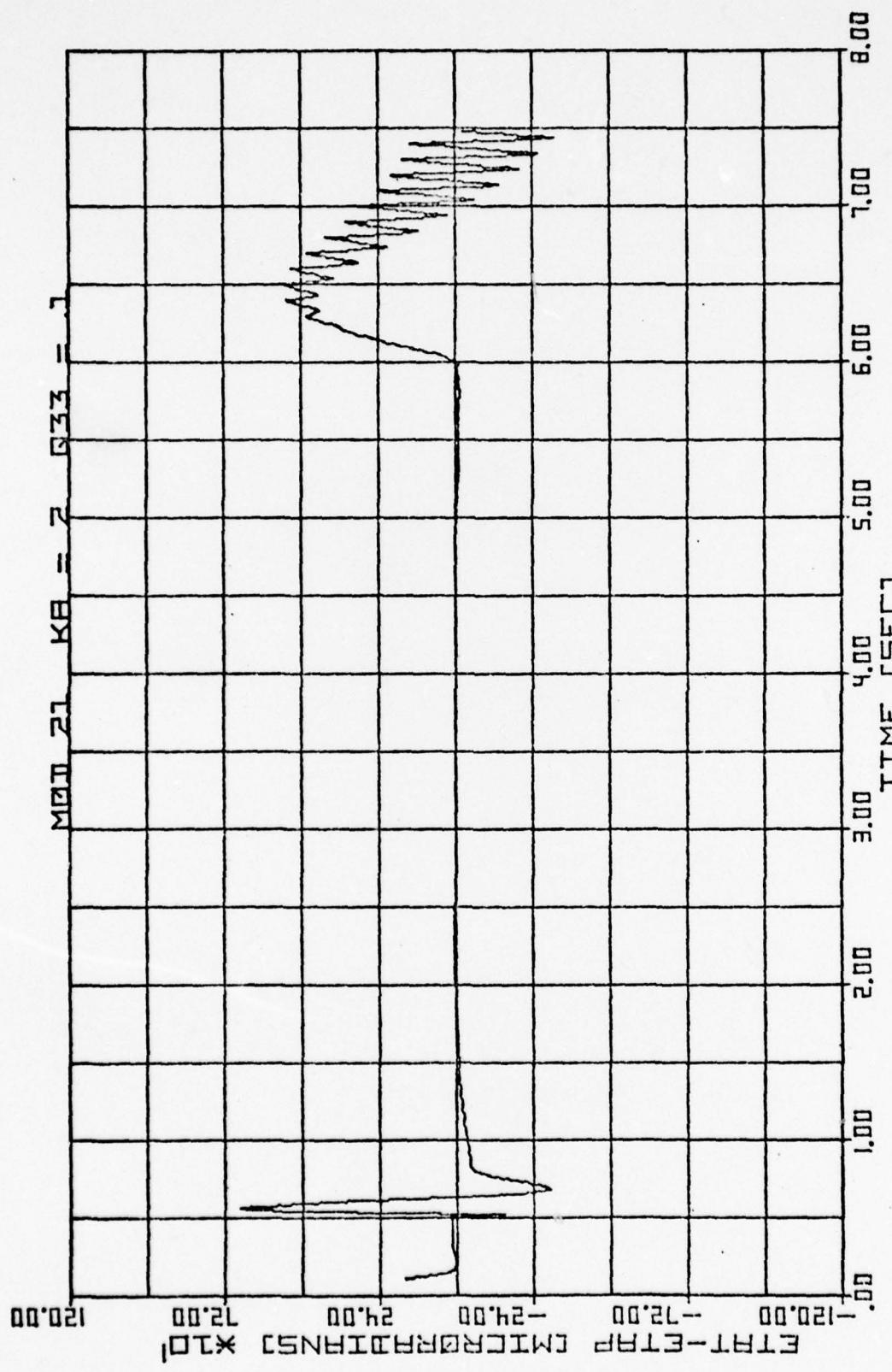
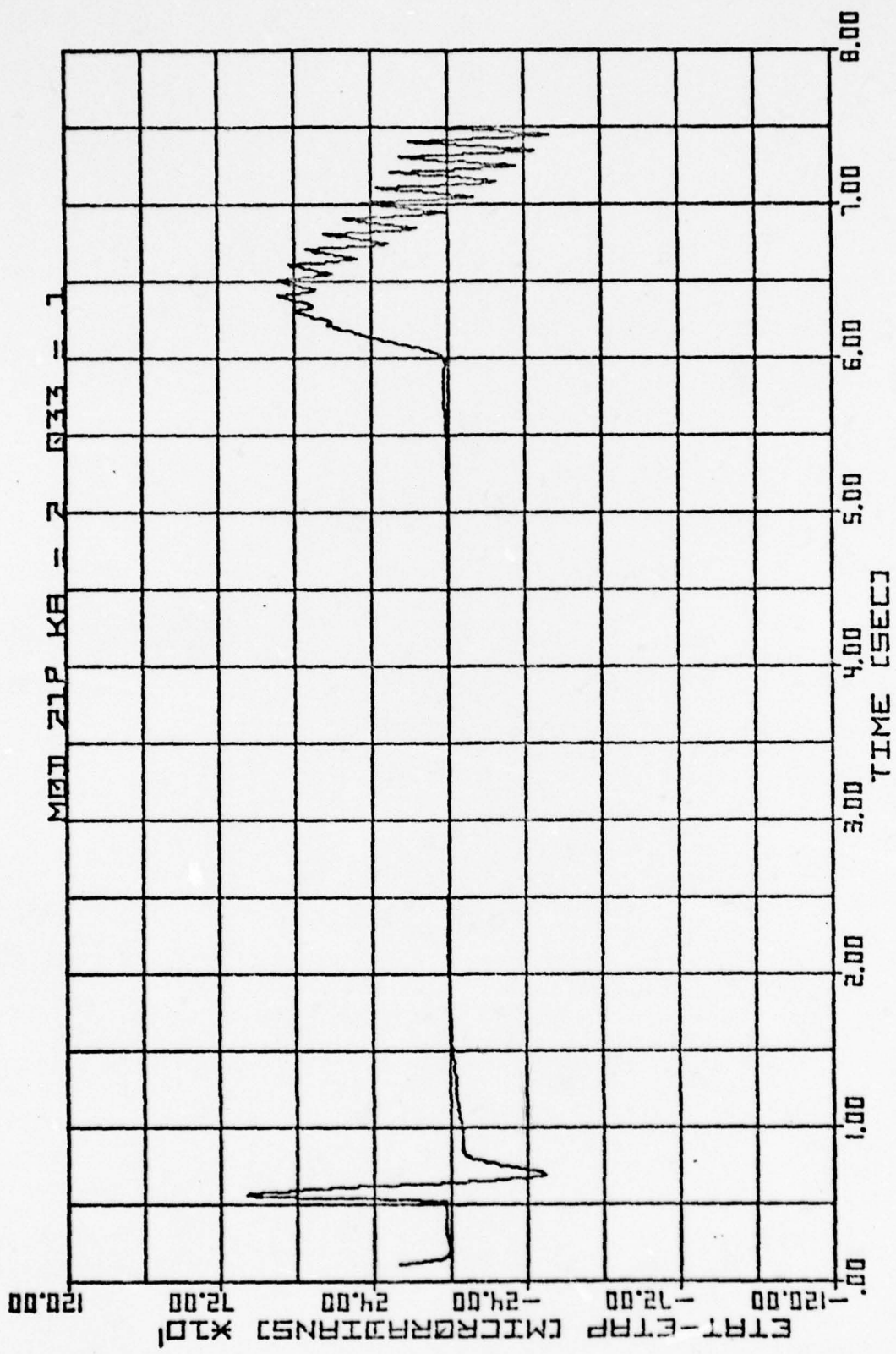


Fig. 16. Aided at 0.01 second rate by Modification Two, with instantaneous update, Scenario Two



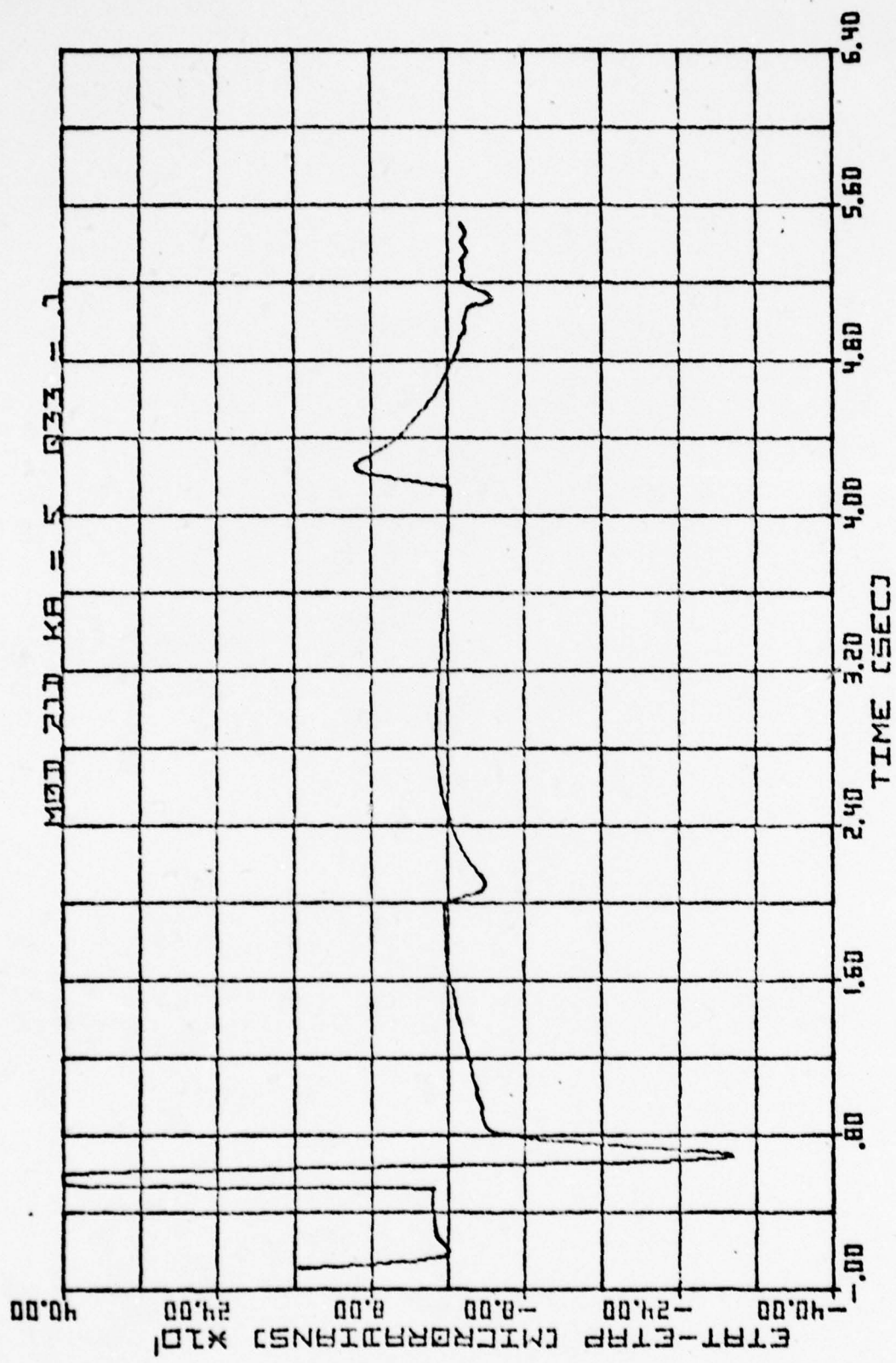


Fig. 18. Aided at 0.01 second rate by Modification Two with computational delay, Scenario Five.

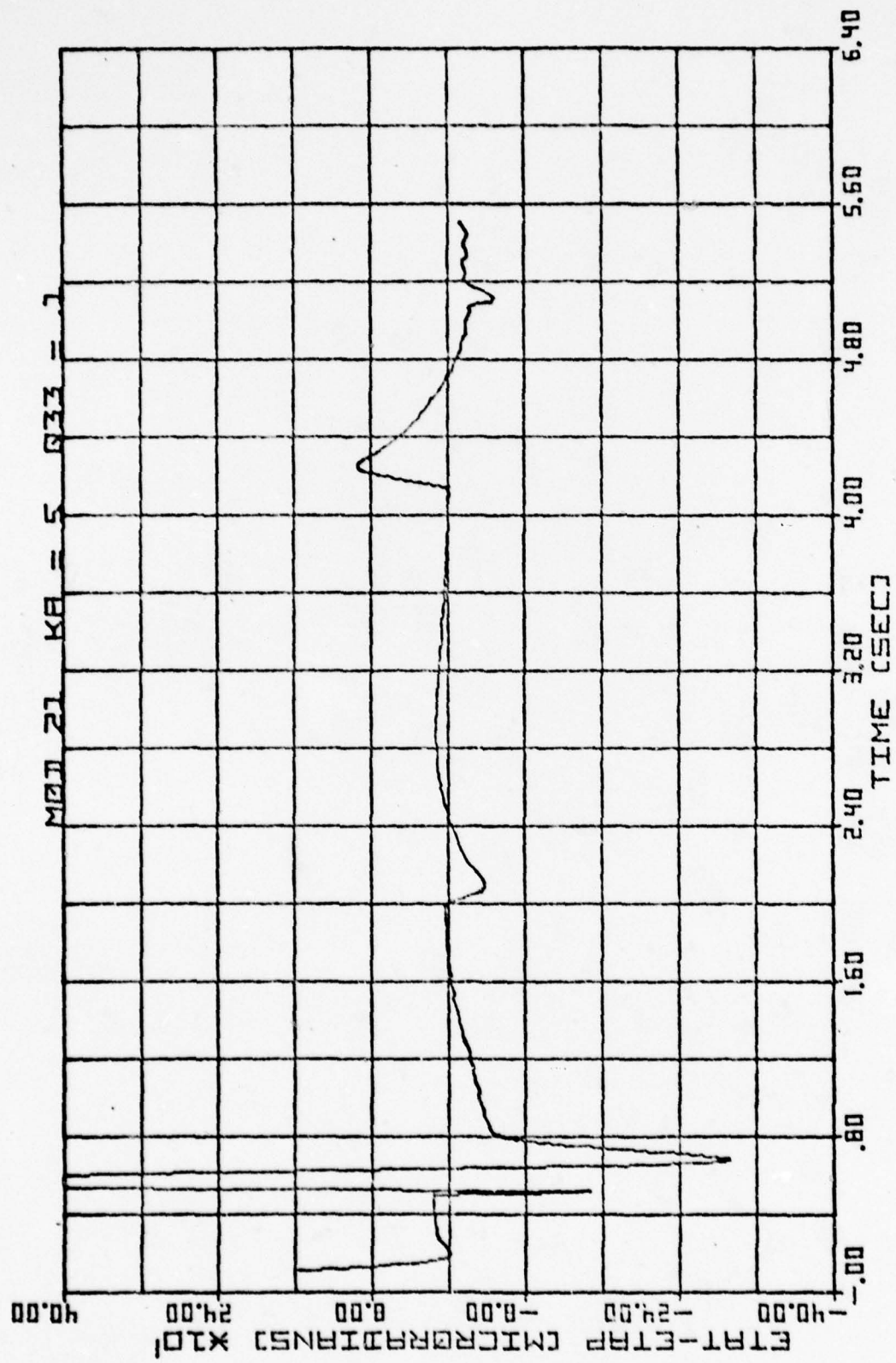


Fig. 19. Aided at 0.01 second rate by Modification Two with instantaneous update, Scenario Five.

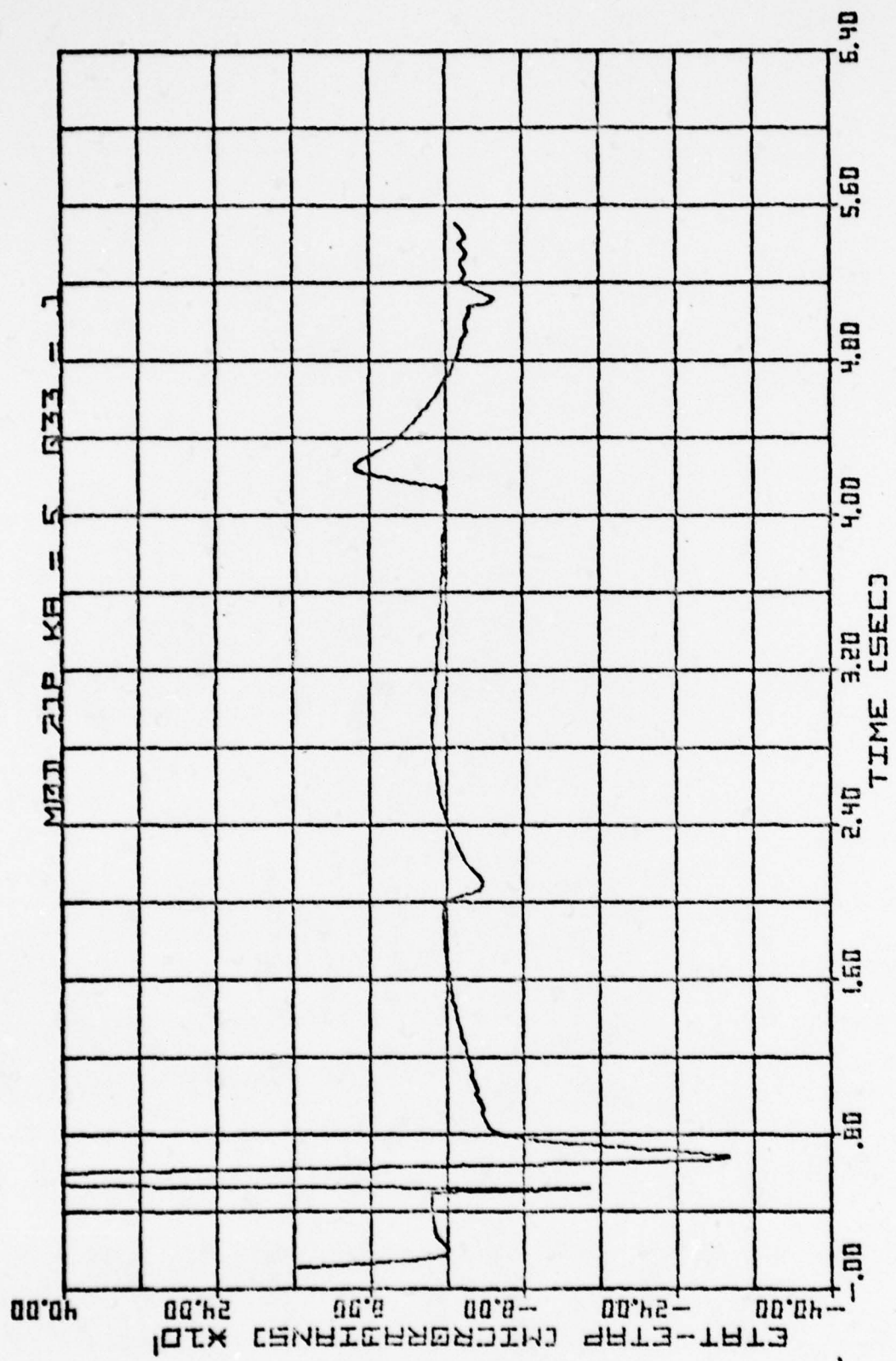
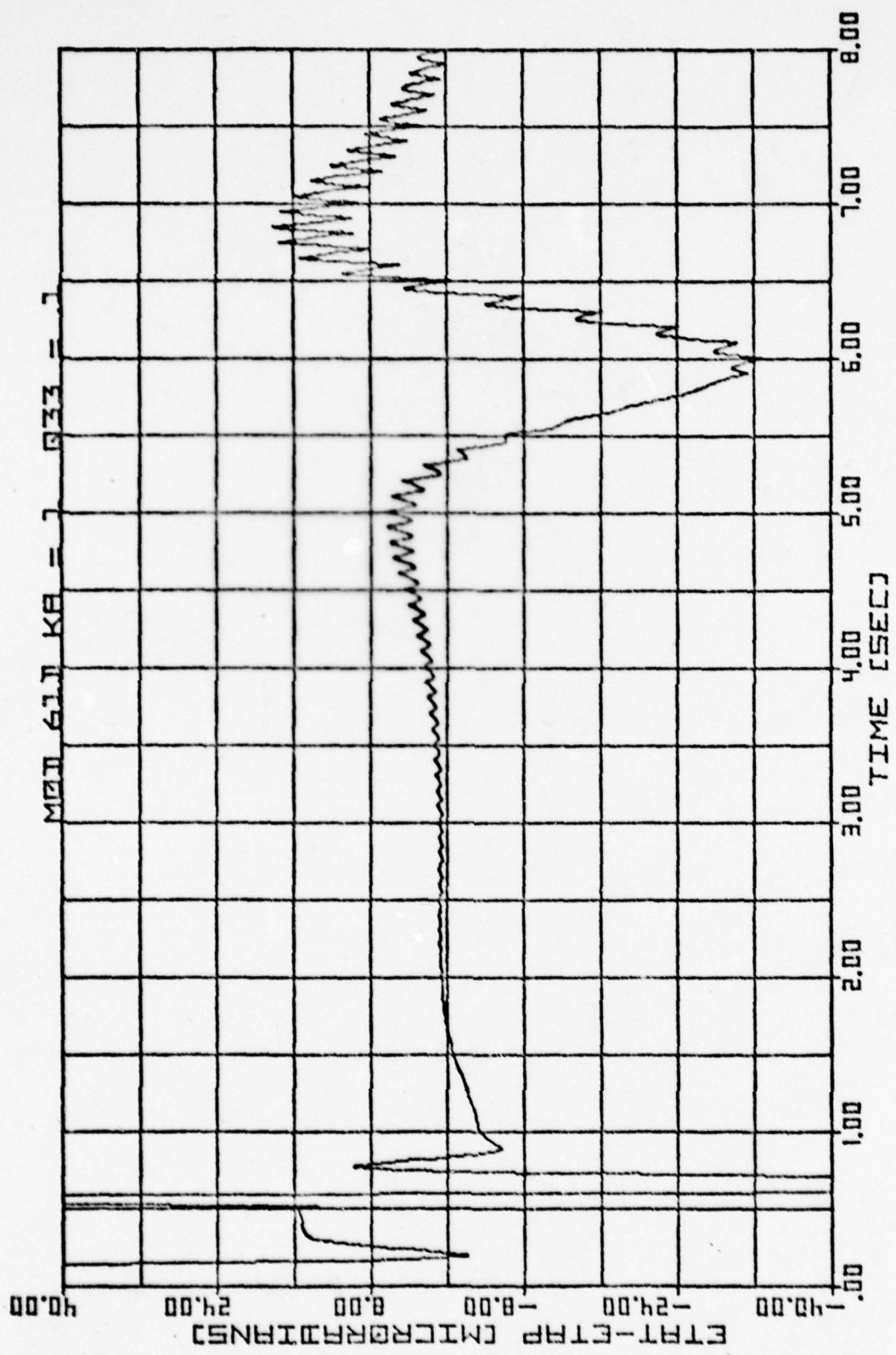


Fig. 20. Aided at 0.01 second rate by Modification Two with predicted update, Scenario Five.



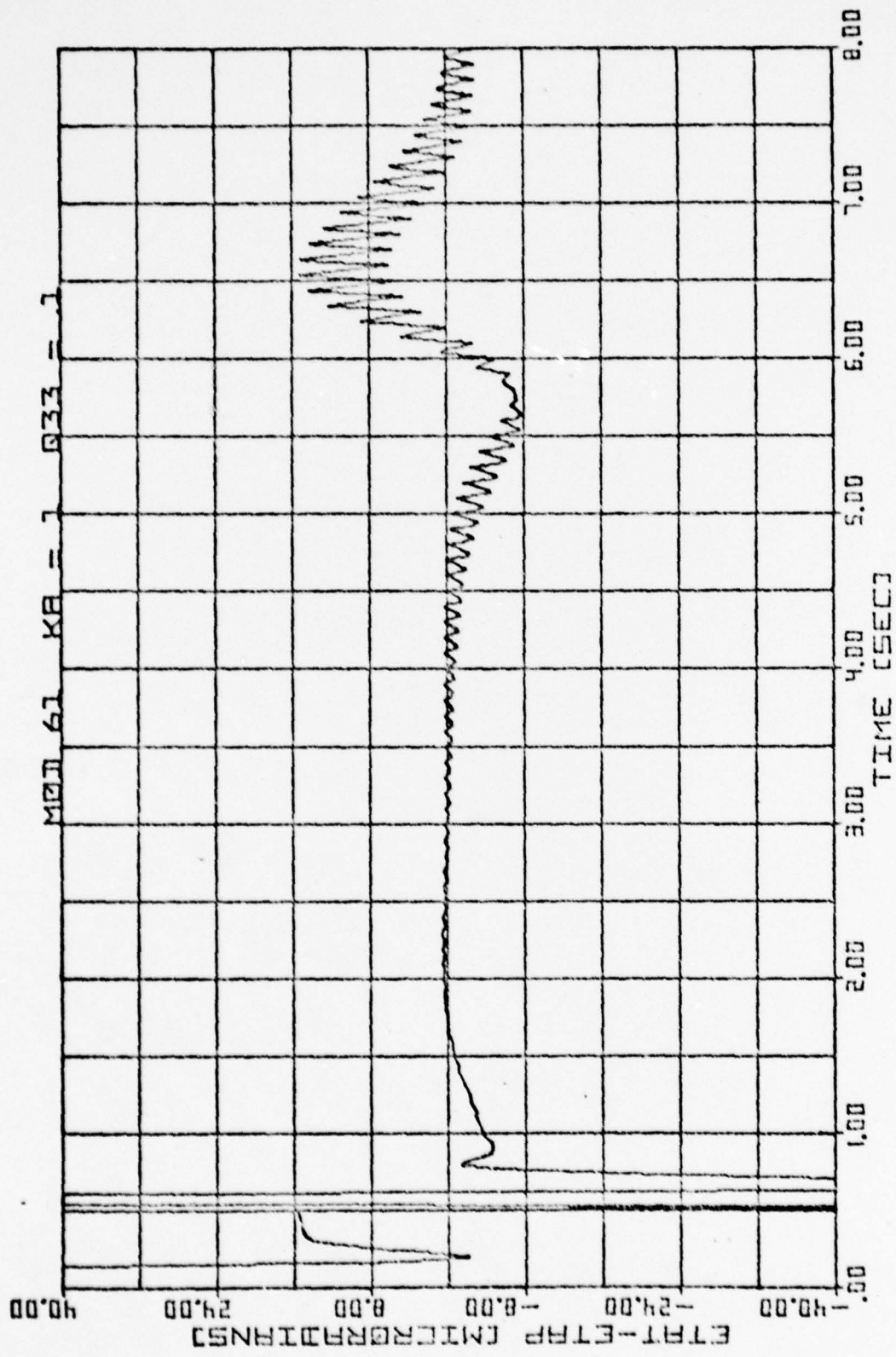


Fig. 22. Aided at 0.01 second rate by Modification Six with instantaneous update, Scenario One.

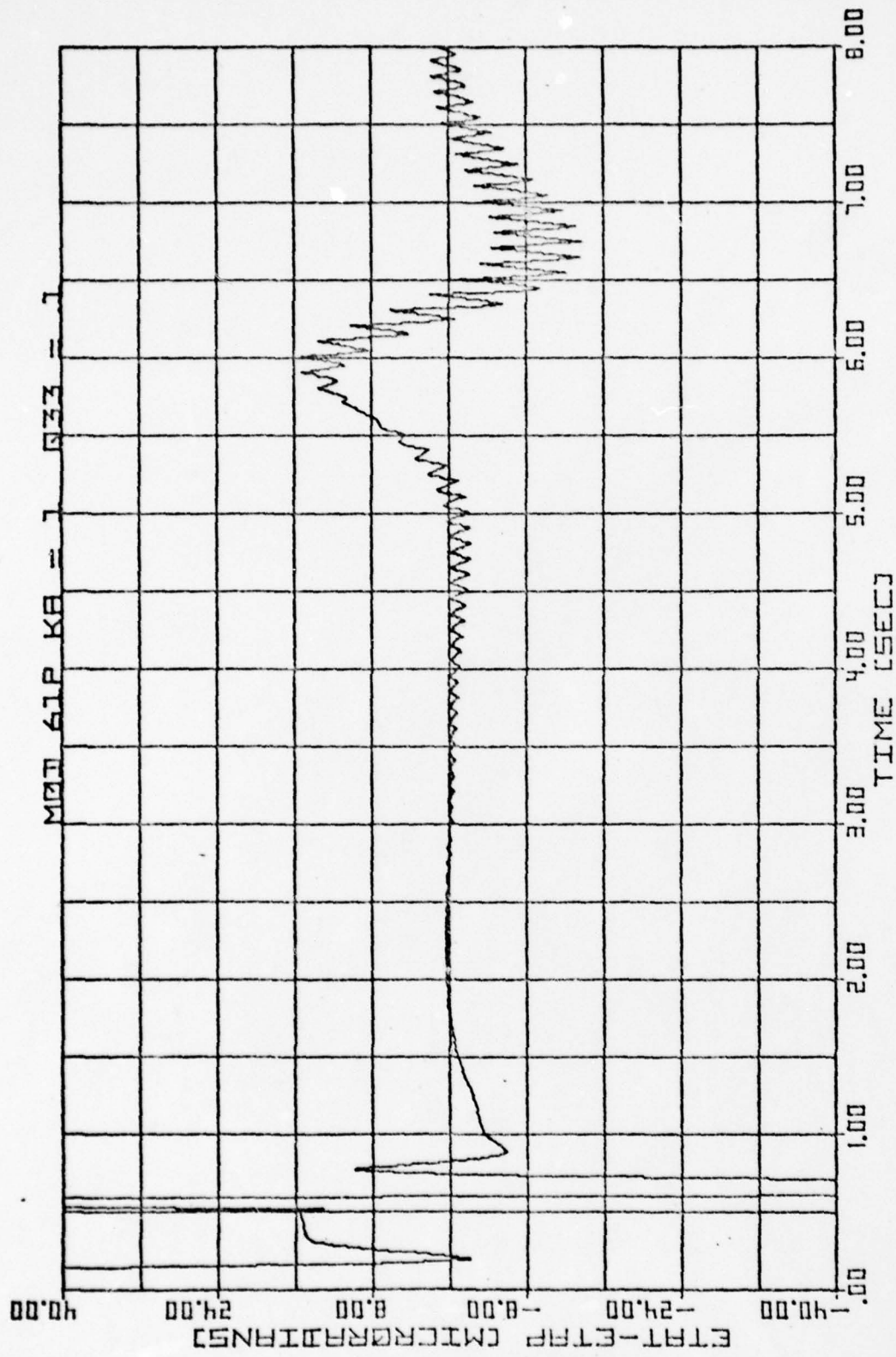


Fig. 23. Aided at 0.01 second rate by Modification Six with predicted update, Scenario One.

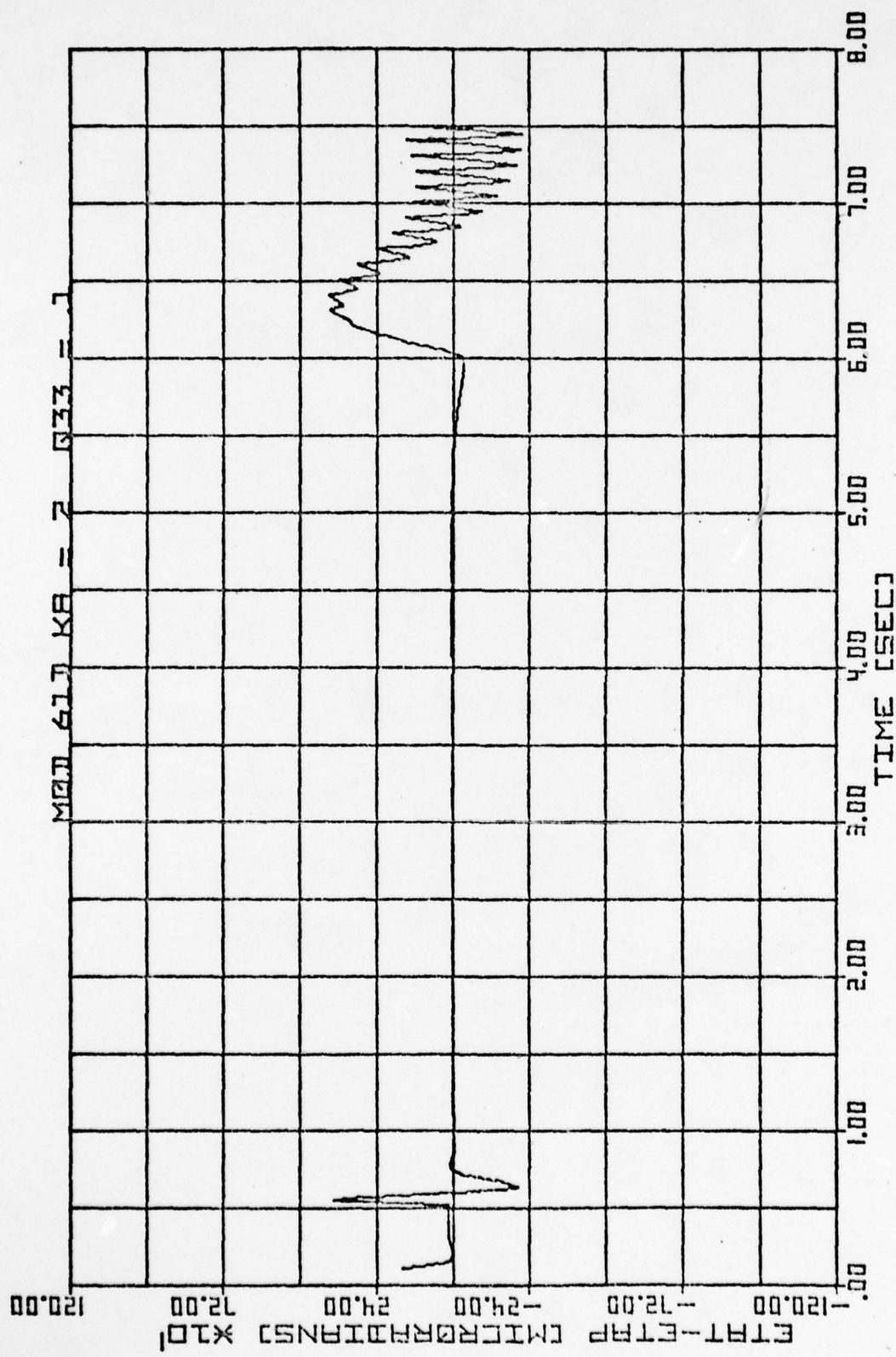


Fig. 24. Aided at 0.01 second rate by Modification Six with computational delay, Scenario Two.

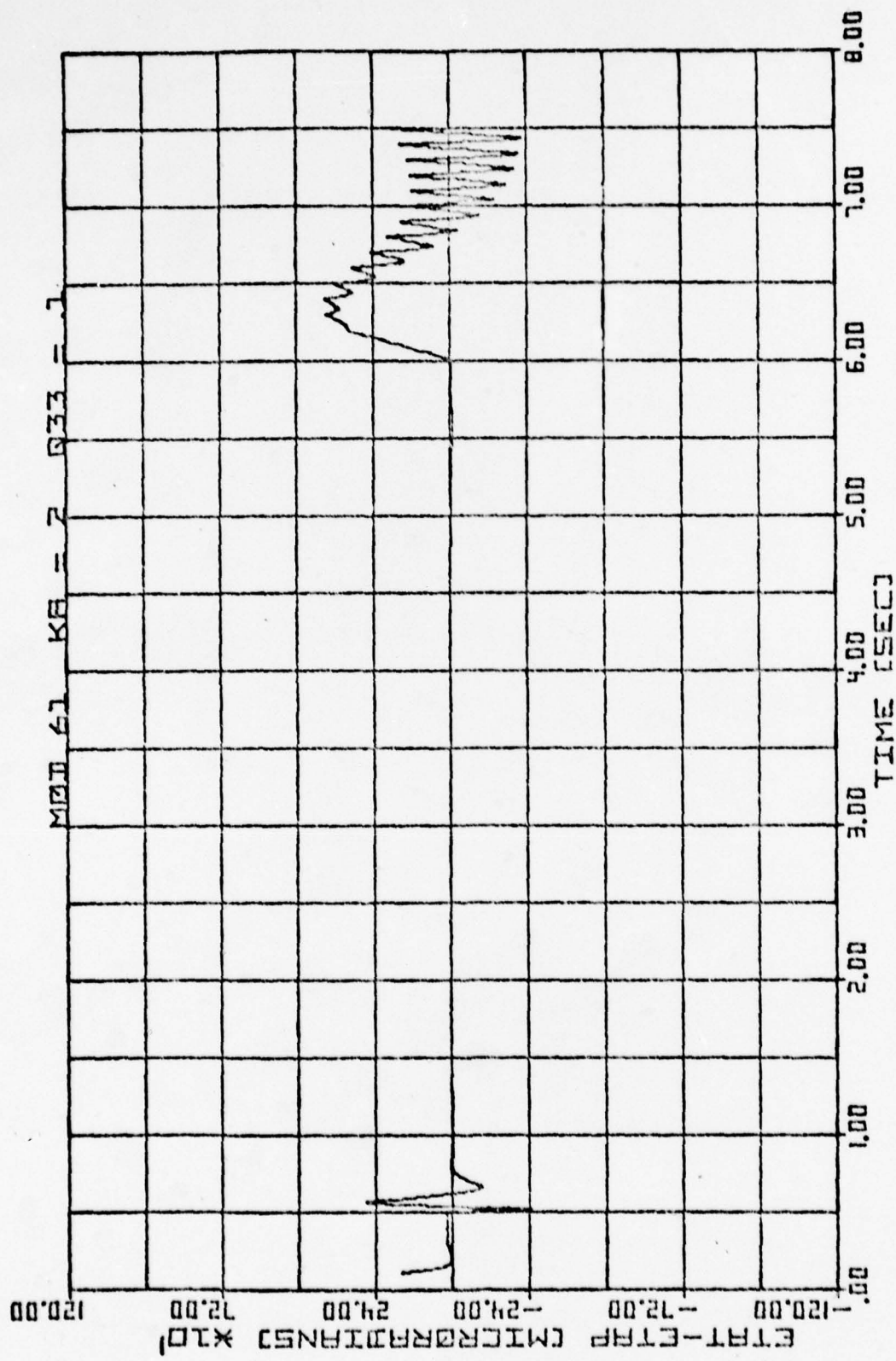


Fig. 25. Aided at 0.01 second rate by Modification Six with instantaneous update, Scenario Two.

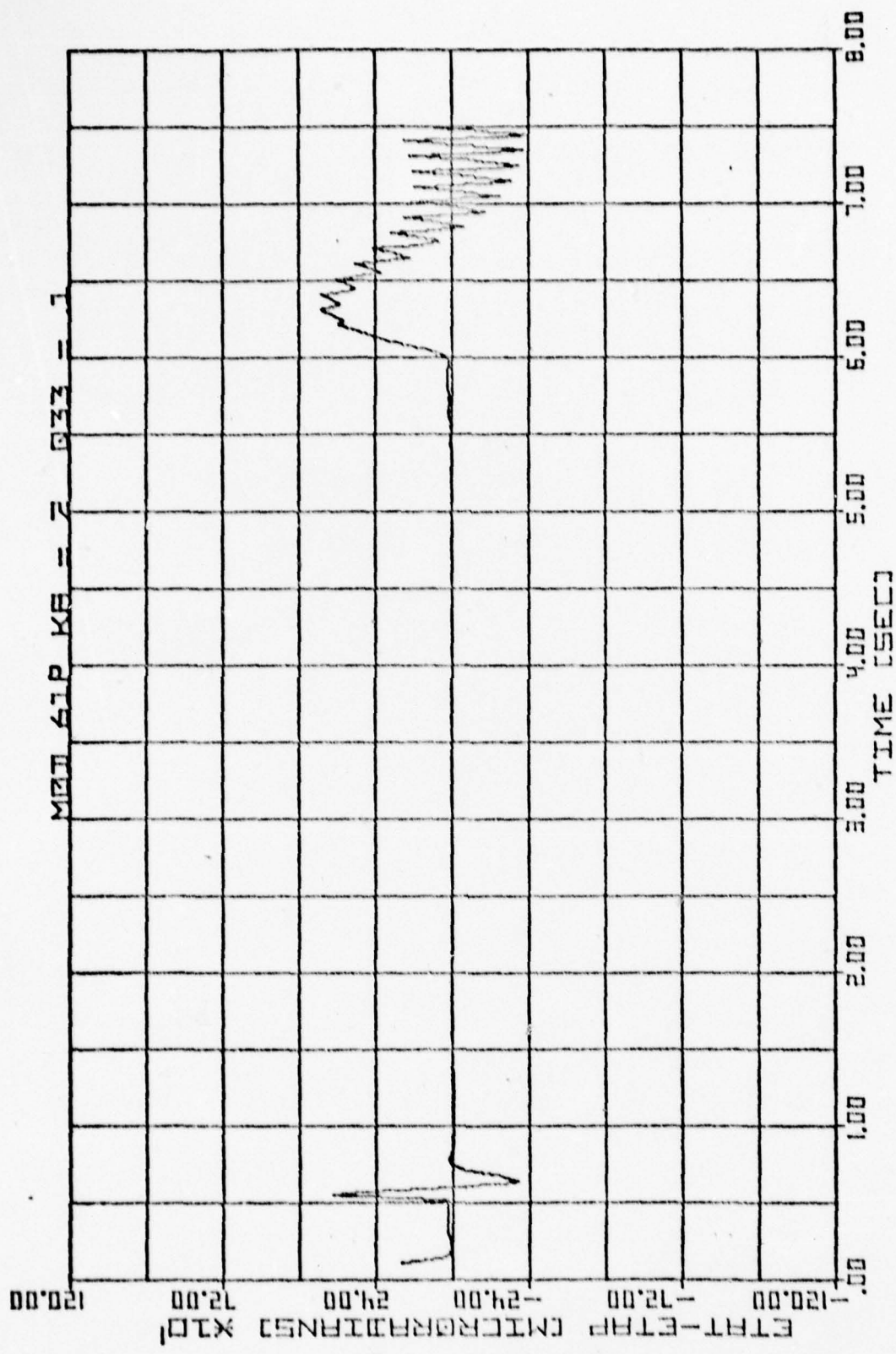


Fig. 26. Aided at 0.01 second rate by Modification Six with predicted update, Scenario Two.

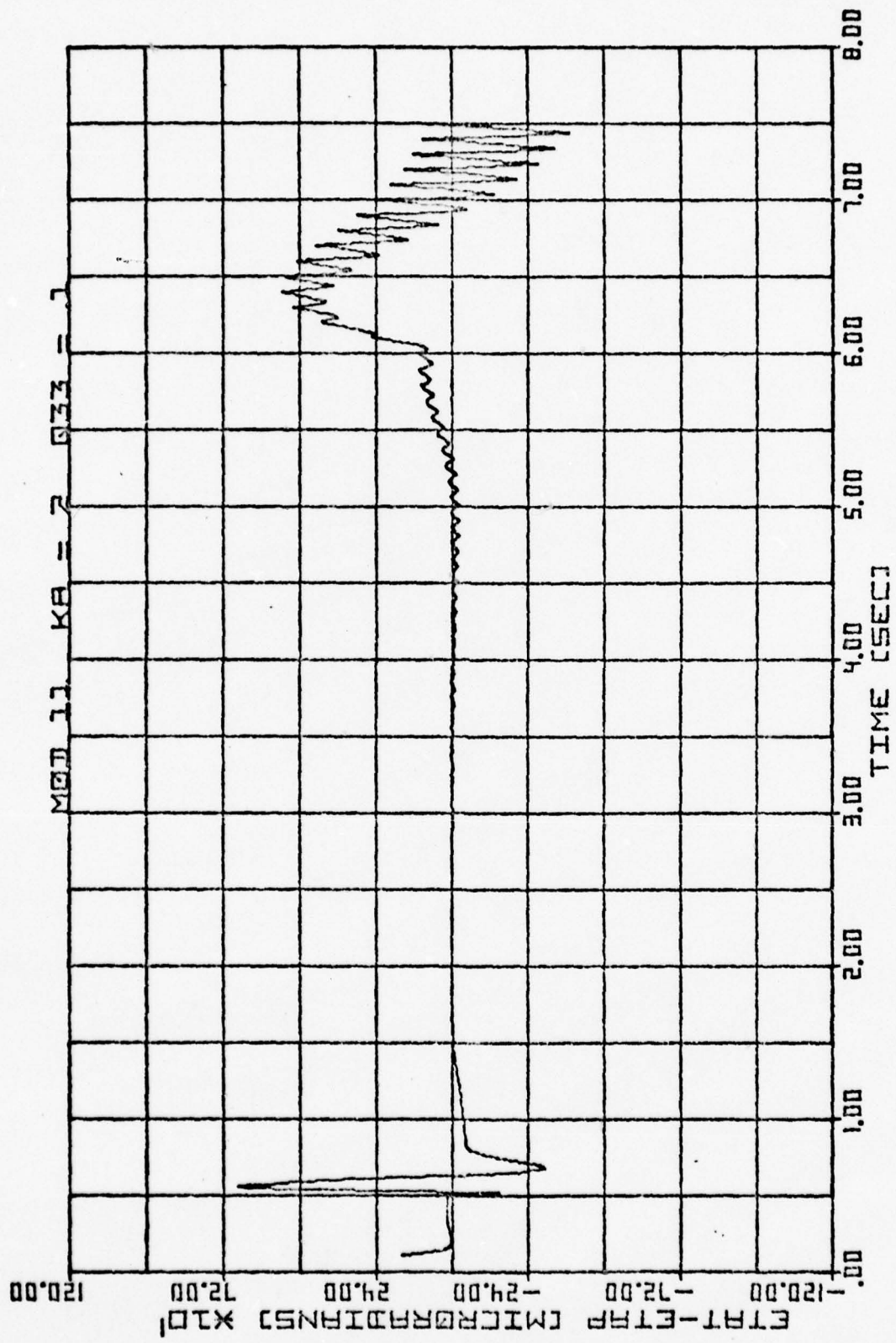


Fig. 27. Aided at 0.01 second rate by Modification One,
Scenario Two.

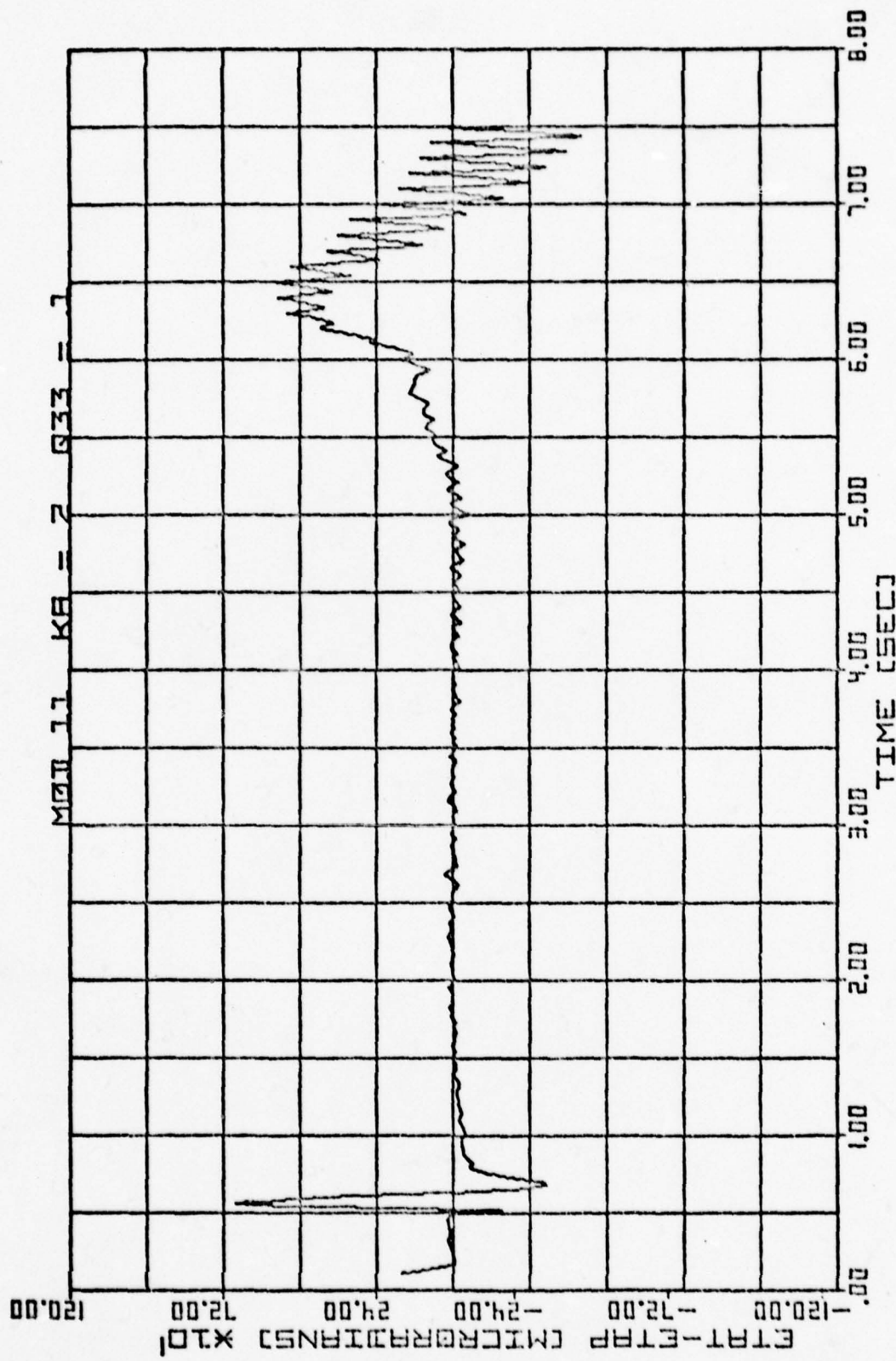


Fig. 28. Aided at 0.01 second rate by Modification One with measurement noise, Scenario Two.

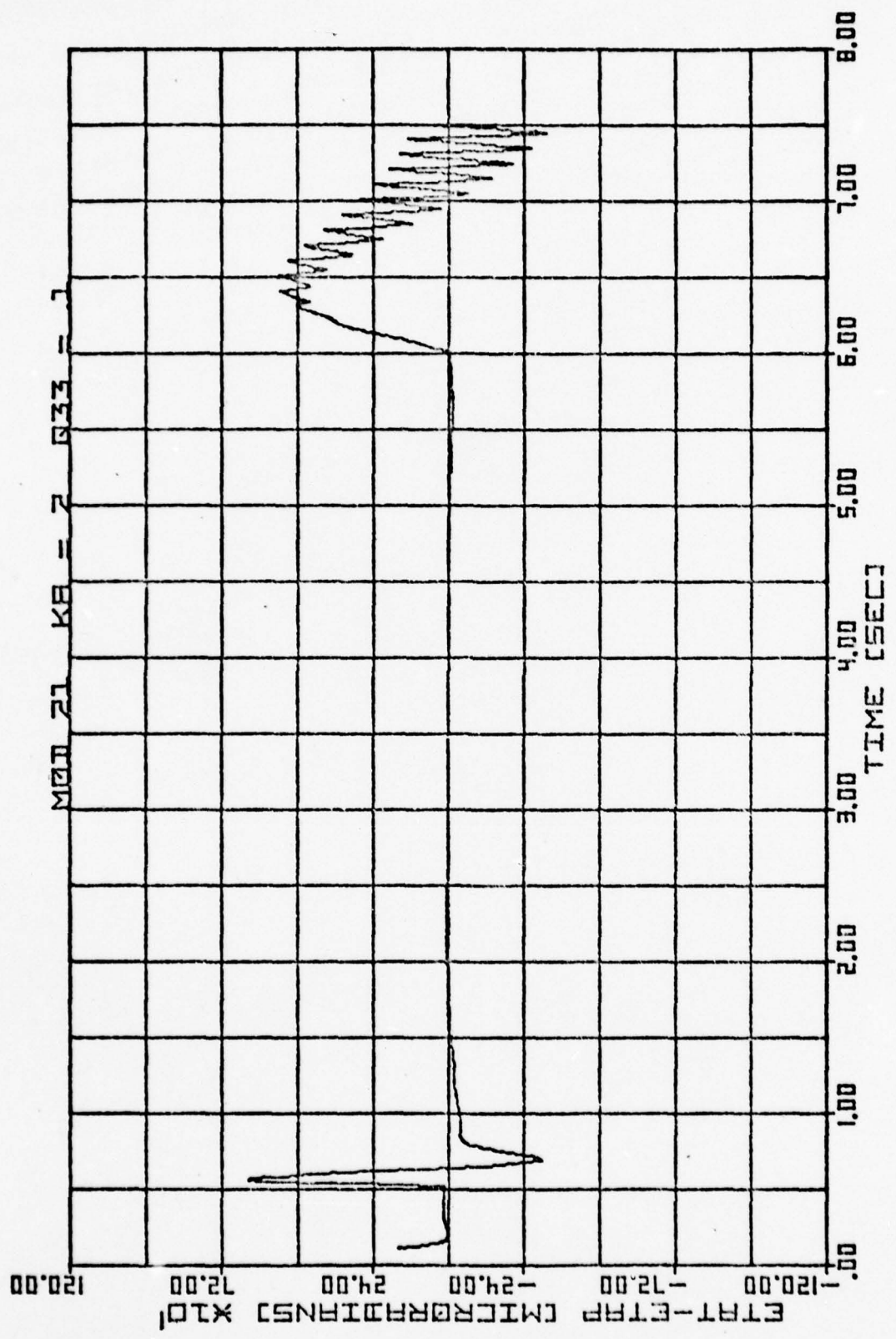


Fig. 29. Aided at 0.01 second rate by Modification Two, Scenario Two.

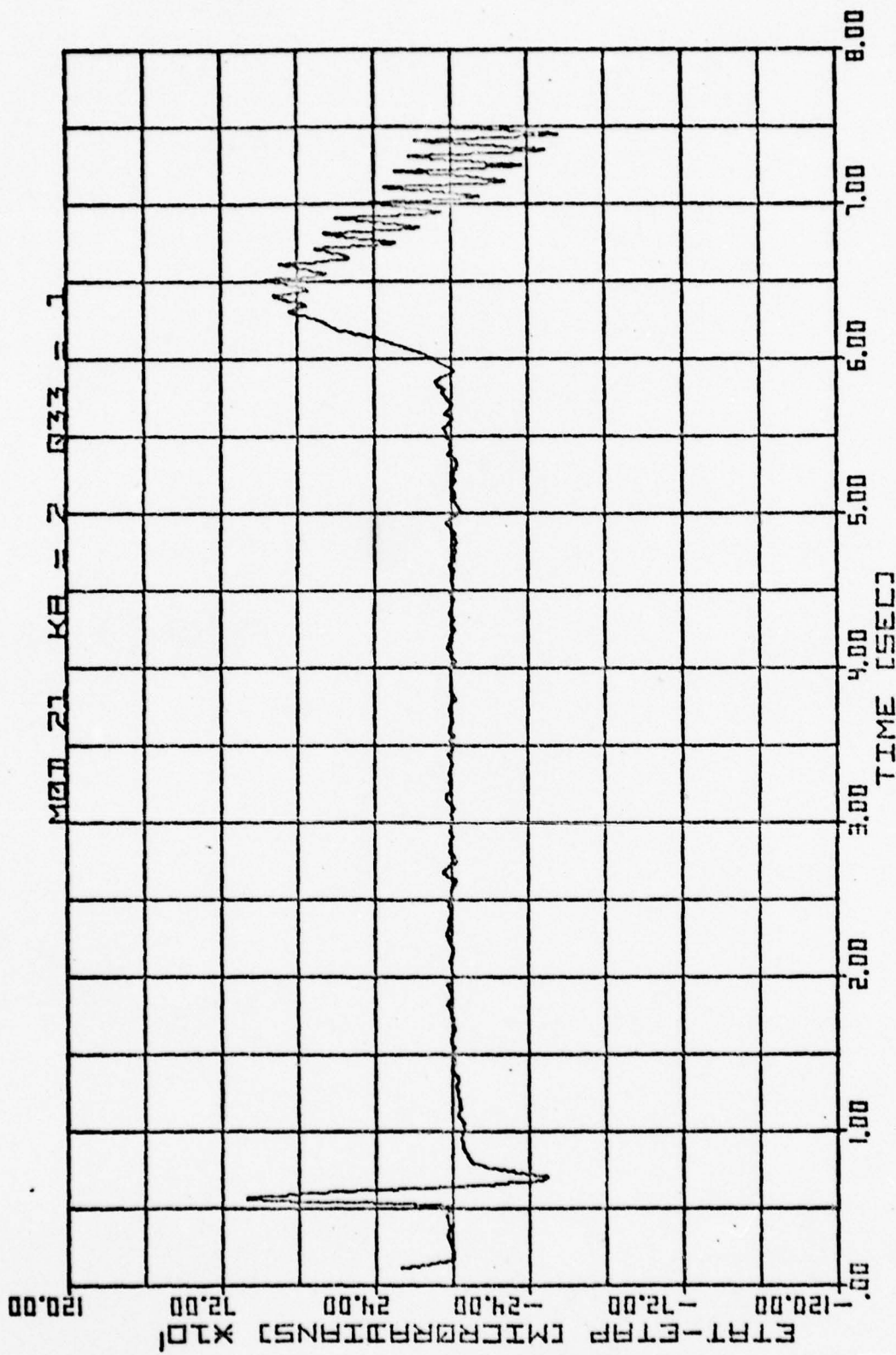


Fig. 30. Aided at 0.01 second rate by Modification Two with measurement noise, Scenario Two.

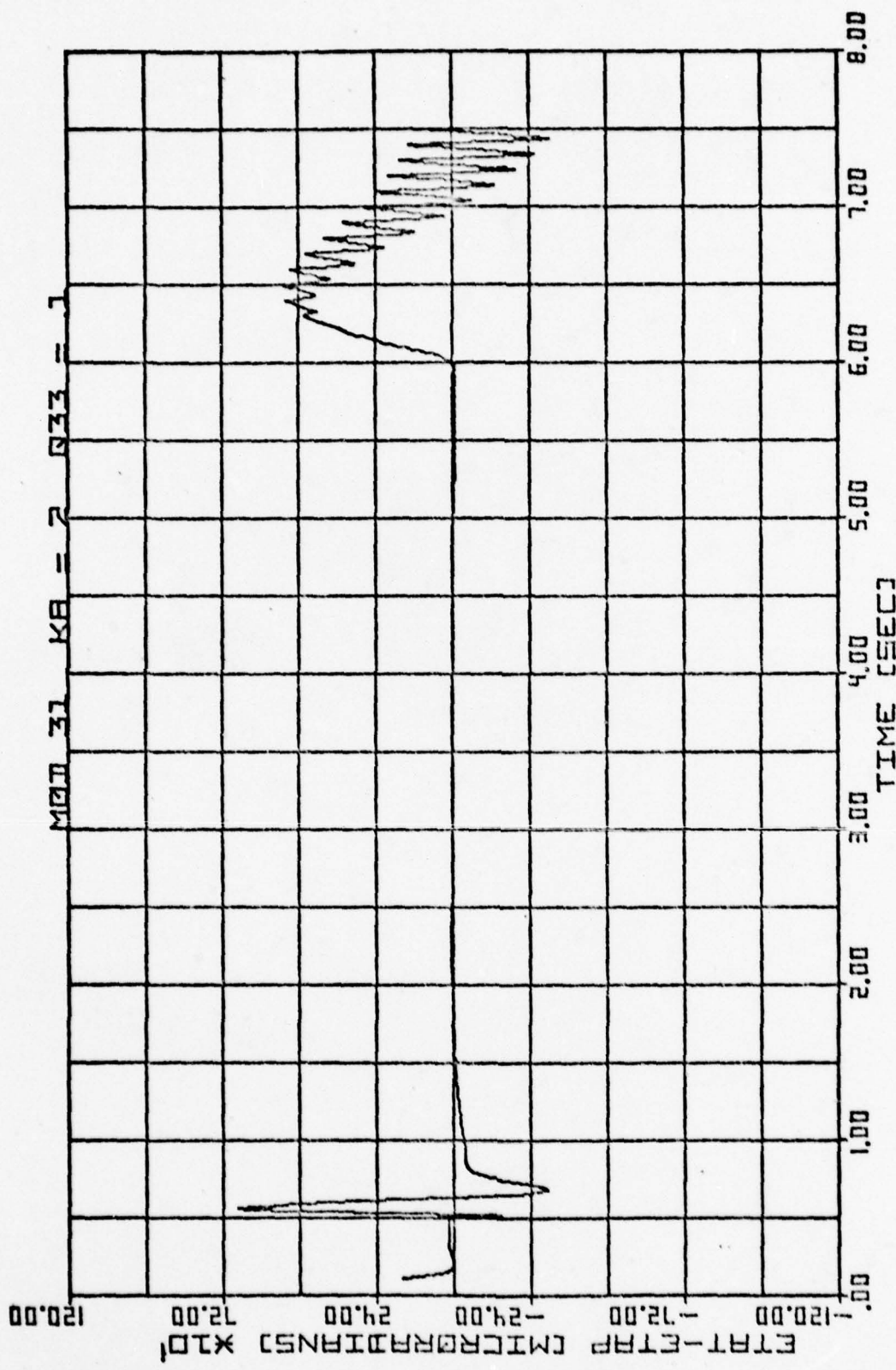


Fig. 31. Aided at 0.01 second rate by Modification Three,
Scenario Two.

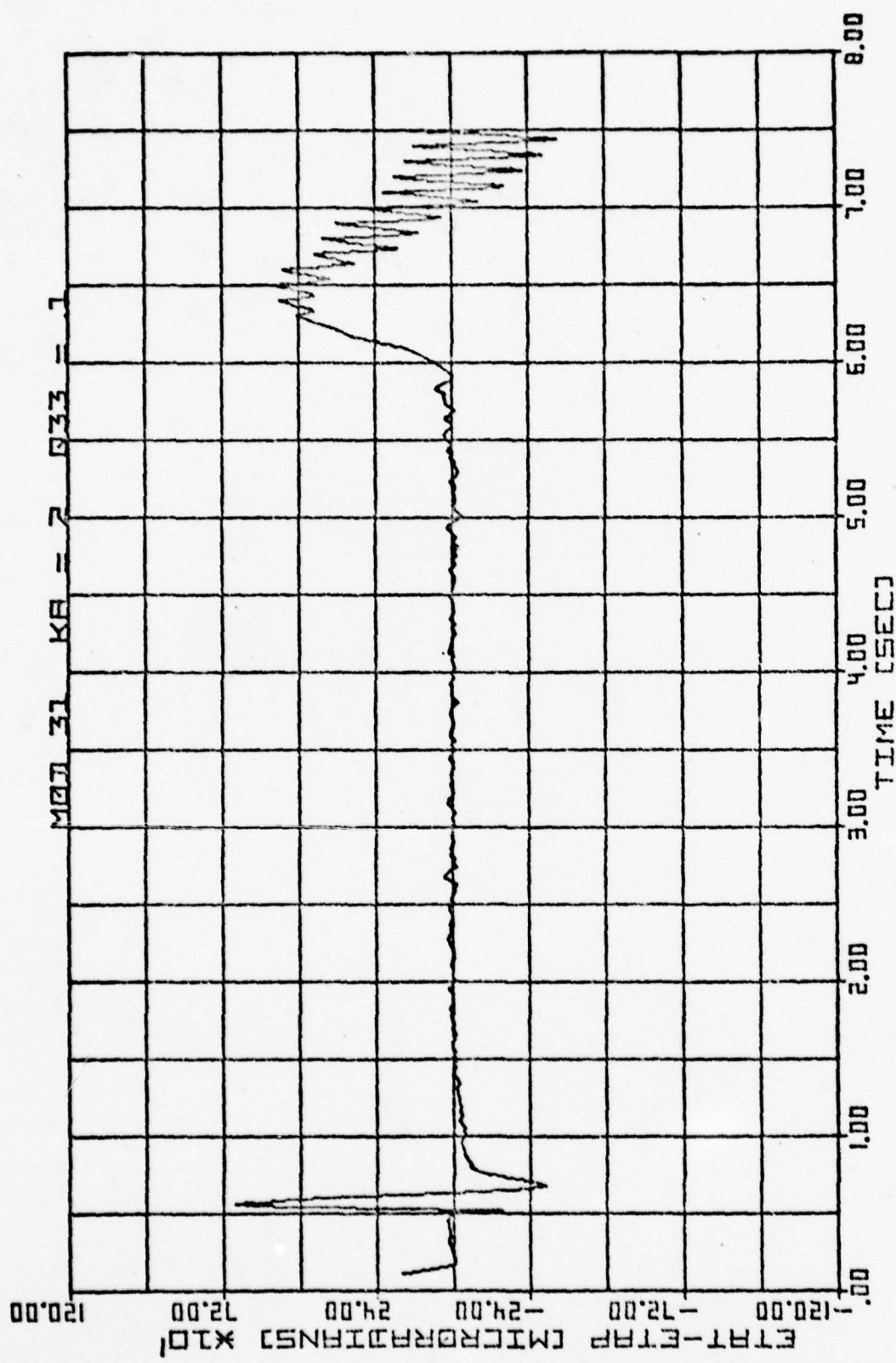


Fig. 32. Aided at 0.01 second rate by Modification Three, with measurement noise, Scenario Two.

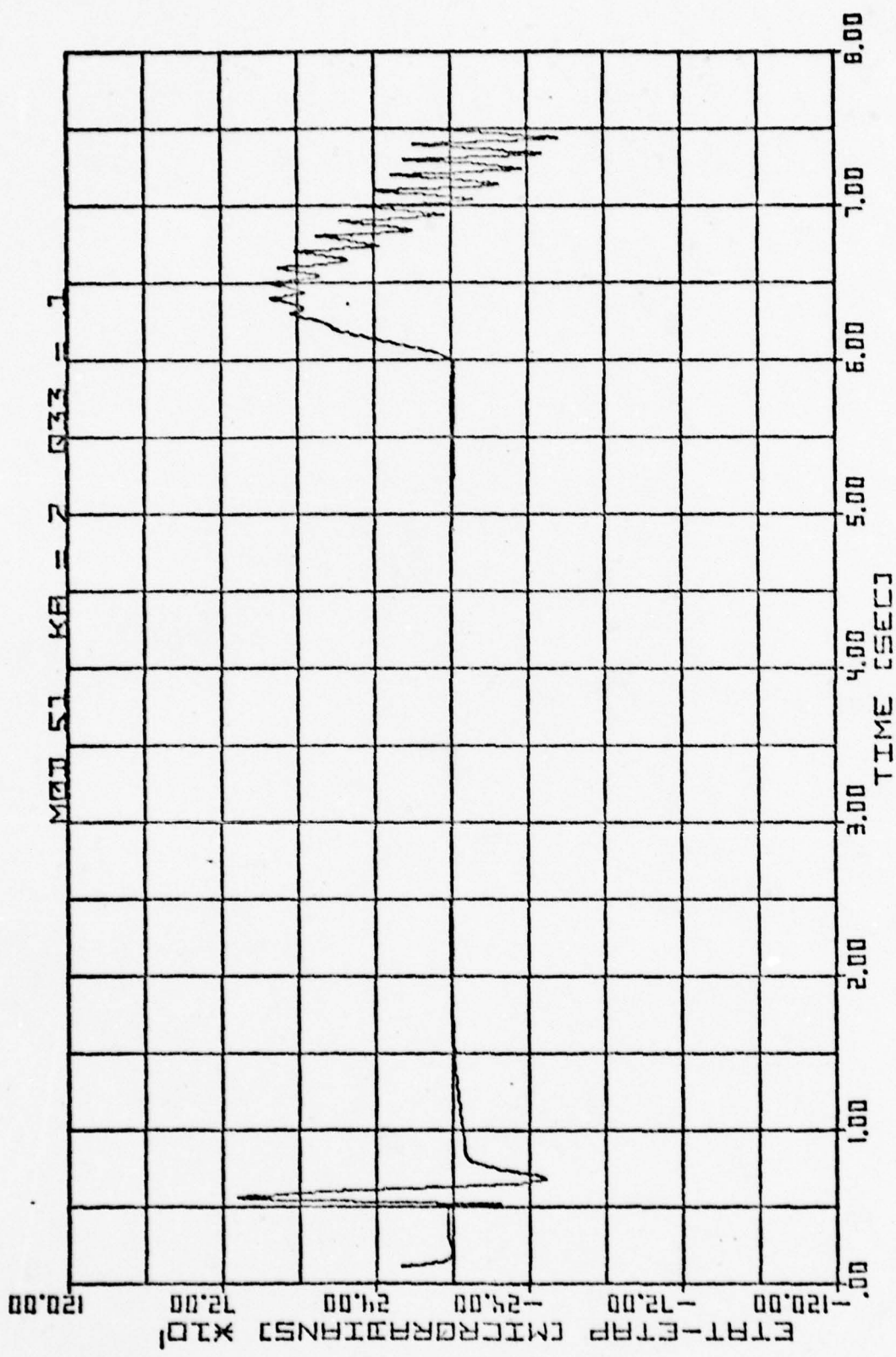


Fig. 33. Aided at 0.01 second rate by Modification Five,
Scenario Two.

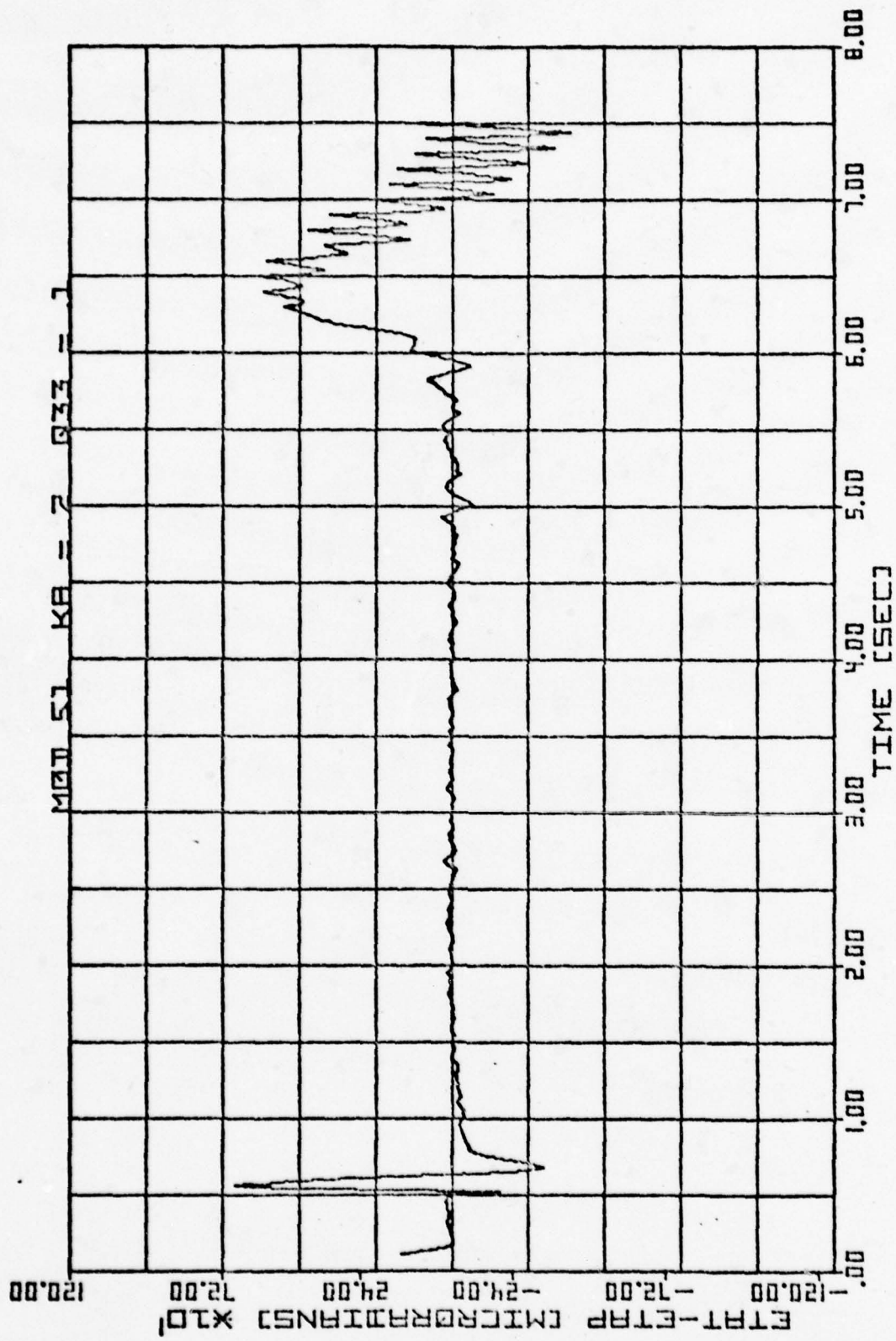


Fig. 34. Aided at 0.01 second rate by Modification Five with measurement noise, Scenario Two.

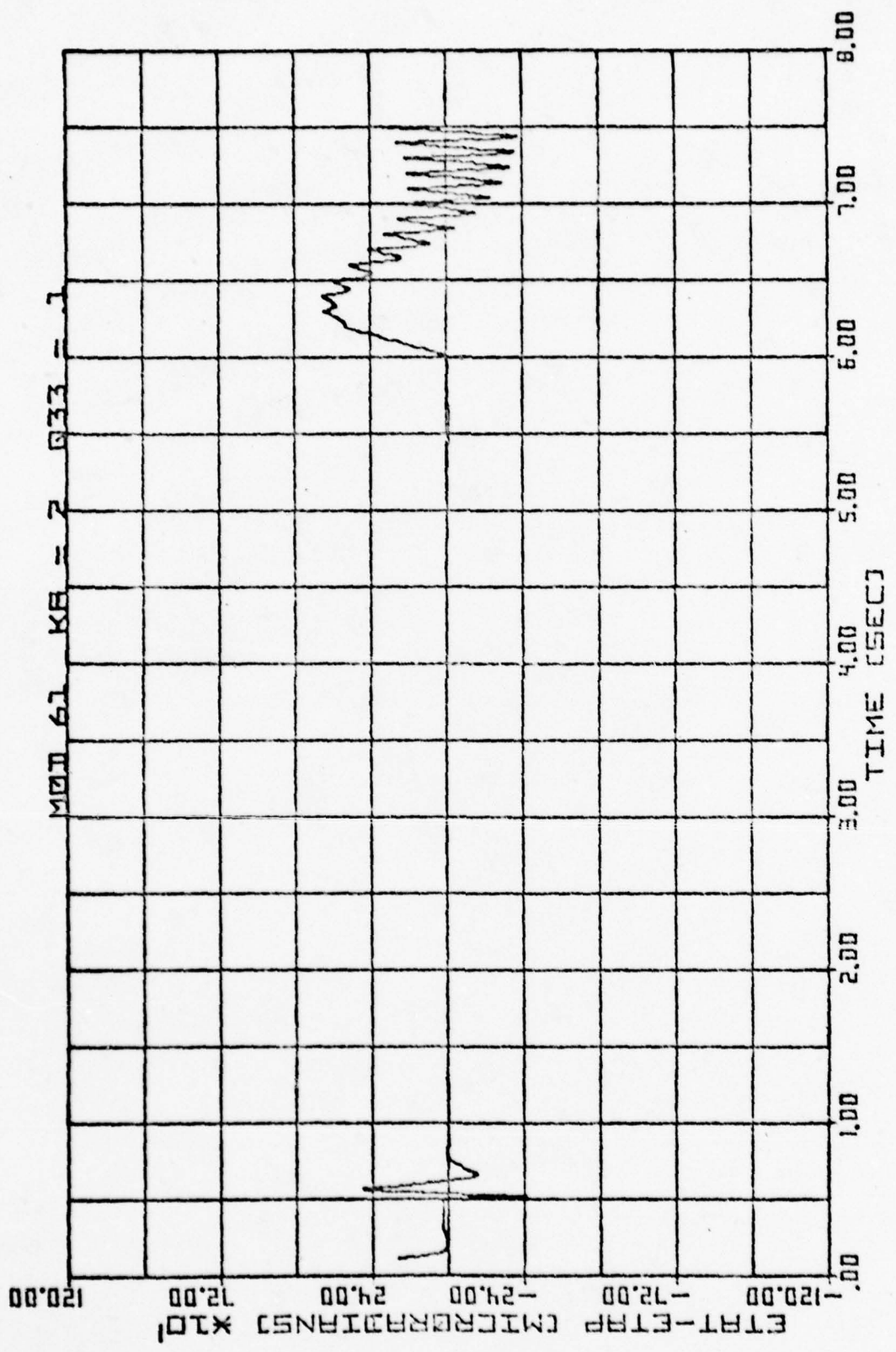


Fig. 35. Aided at 0.01 second rate by Modification Six, Scenario Two.

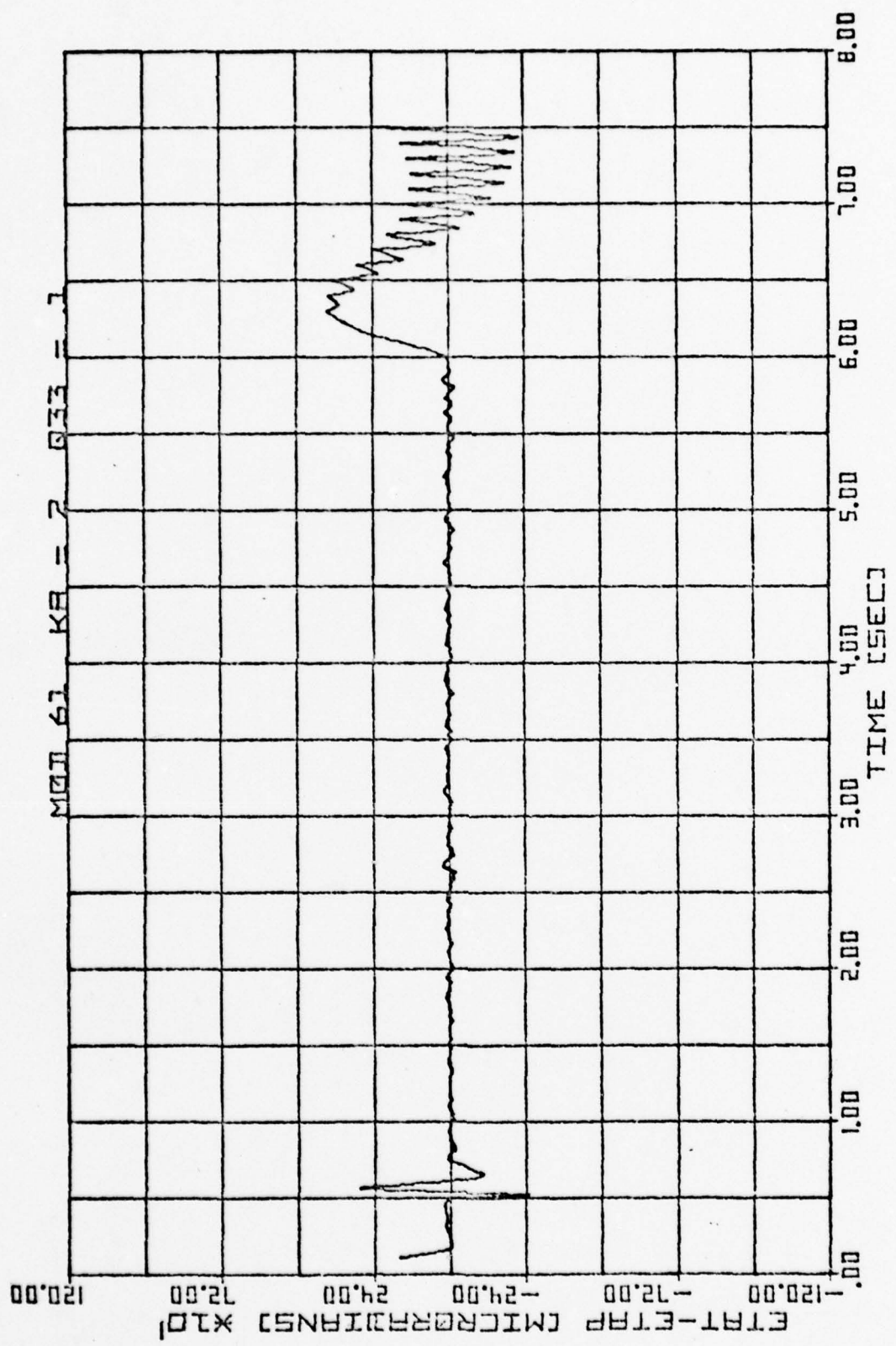


Fig. 36. Aided at 0.01 second rate by Modification Six, with measurement noise, Scenario Two

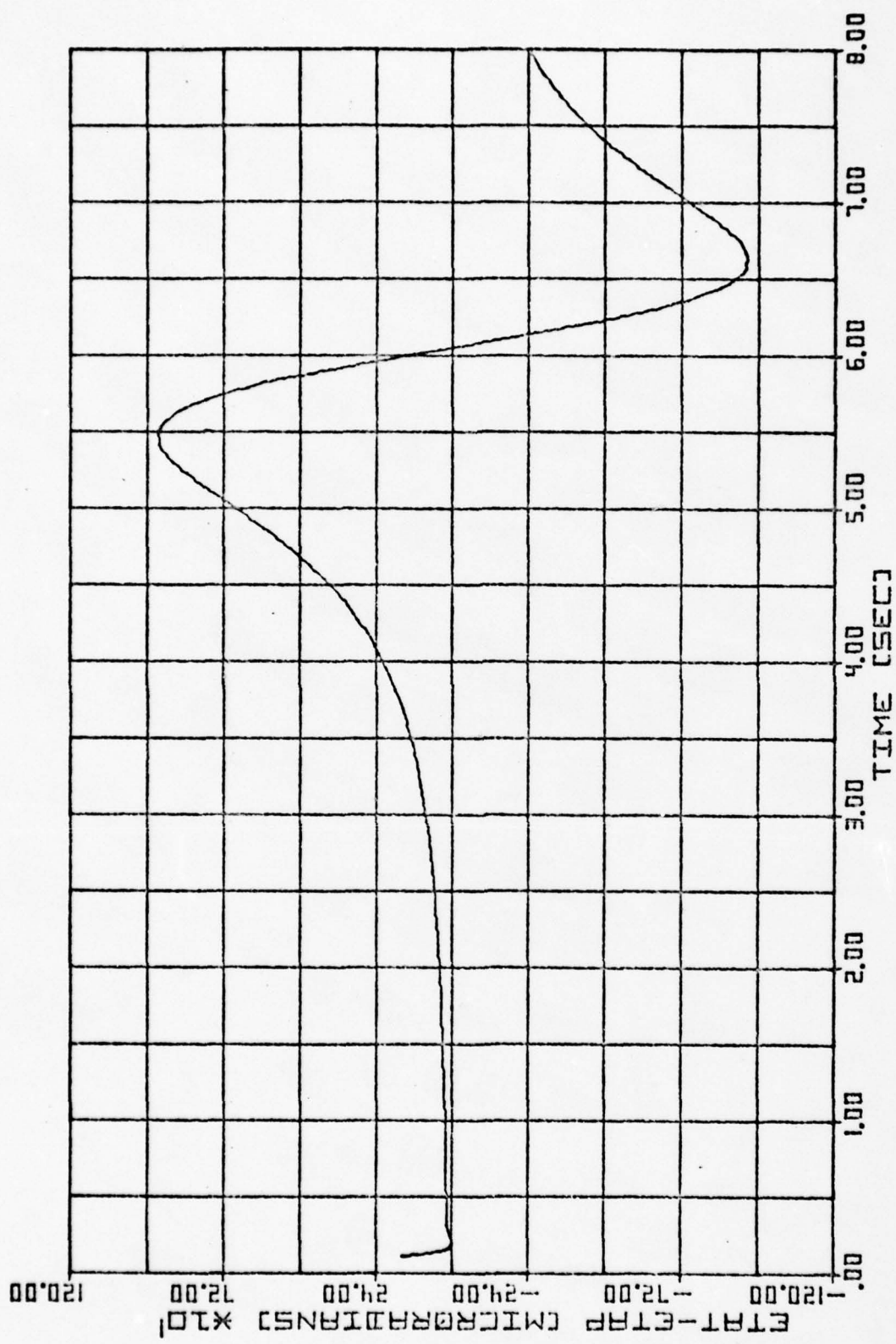


Fig. 37. Unaided tracking of Scenario One.

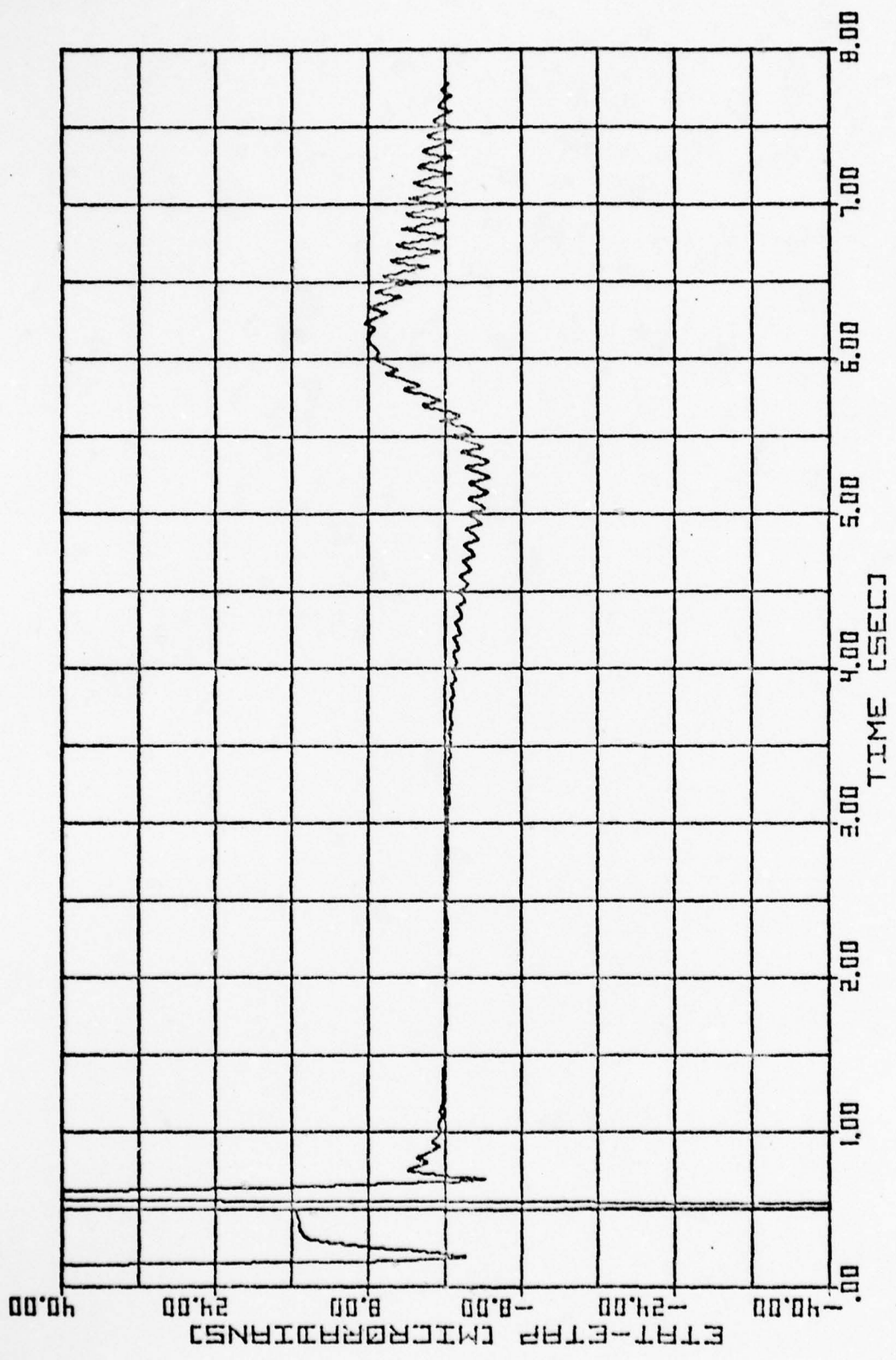


Fig. 38. Aided at 0.1 second rate, $Q_{33} = 1.0$, Scenario One.

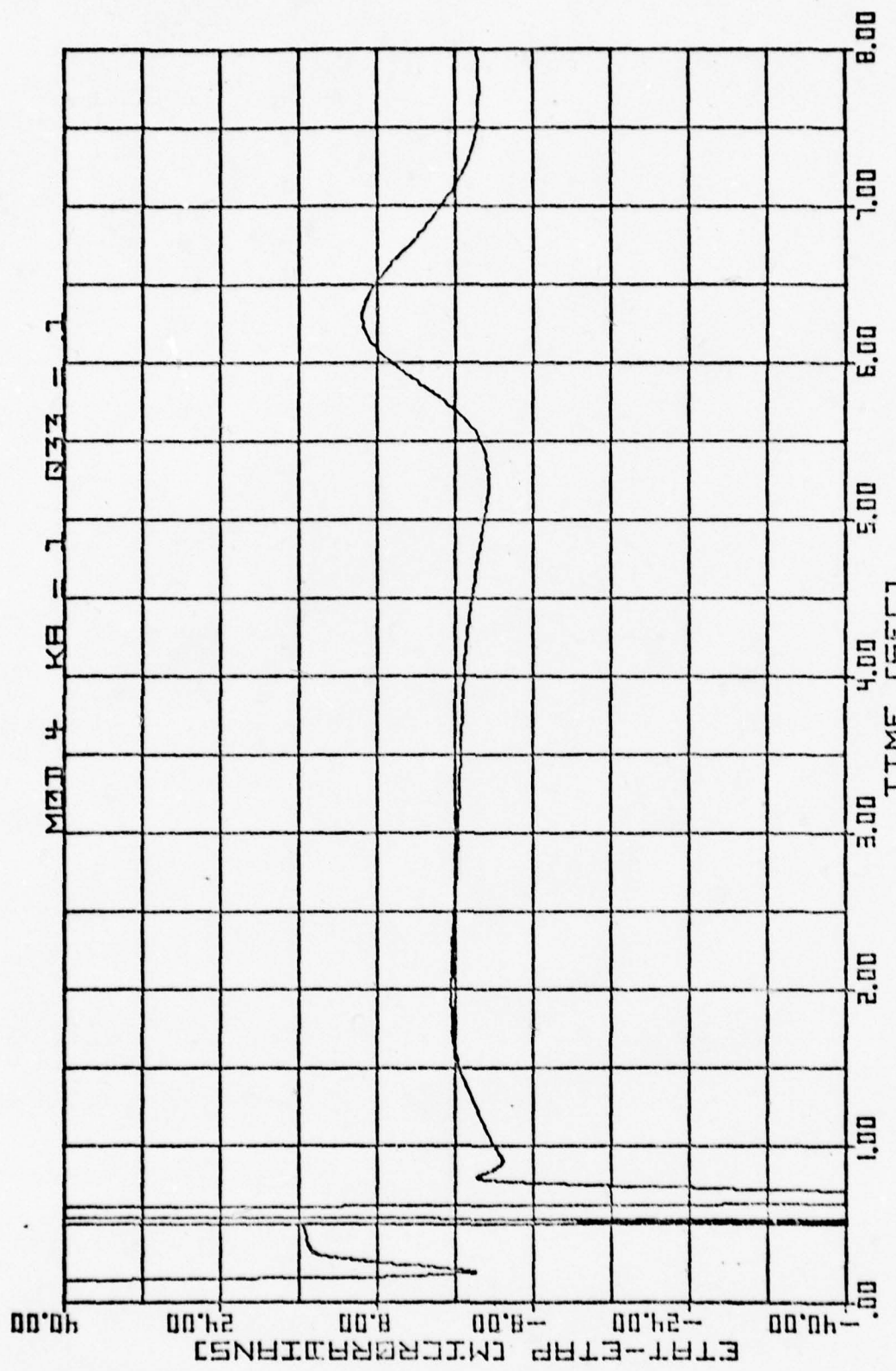


Fig. 39. Aided at 0.01 second rate with laser rangefinder
Optimal modification, Scenario One.

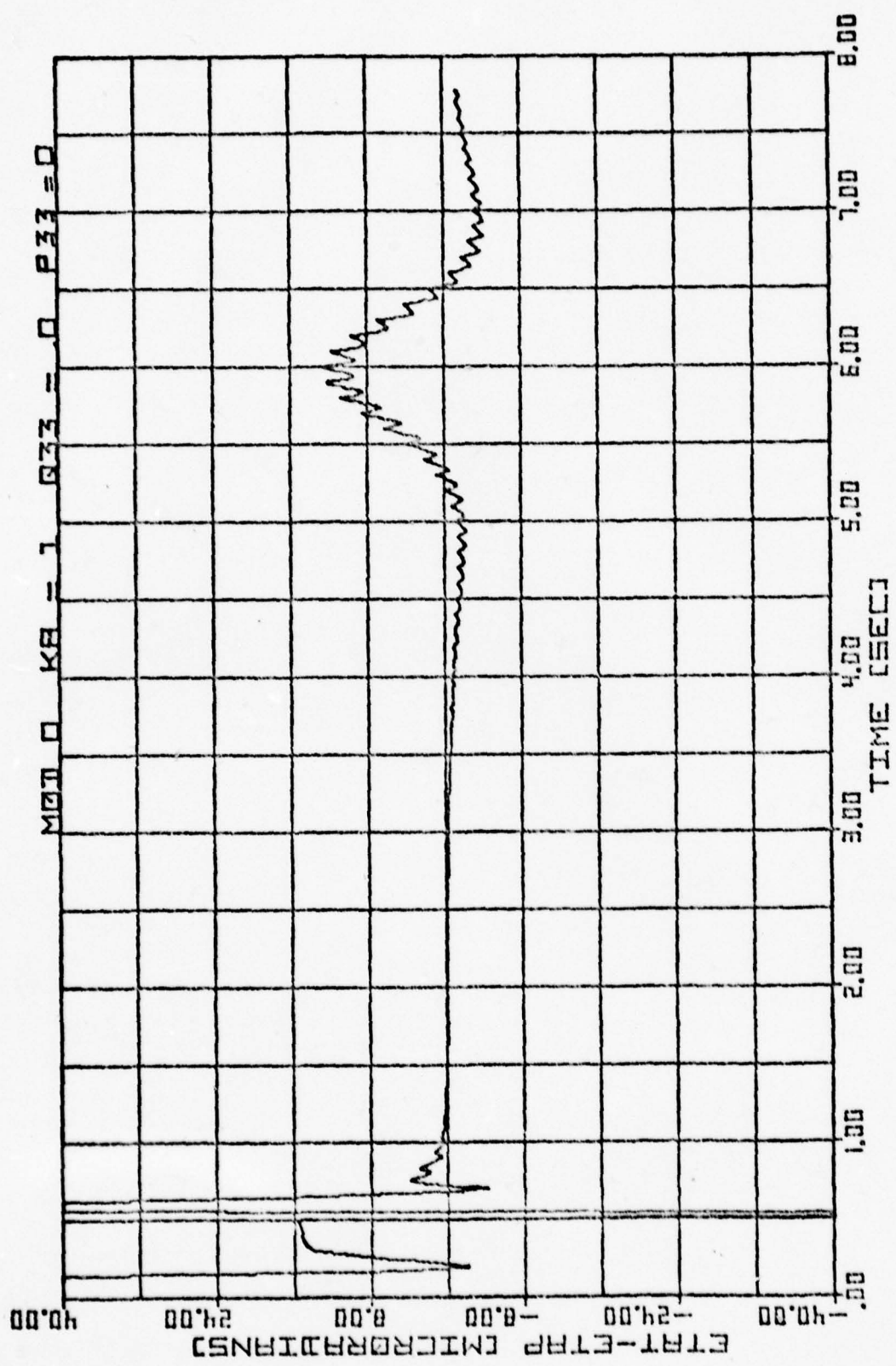


Fig. 40. Aided at 0.1 second rate, $Q_{33} = P_{33} = 0.0$, Scenario One.

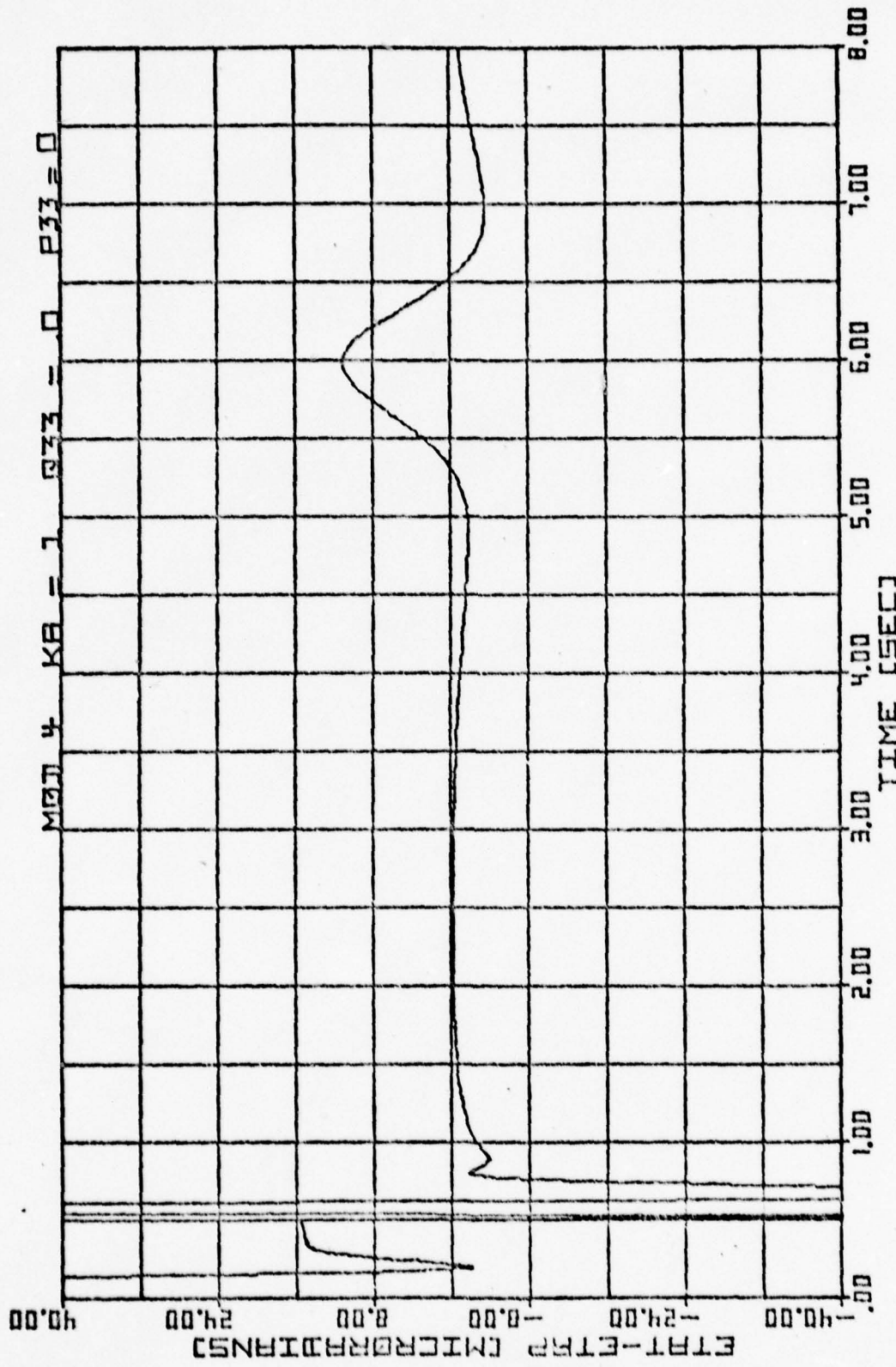


Fig. 41. Aided at 0.01 second rate by Modification Four,
 $Q_{33} = 0.0$, Scenario One.

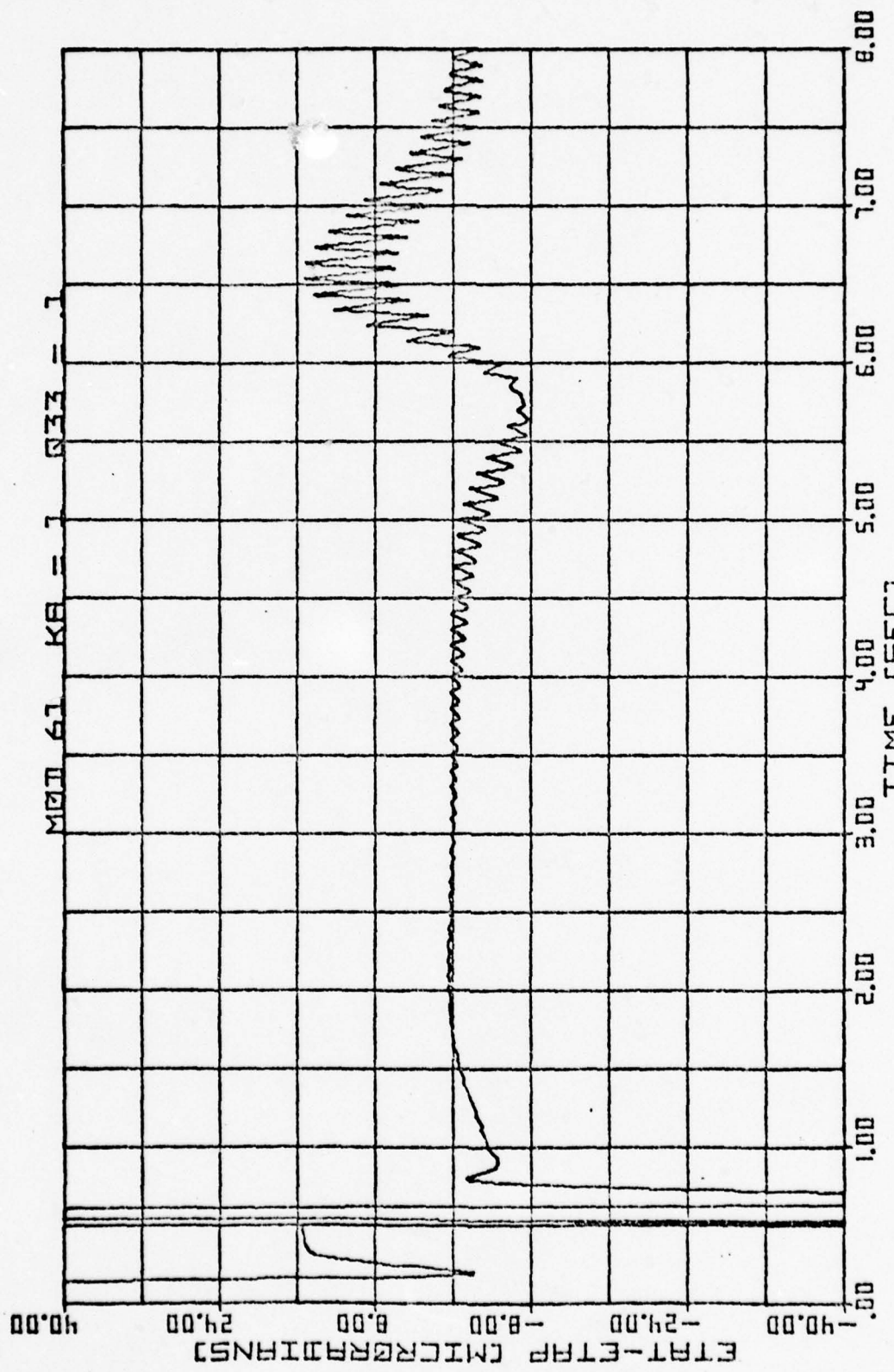


Fig. 42. Aided at 0.01 second rate by Modification Six, Scenario One.

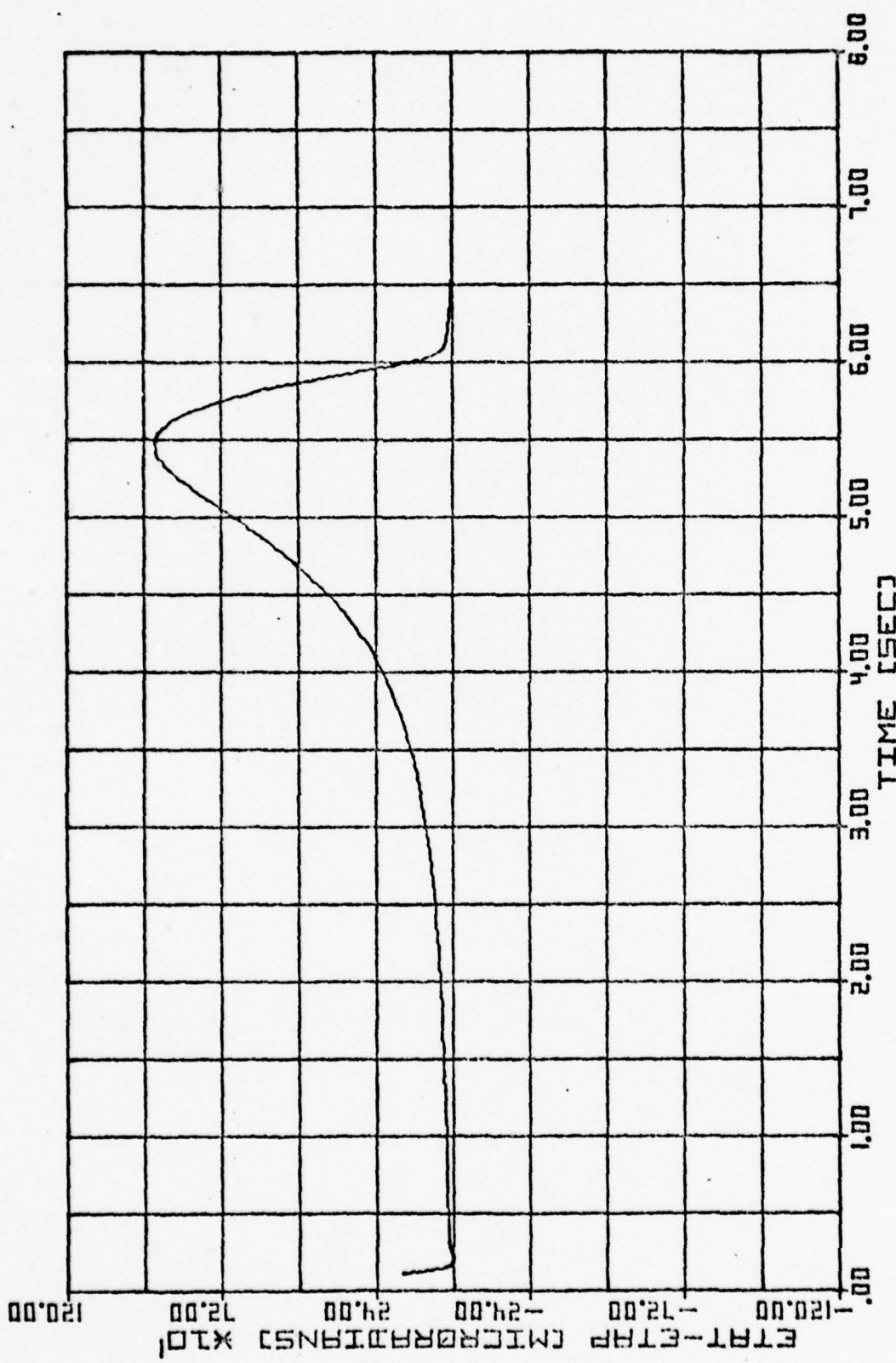
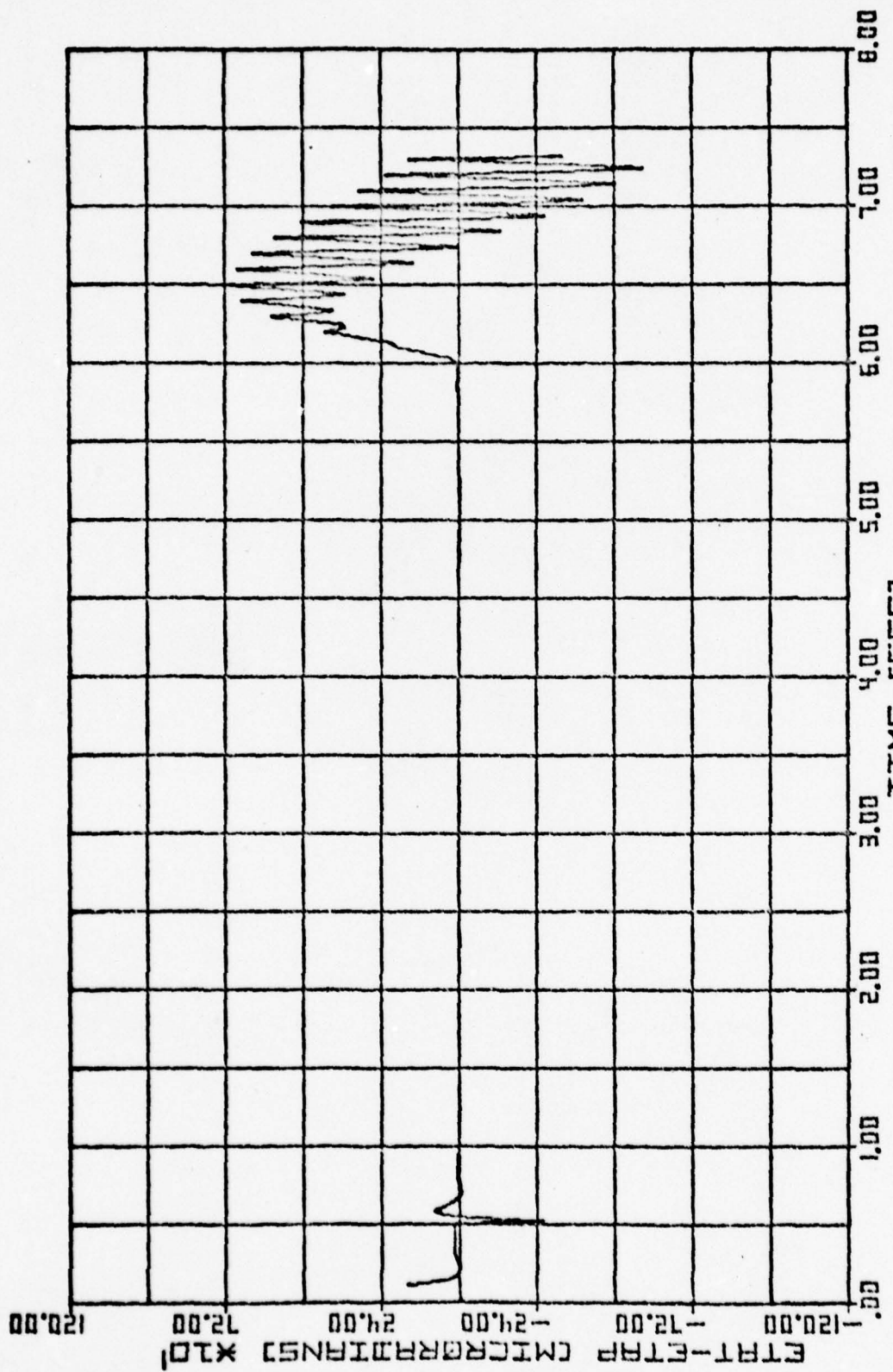


Fig. 43. Unaided tracking of Scenario Two.



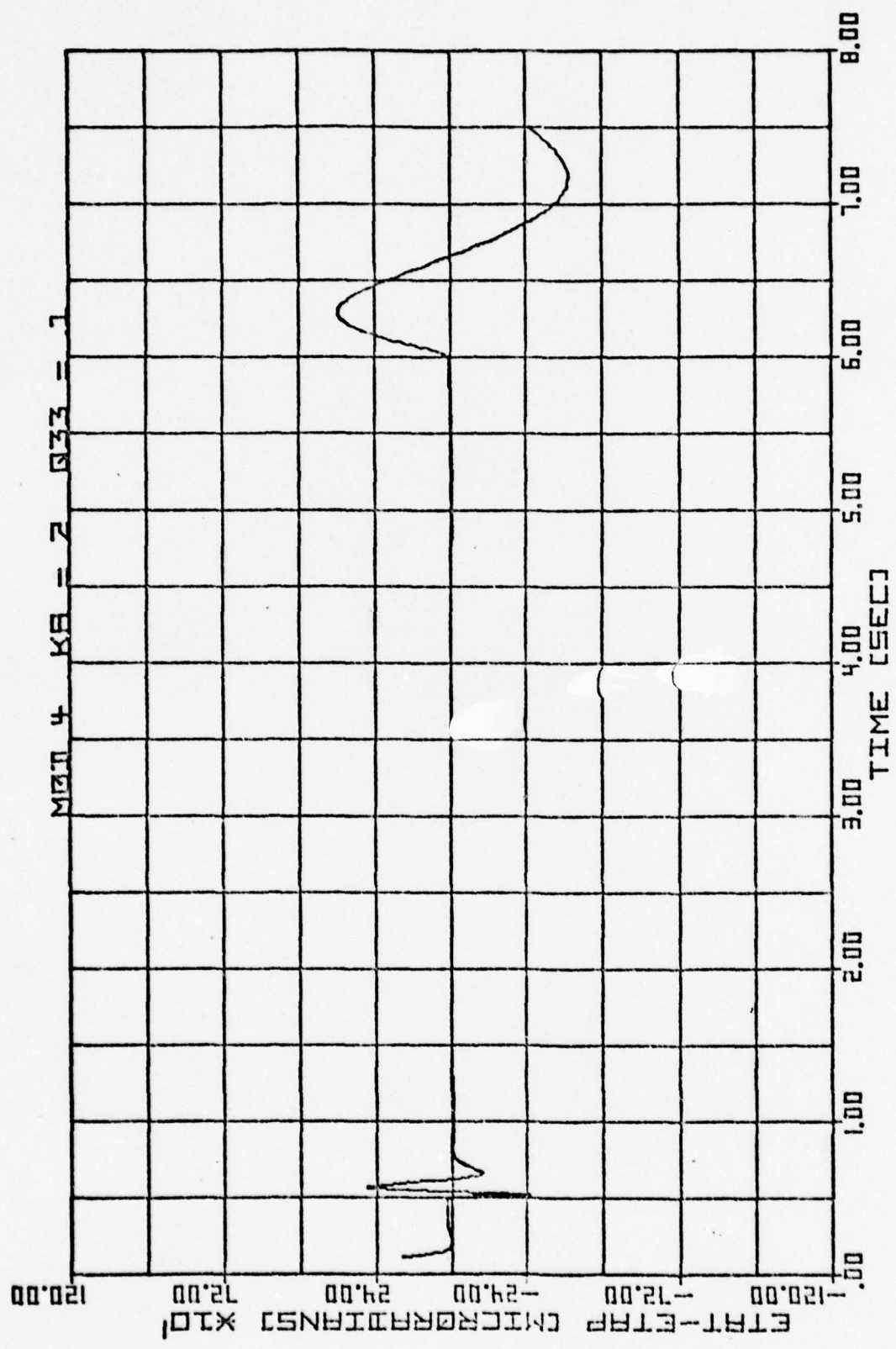
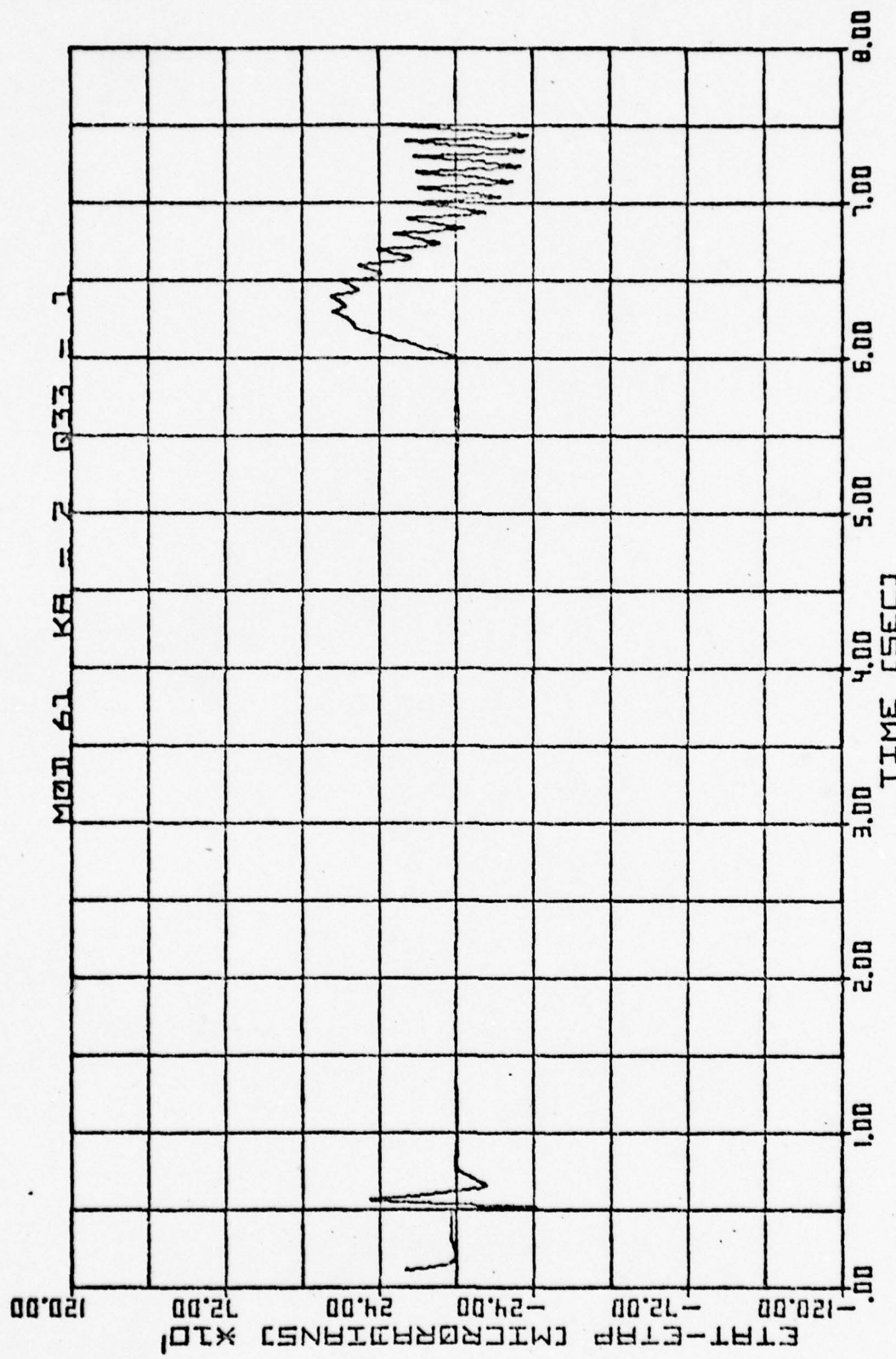
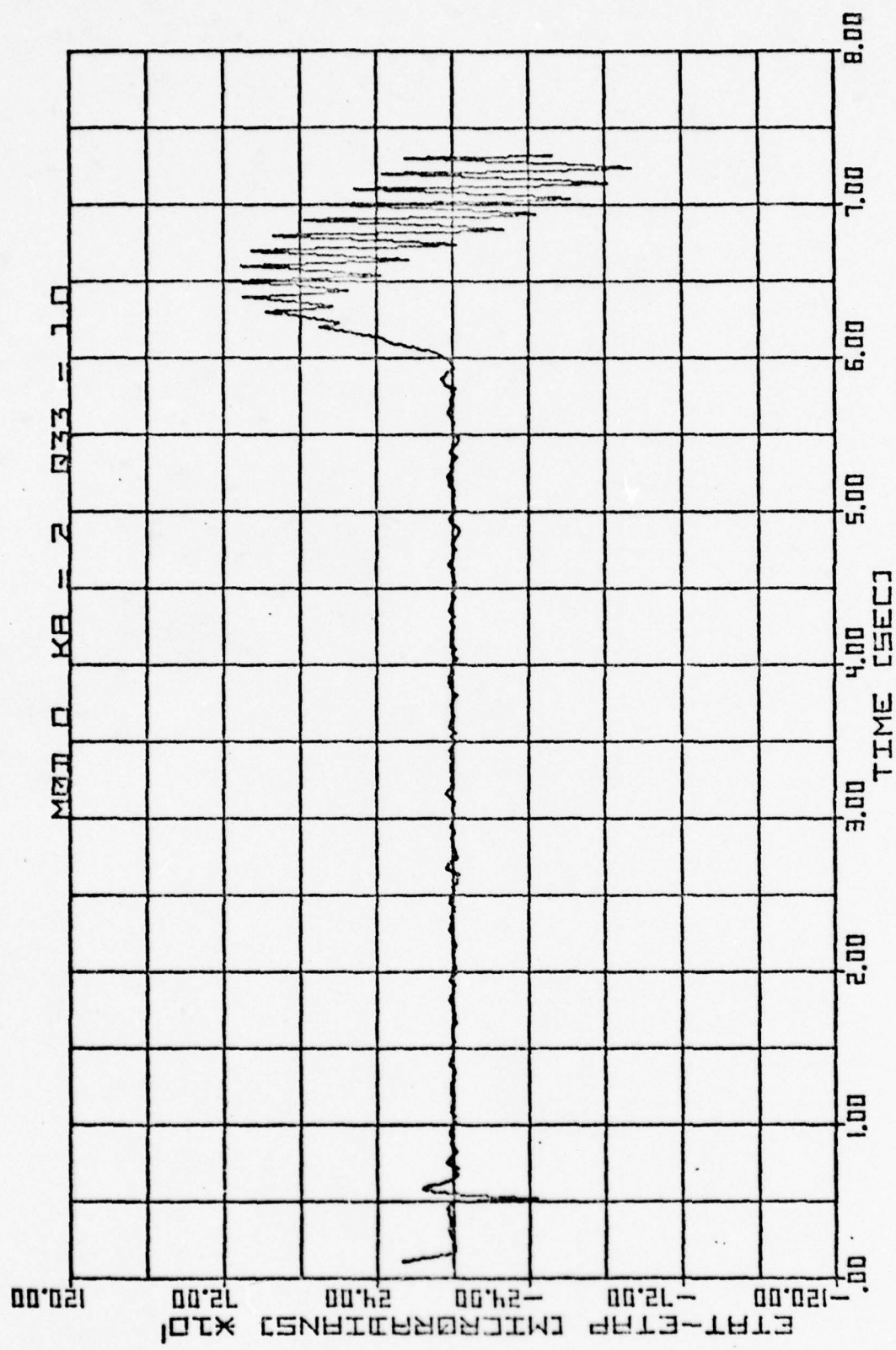


Fig. 45. Aided at 0.01 second rate with laser rangefinder,
Optimal modification, Scenario Two.





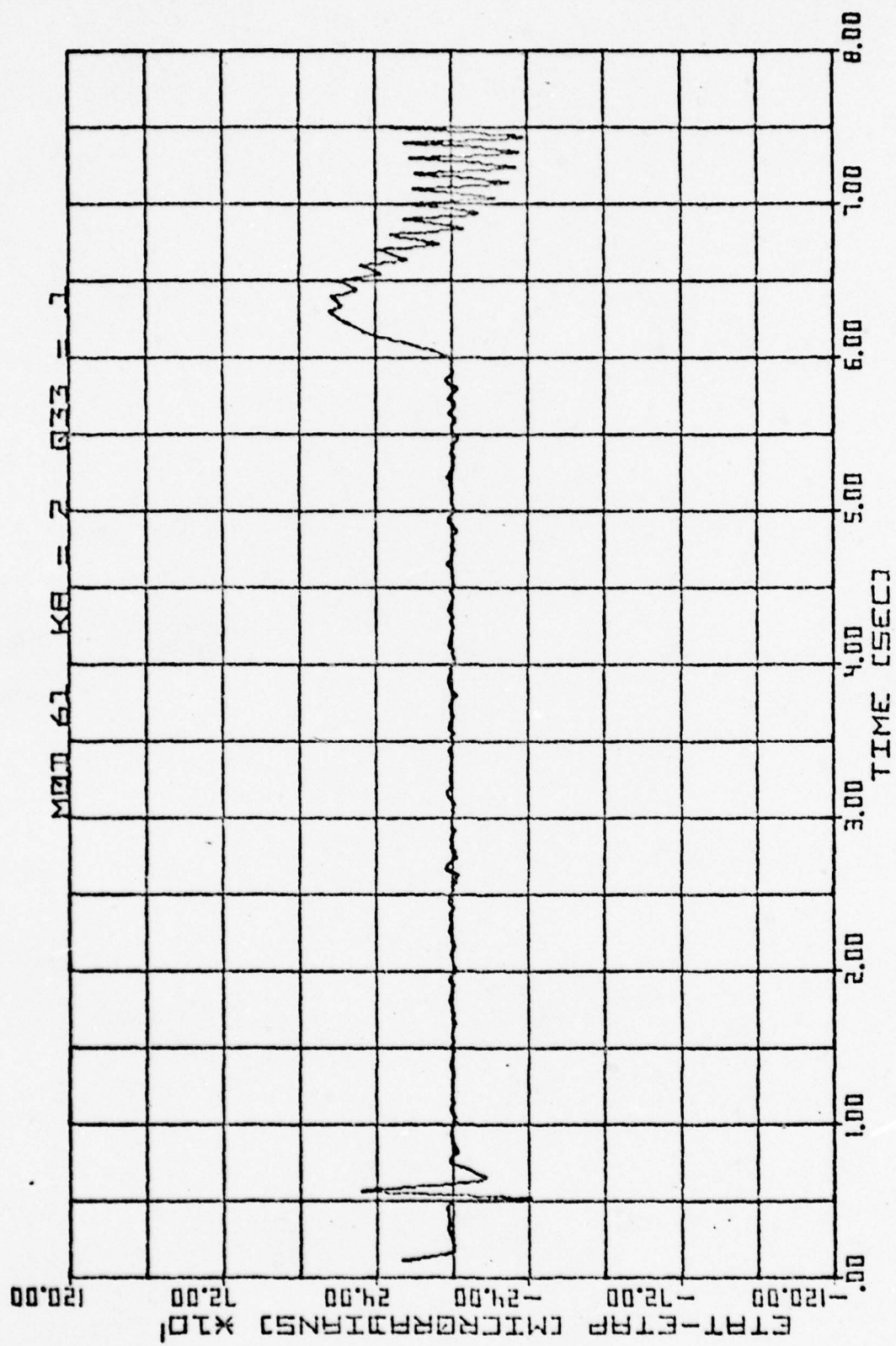


Fig. 48. Aided at 0.01 second rate by Modification Six with measurement noise, Scenario Two.

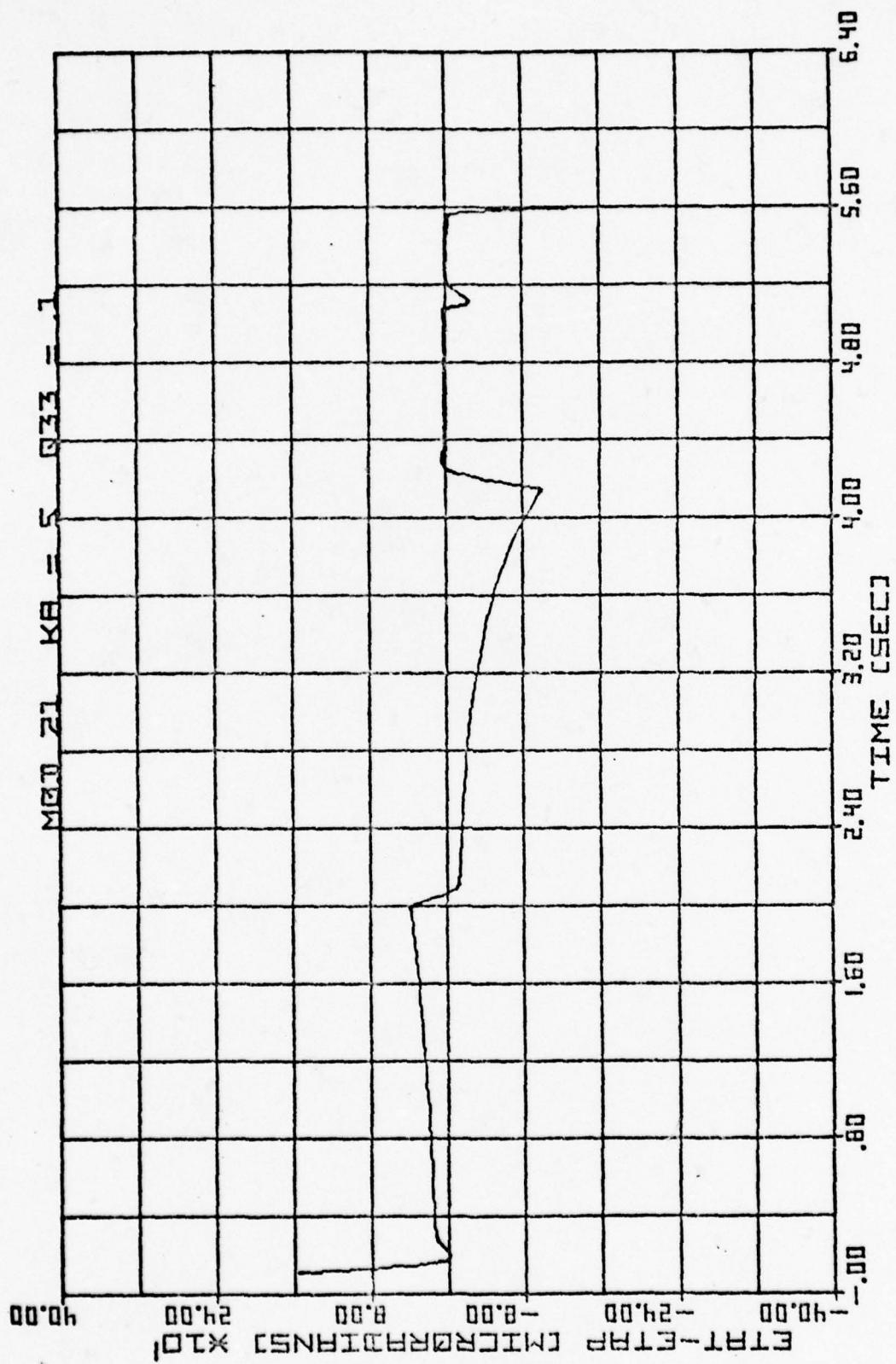
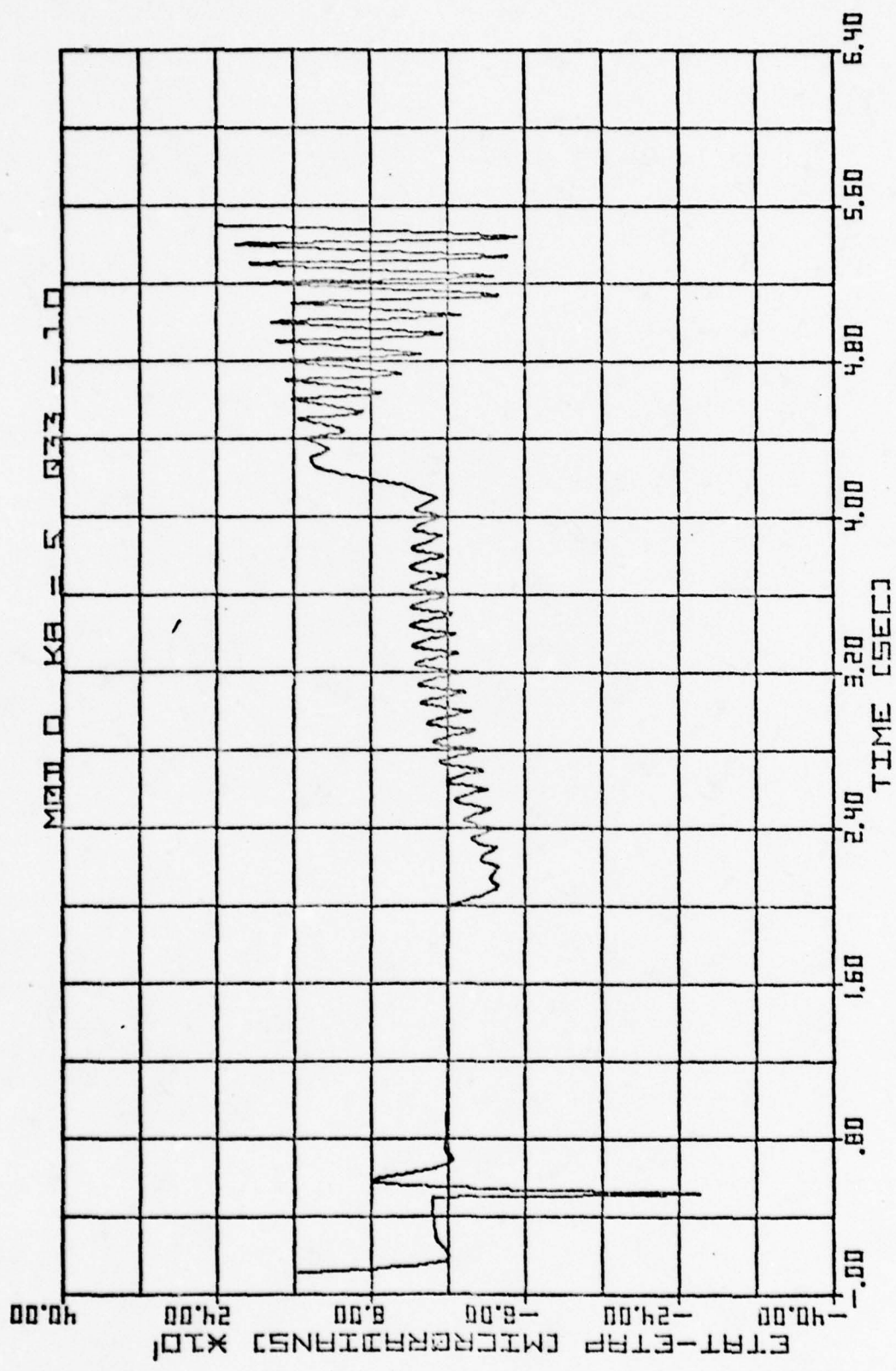


Fig. 49. Unaided tracking of Scenario Five.



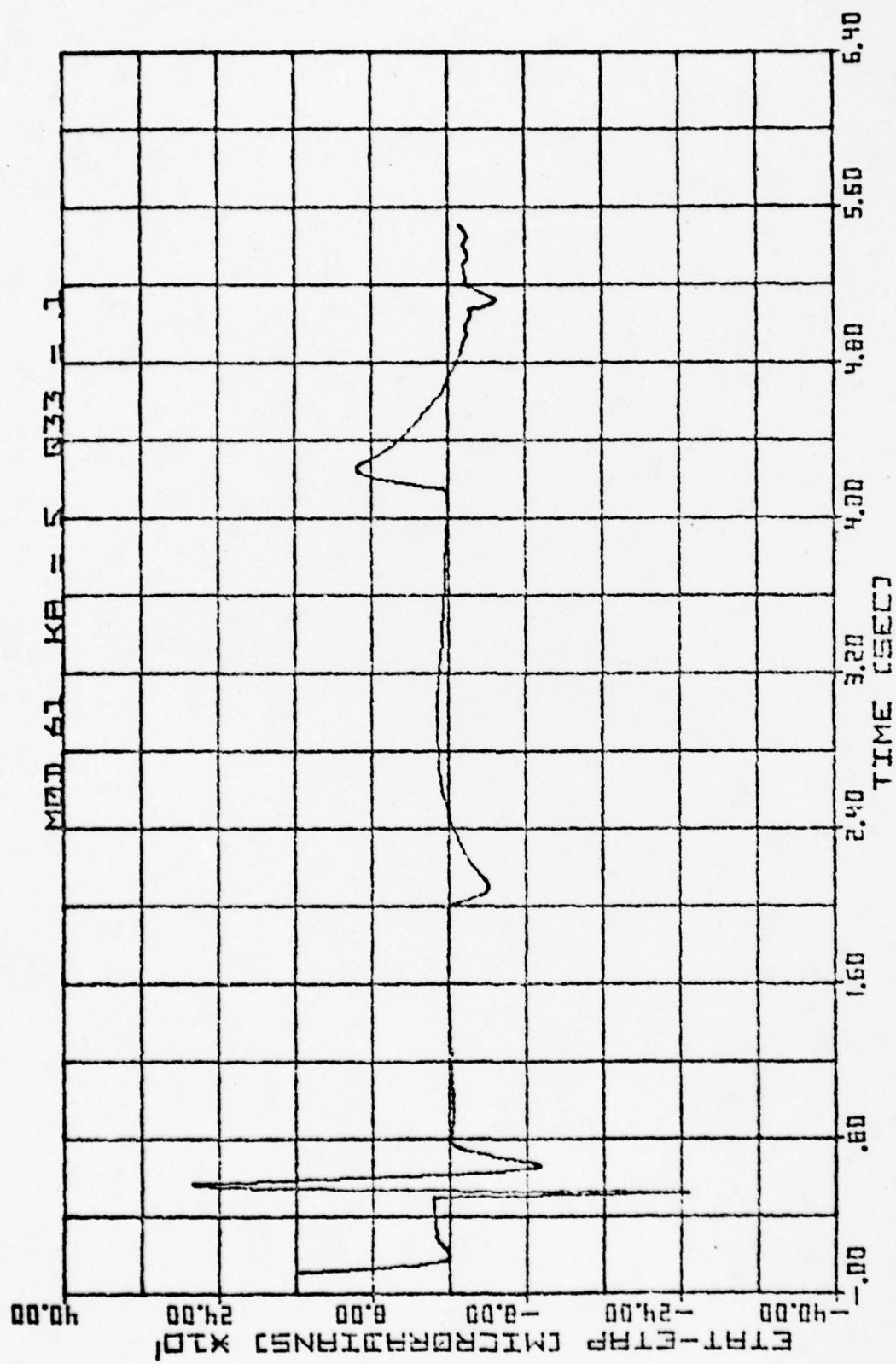


Fig. 51. Aided at 0.01 second rate by Modification Six,
Scenario Five.

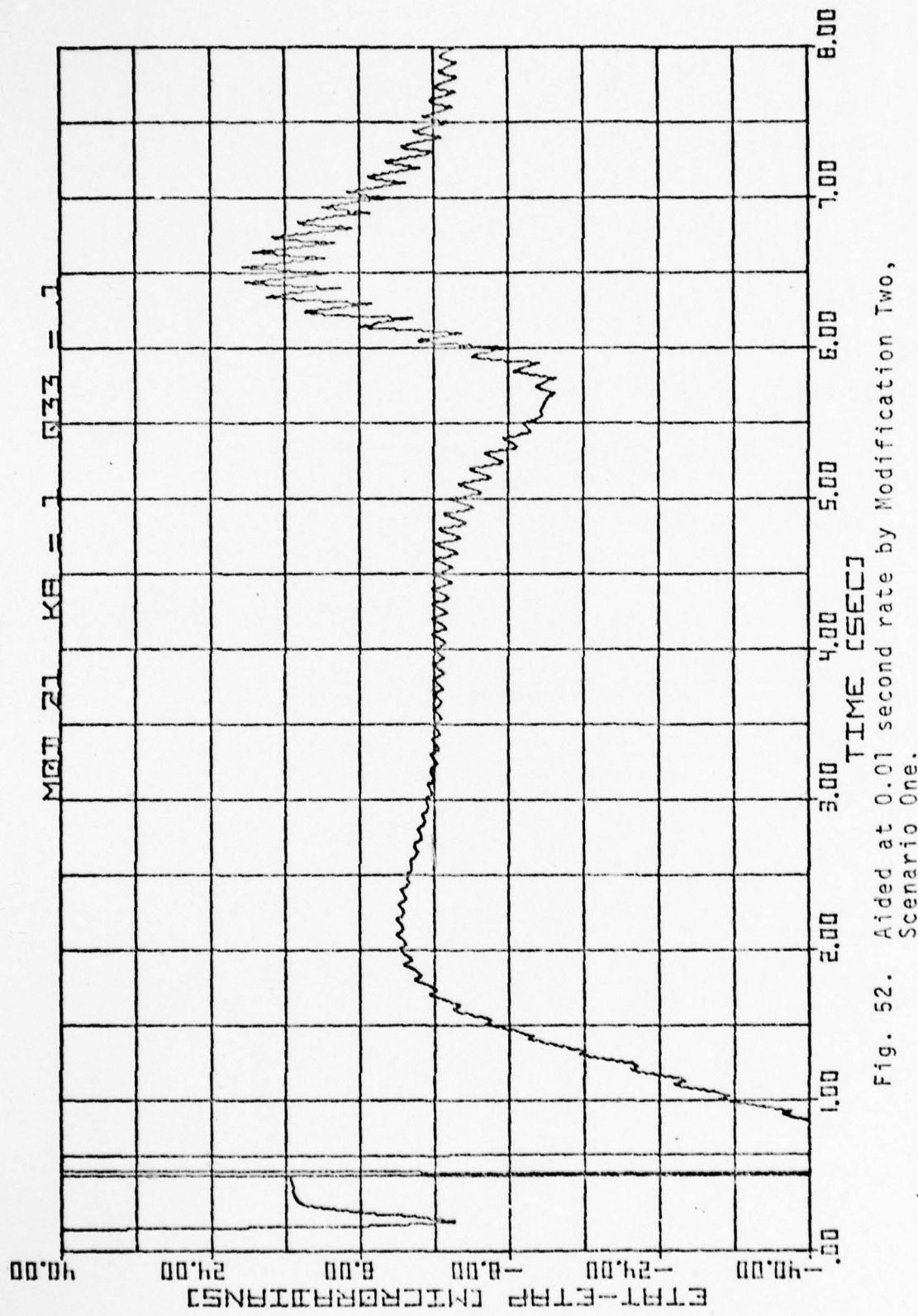


Fig. 52. Aided at 0.01 second rate by Modification Two, Scenario One.

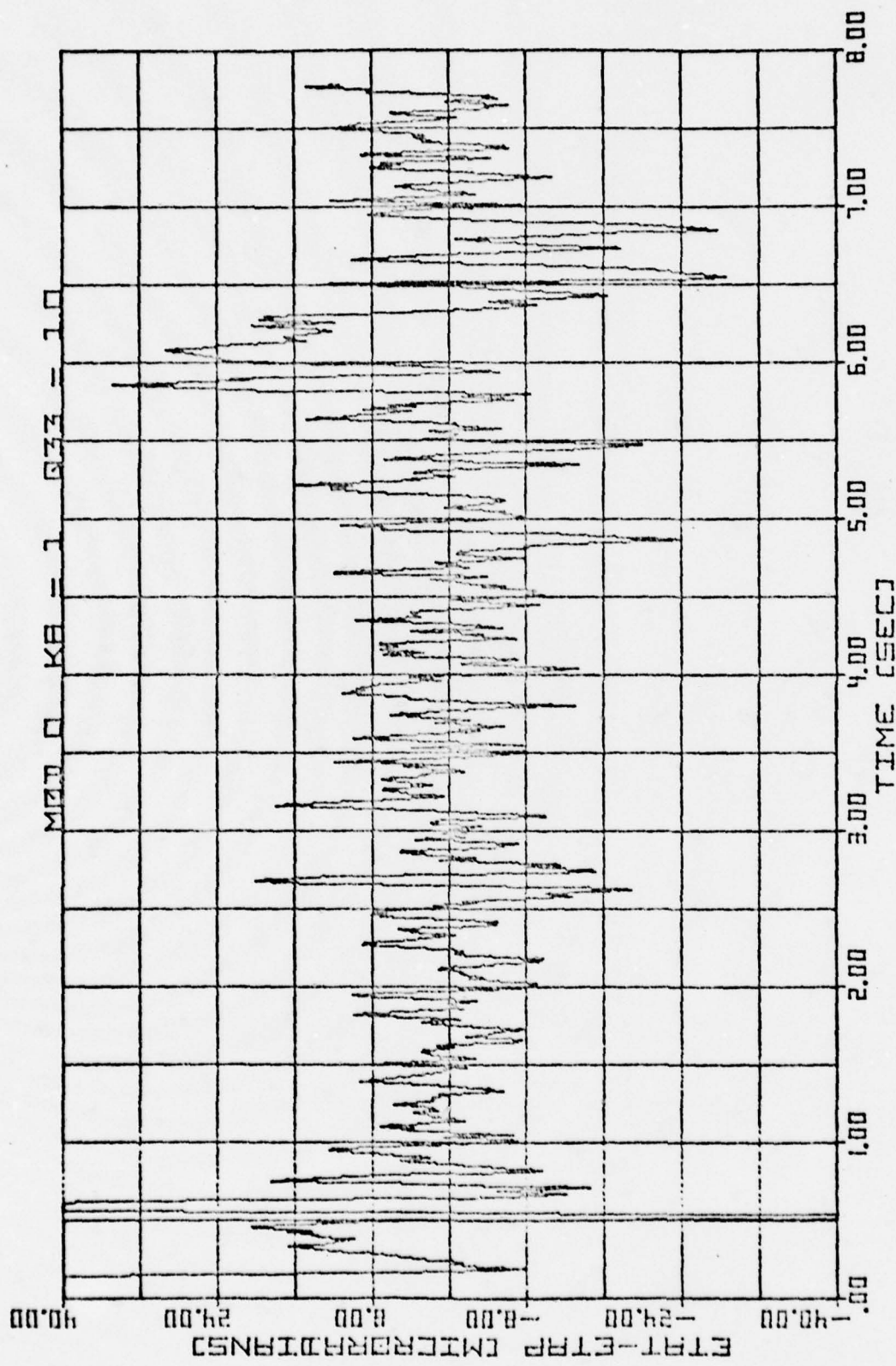


Fig. 53. Aided at 0.1 second rate, with noise, Scenario One.

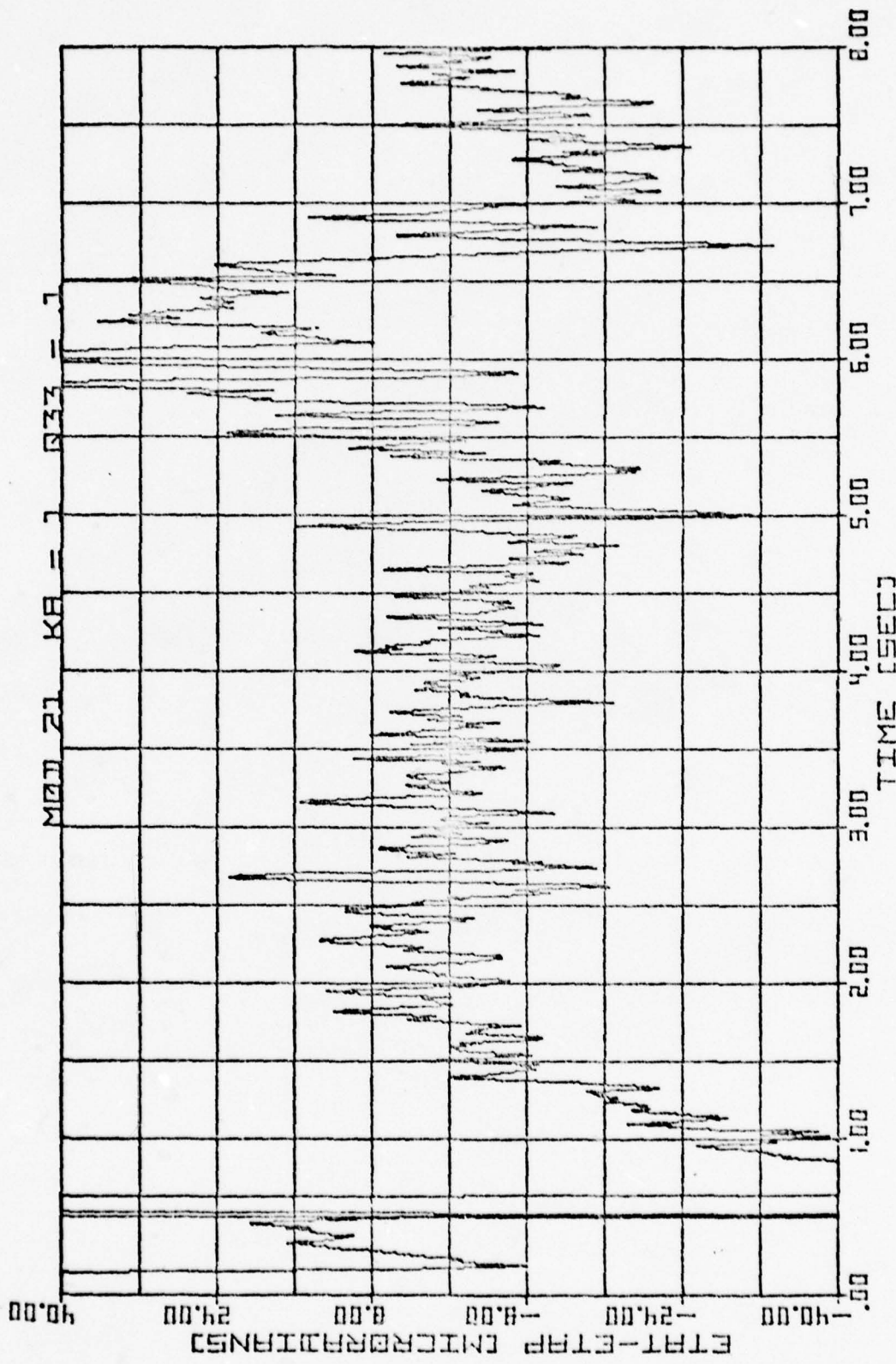
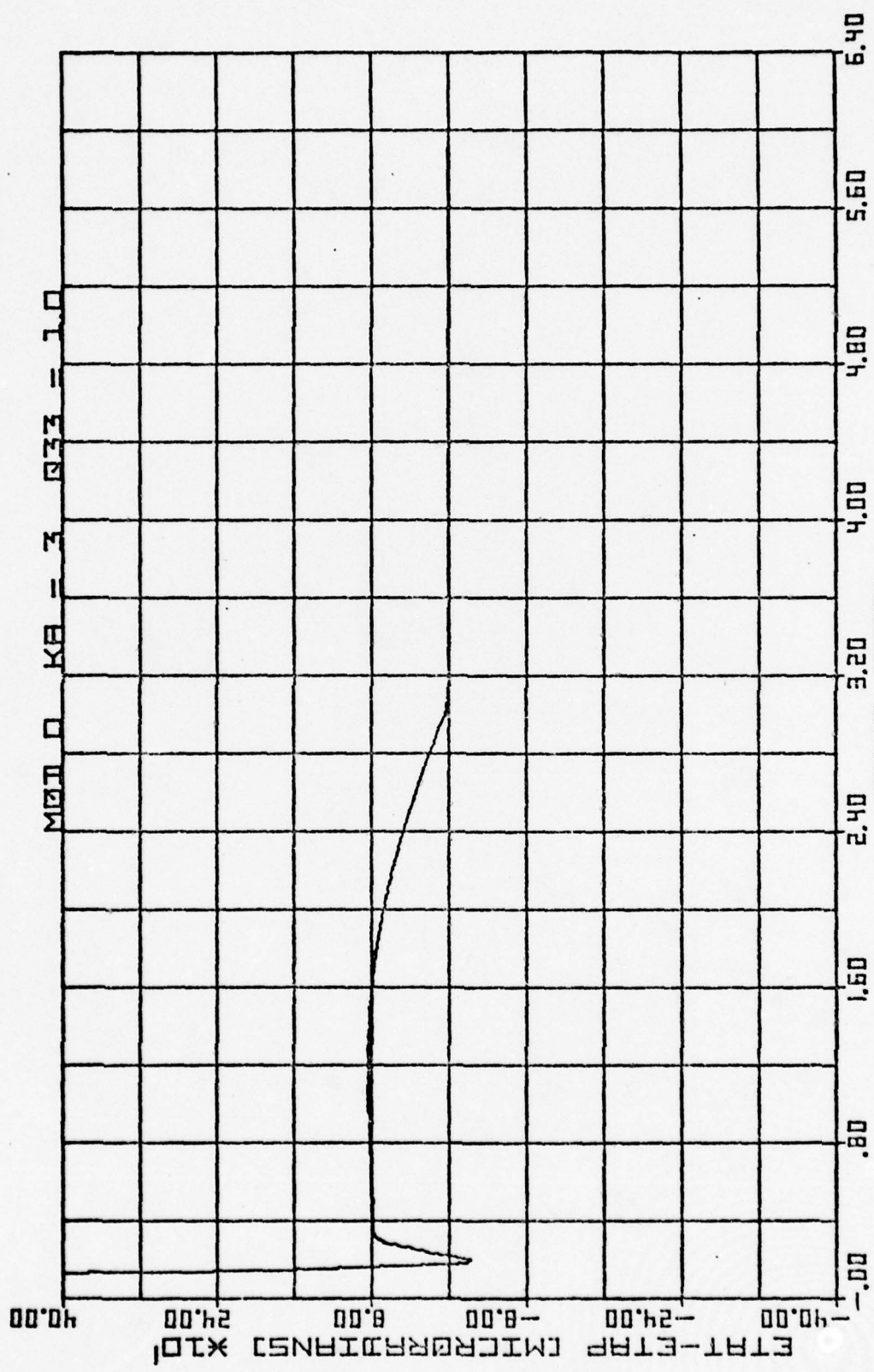


Fig. 54. Aided at 0.01 second rate by Modification Two, with noise, Scenario One.



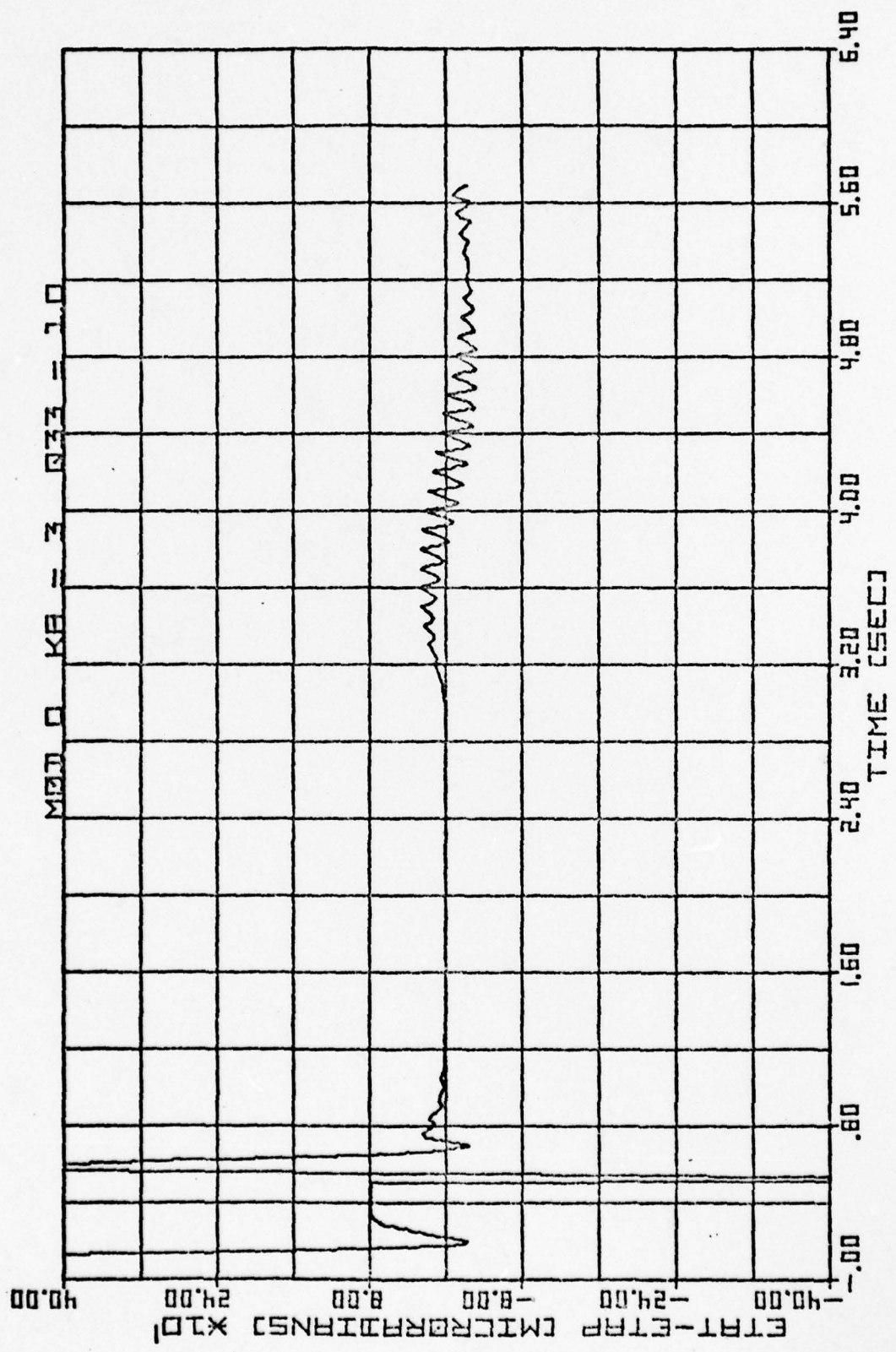


Fig. 56. Aided at 0.1 second rate, Scenario Three.

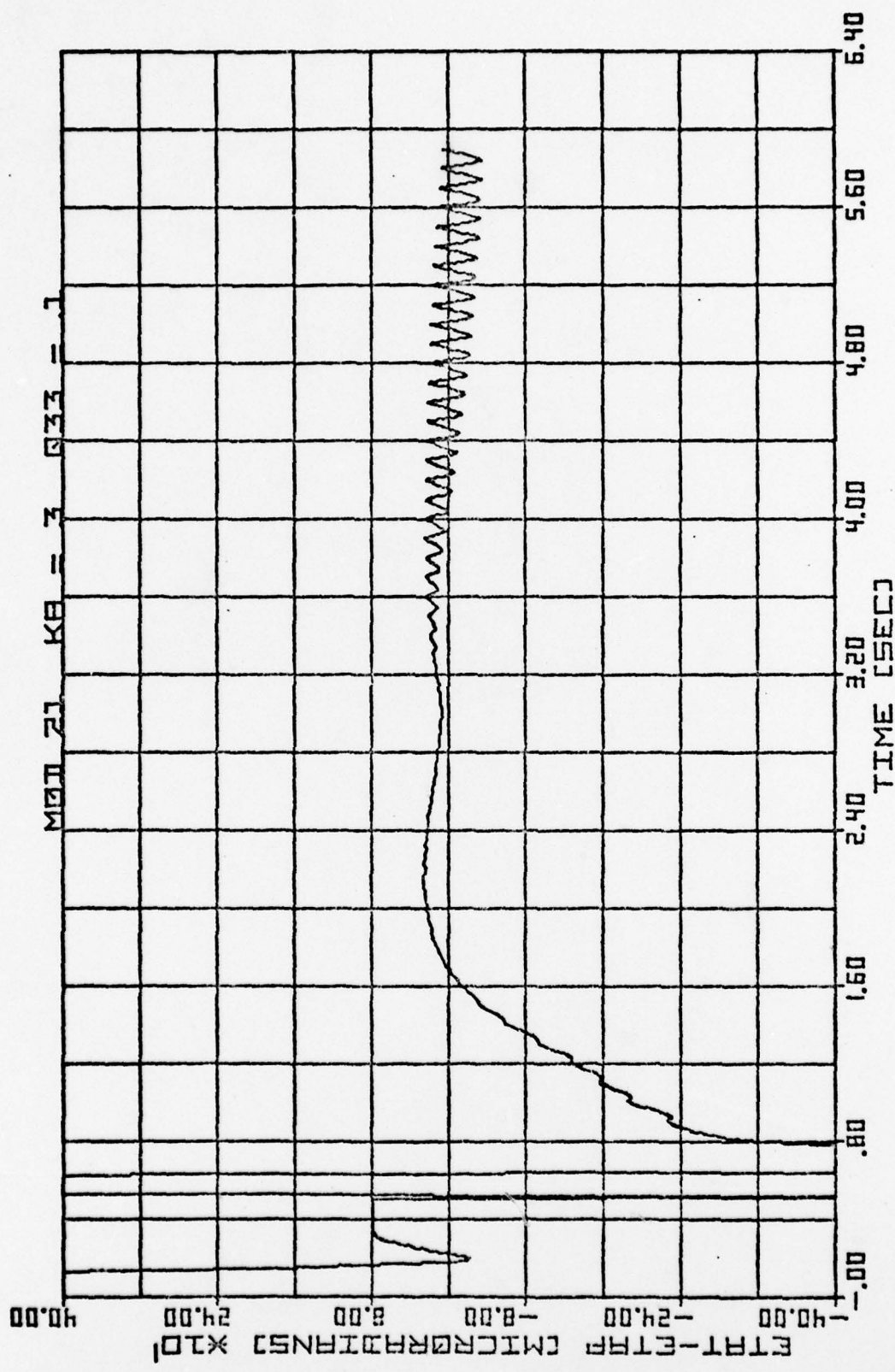


Fig. 57. Aided at 0.01 second rate by Modification Two,
Scenario Three.

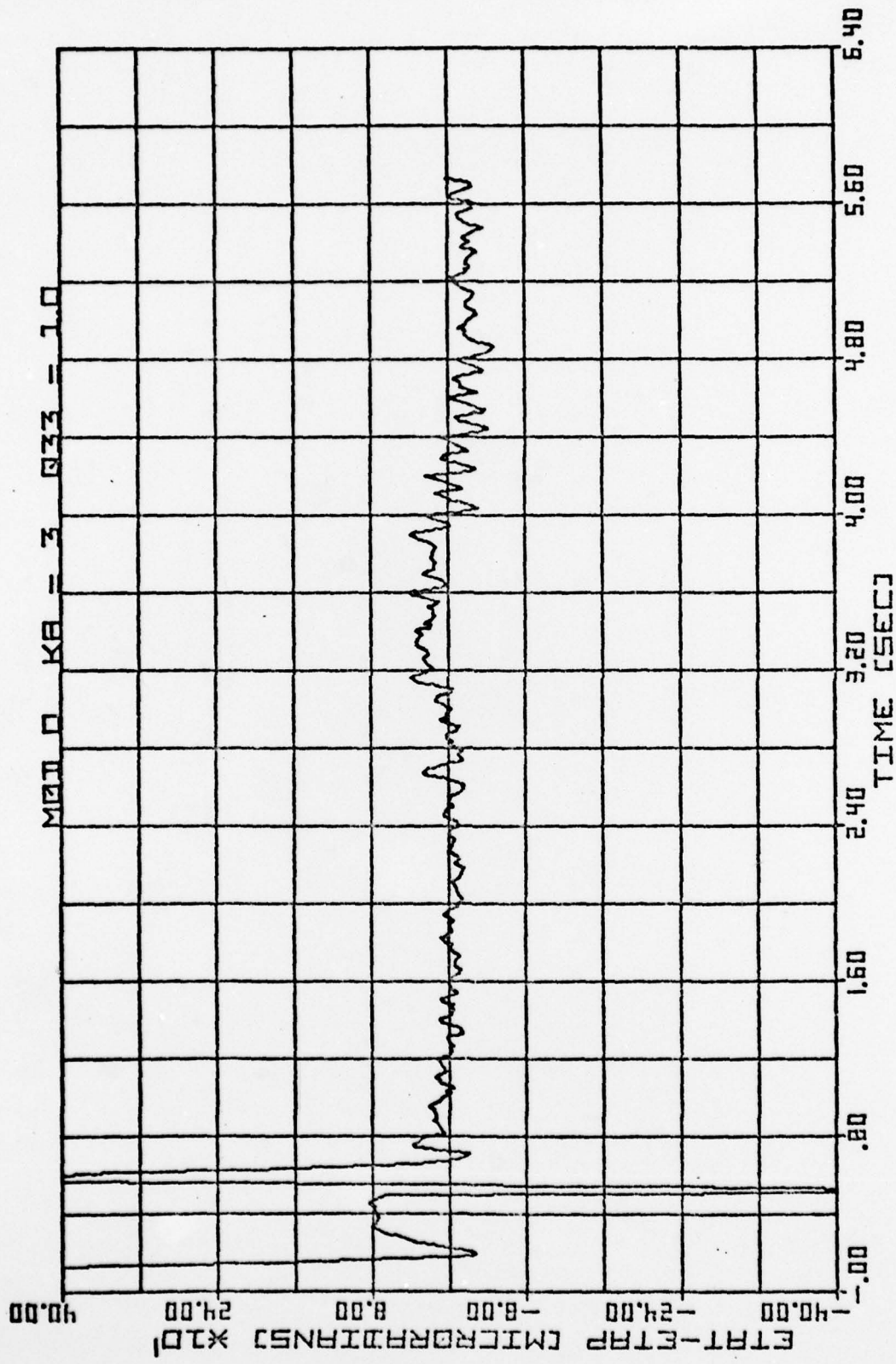


Fig. 58. Aided at 0.1 second rate, with noise, Scenario Three.

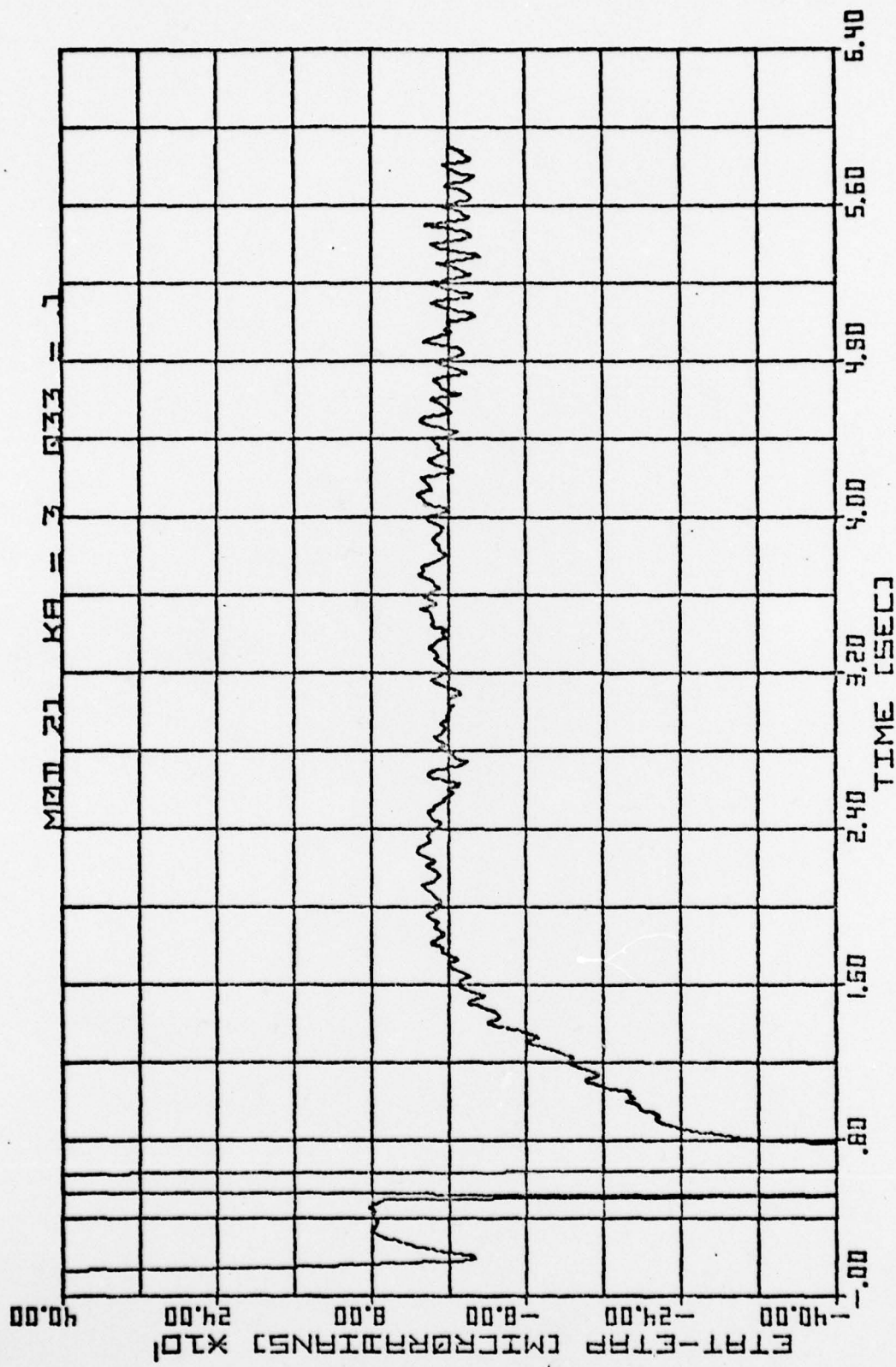
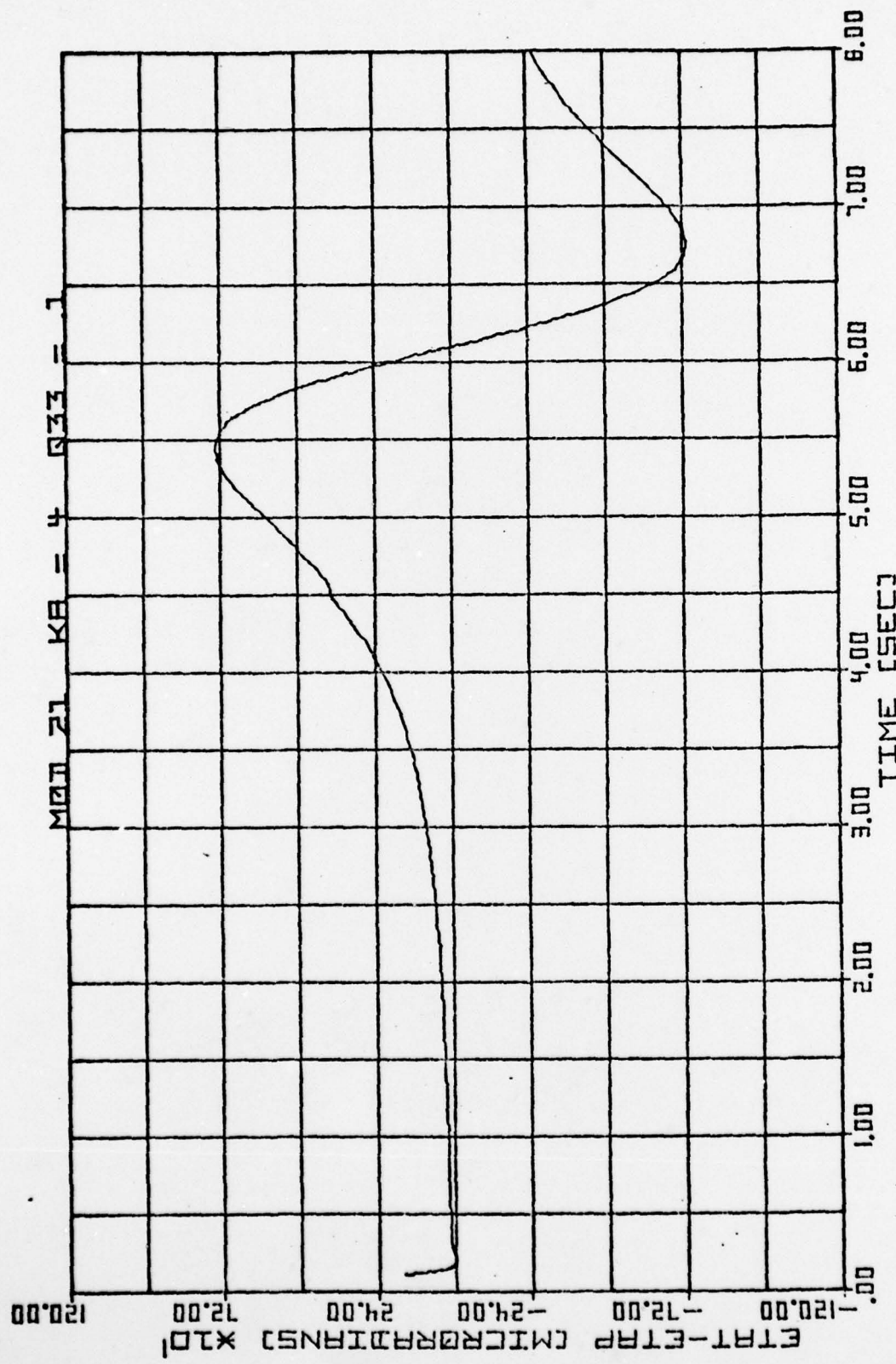


Fig. 59. Aided at 0.01 second rate by Modification Two, with noise, Scenario Three.



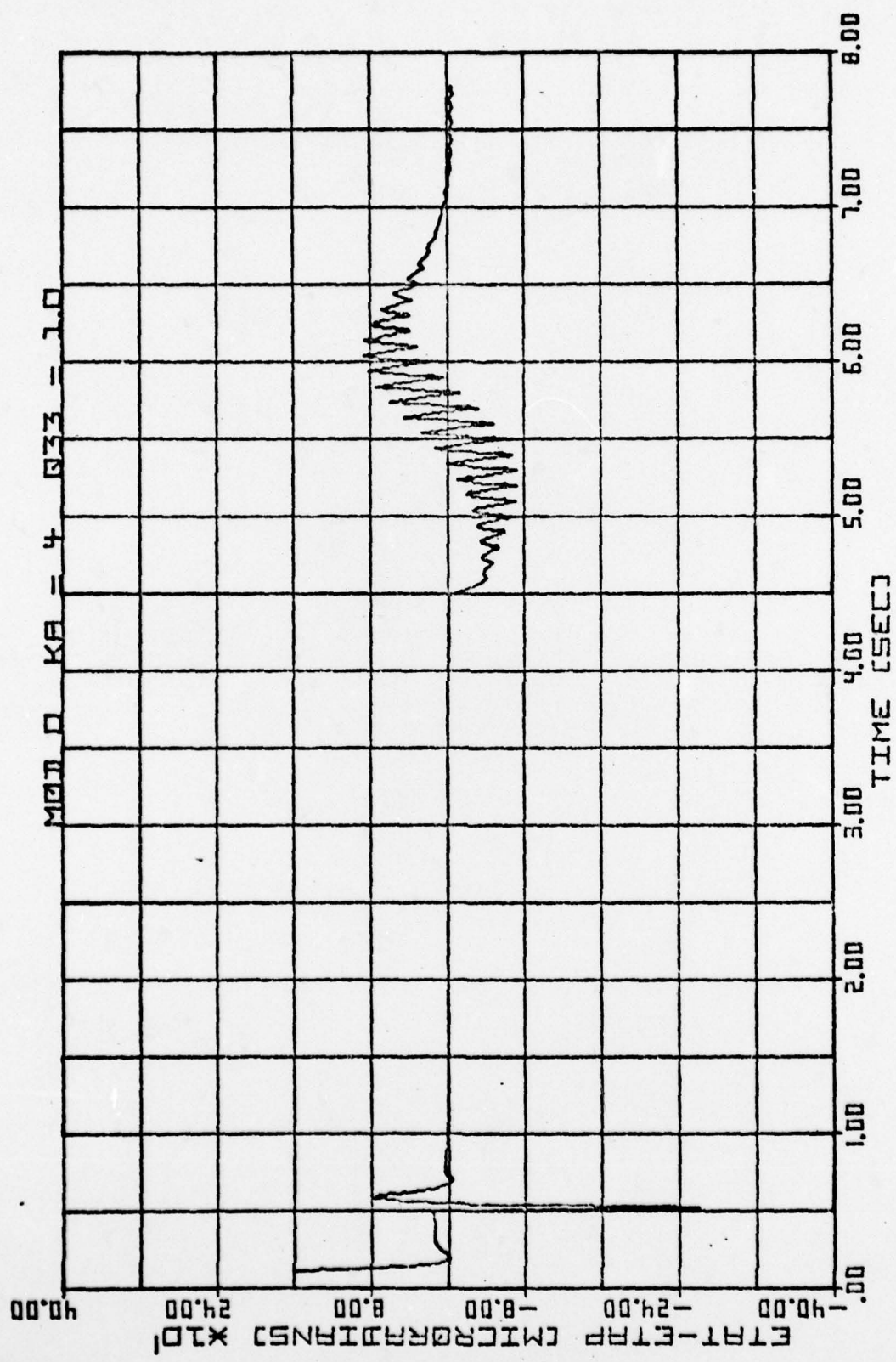


Fig. 61. Aided at 0.1 second rate, Scenario Four.

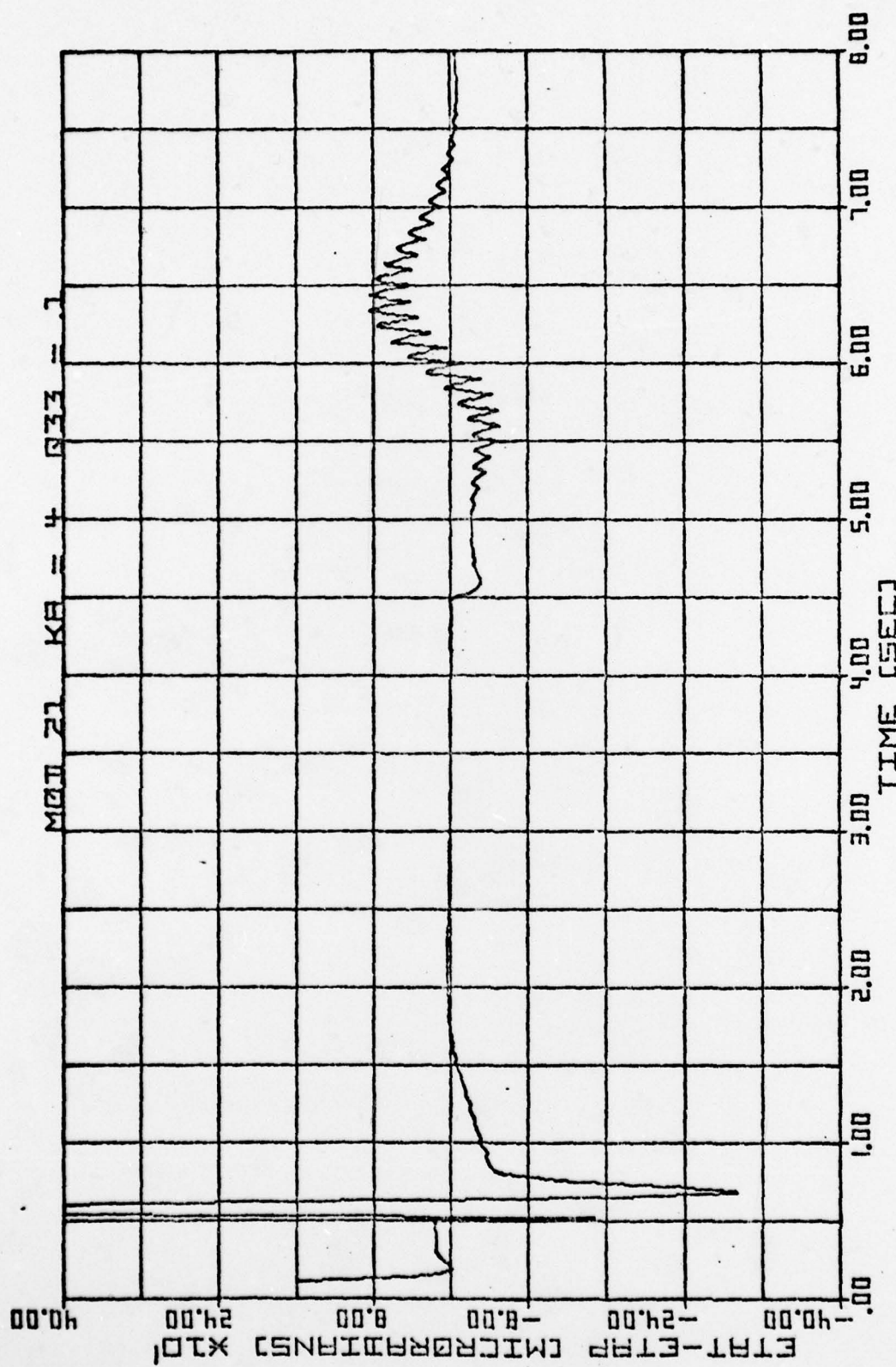


Fig. 62. Aided at 0.01 second rate by Modification Two,
Scenario Four.

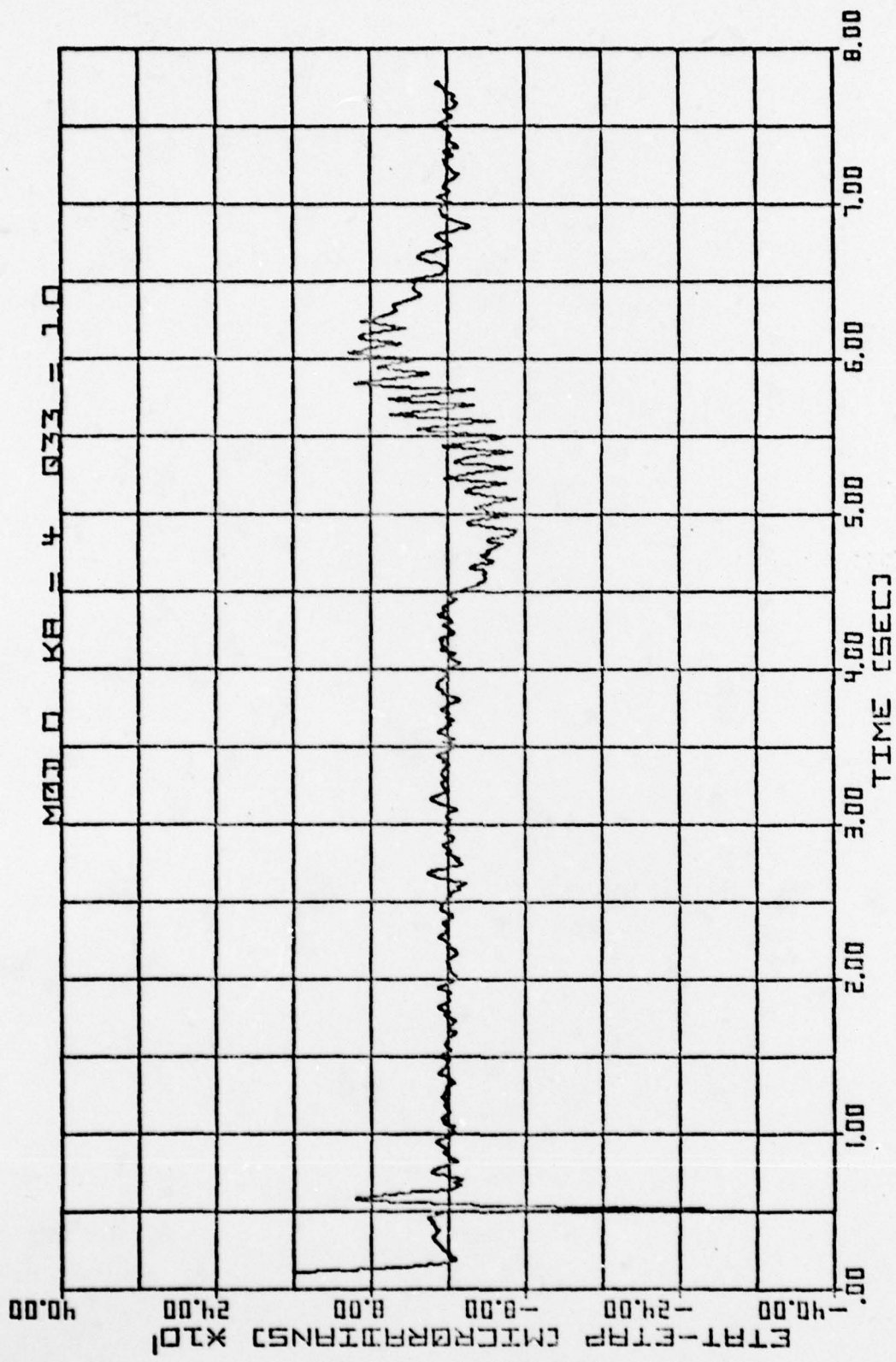


Fig. 63. Aided at 0.1 second rate, with noise,
Scenario Four.

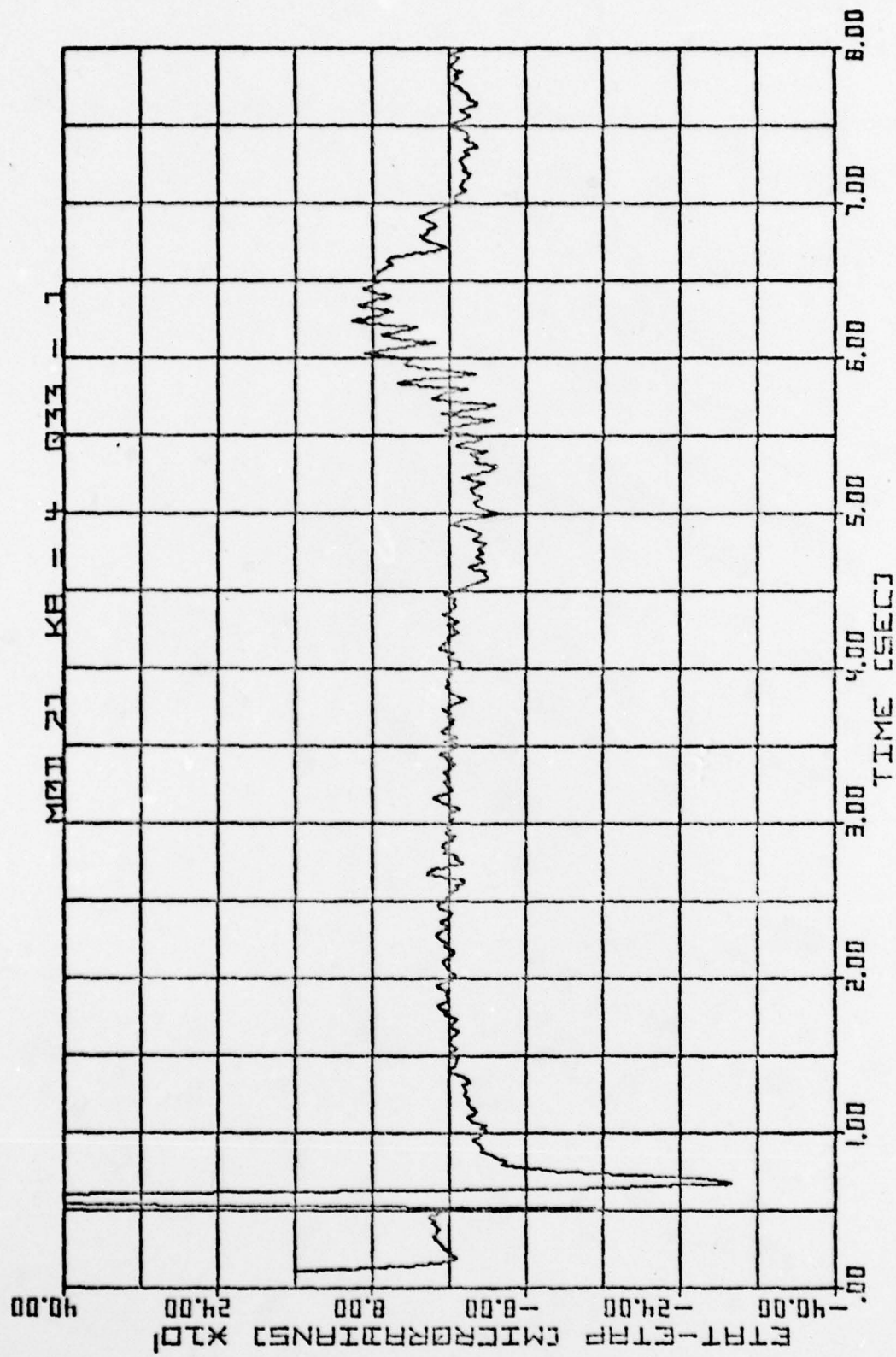


Fig. 64. Aided at 0.01 second rate by Modification Two, with Noise, Scenario Four.

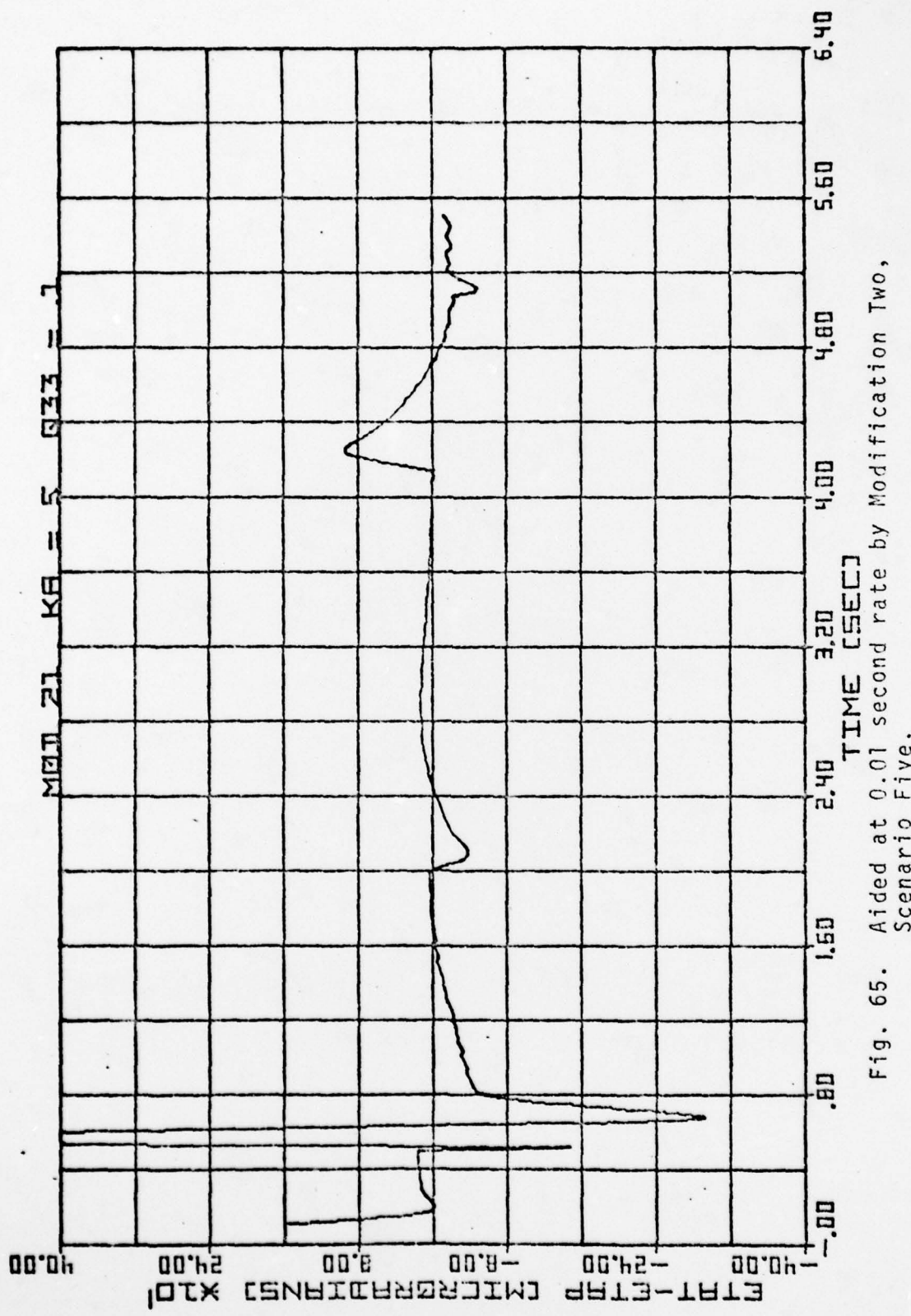
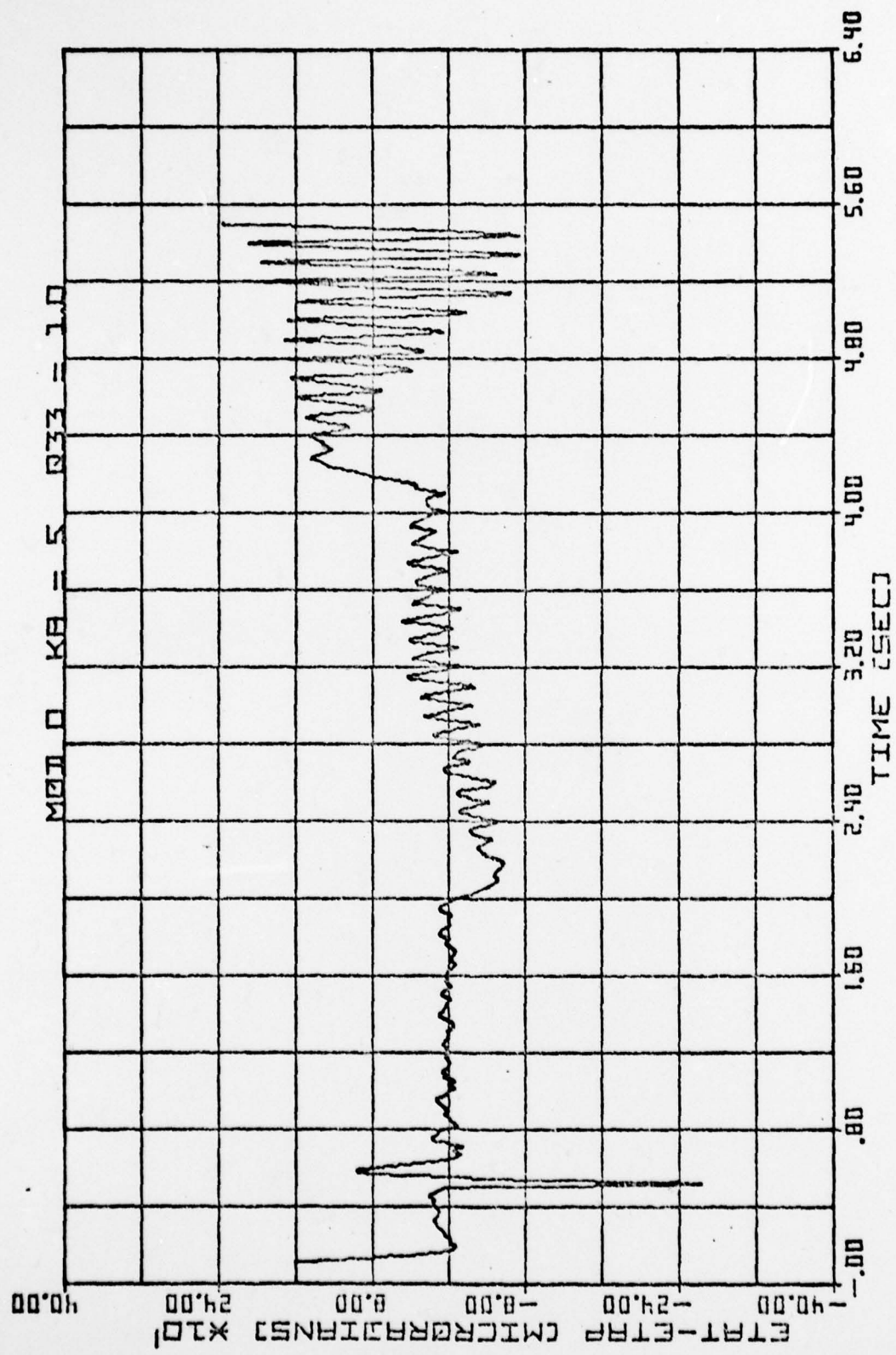


Fig. 65. Aided at 0.01 second rate by Modification Two,
Scenario Five.



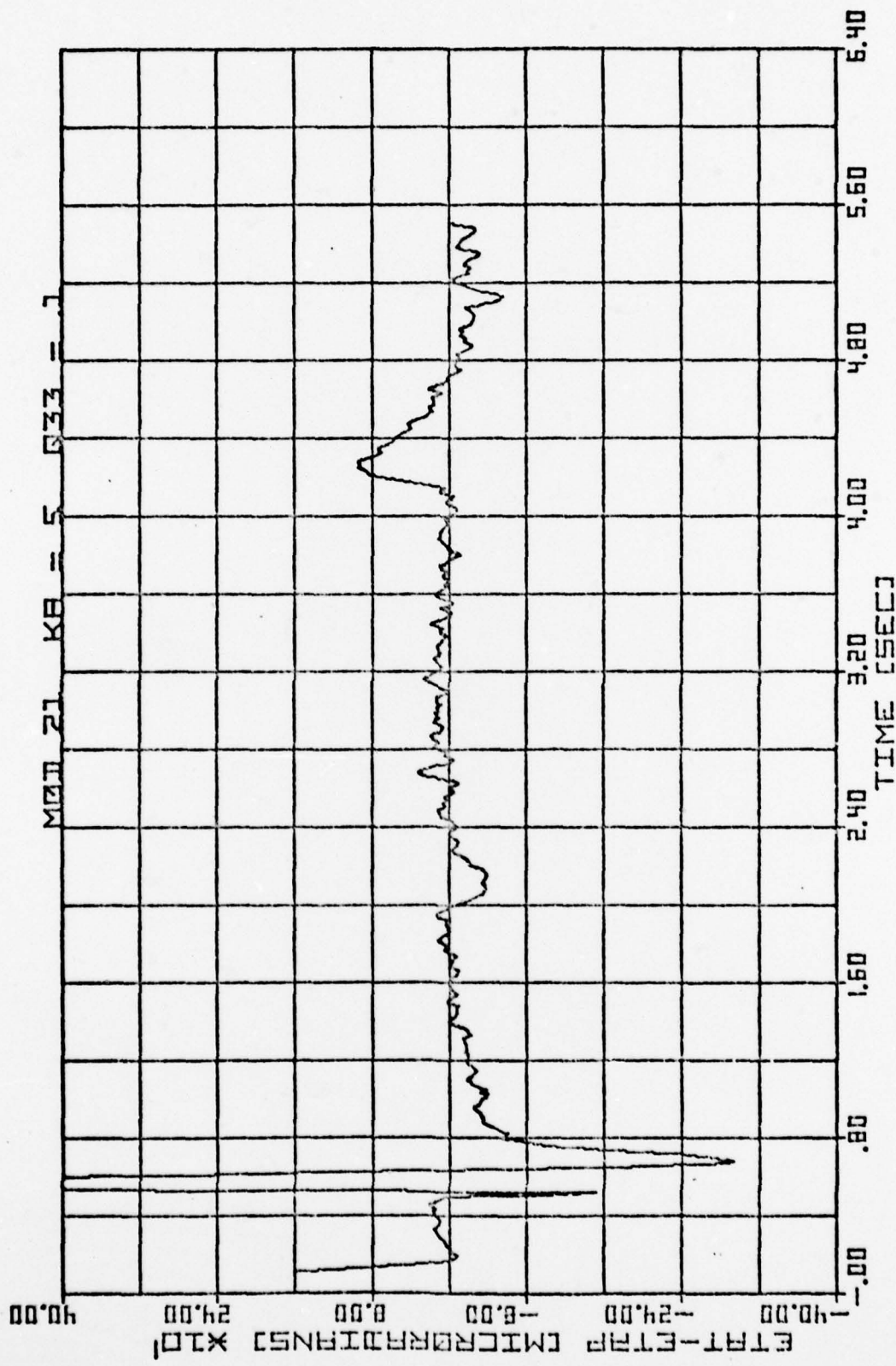


Fig. 67. Aided at 0.01 second rate by Modification Two, with noise, Scenario Five.

Vita

James M. Petek was born on 14 August 1947 in Cleveland, Ohio. After his graduation from John Marshall High School in Cleveland, he attended Ohio State University, Lakewood Extension, for one year. In 1965, he entered the United States Air Force Academy. After graduation and receiving his commission in June 1969, he was assigned to Under-graduate Pilot Training at Williams AFB, Arizona. In July 1970, he received his wings and was assigned to Grand Forks AFB, North Dakota as an F-101 interceptor pilot. His next assignment was to Da Nang AB, Republic of Viet Nam as a Forward Air Controller. Upon returning from Viet Nam, he was assigned to Vance AFB, Oklahoma as a T-38 Instructor Pilot and Flight Commander. In June 1976, he entered the Graduate Astronautical Engineering program at the Air Force Institute of Technology.

~~UNCLASSIFIED~~

SECURITY CLASSIFICATION OF THIS PAGE (When Data Entered)

DD FORM 1473 EDITION OF 1 NOV 65 IS OBSOLETE
1 JAN 73

UNCLASSIFIED *(b)(1)*
SECURITY CLASSIFICATION OF THIS PAGE (When Data Entered)

UNCLASSIFIED
EXPIRATION OF THIS PAGE

3 next
page

UNCLASSIFIED

SECURITY CLASSIFICATION OF THIS PAGE (When Data Entered)

Block 20.

performance of all methods tested. This method demonstrated a definite improvement over the slower system when tracking highly maneuverable targets.



UNCLASSIFIED

SECURITY CLASSIFICATION OF THIS PAGE (When Data Entered)